# DANSYNC

## *Annual Report 1996*

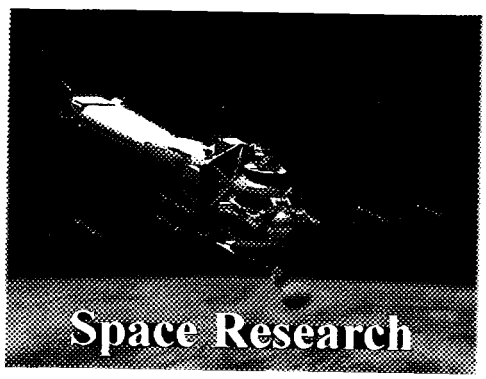


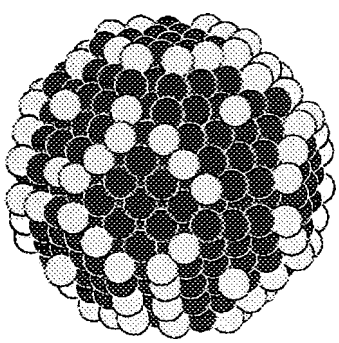

Catalysis

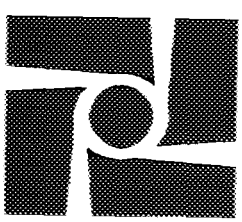

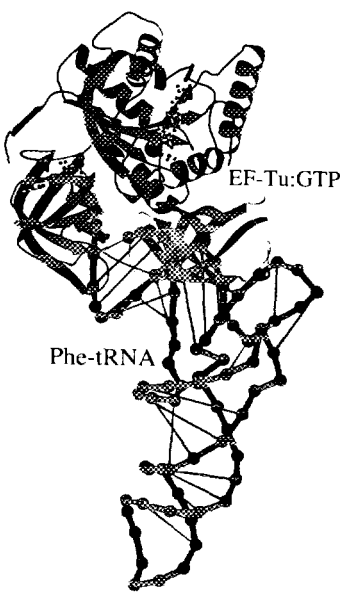


Biochemistry

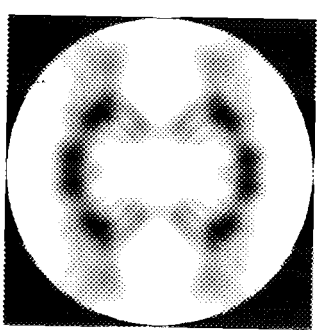

Material Science

We regret that some of the pages in this report may not be up to the proper legibility standards, even though the best possible copy was used for scanning

# *Preface*

DANSYNC is an organisation of danish users of hard X-ray synchrotron facilities, funded by the The Danish Natural Science Research Council.
It was founded in the beginning of 1996, and this is the first Annual Report from DANSYNC.

Users span from basic physics at Risø National Laboratory, Ørsted Laboratory and Denmarks Technical University over materials science from Risø National Laboratory to chemistry and biology at Aarhus University, Copenhagen University and Denmarks Technical University, as well as industrial research represented by Haldor Topsøe A/S and space research at Danish Space Research Institute. These groups are represented in the diagram below showing the number of 8 hour beam shifts during 1996 where members of the groups participated, often in collaboration with their international partners. The total number of shifts were 1433.

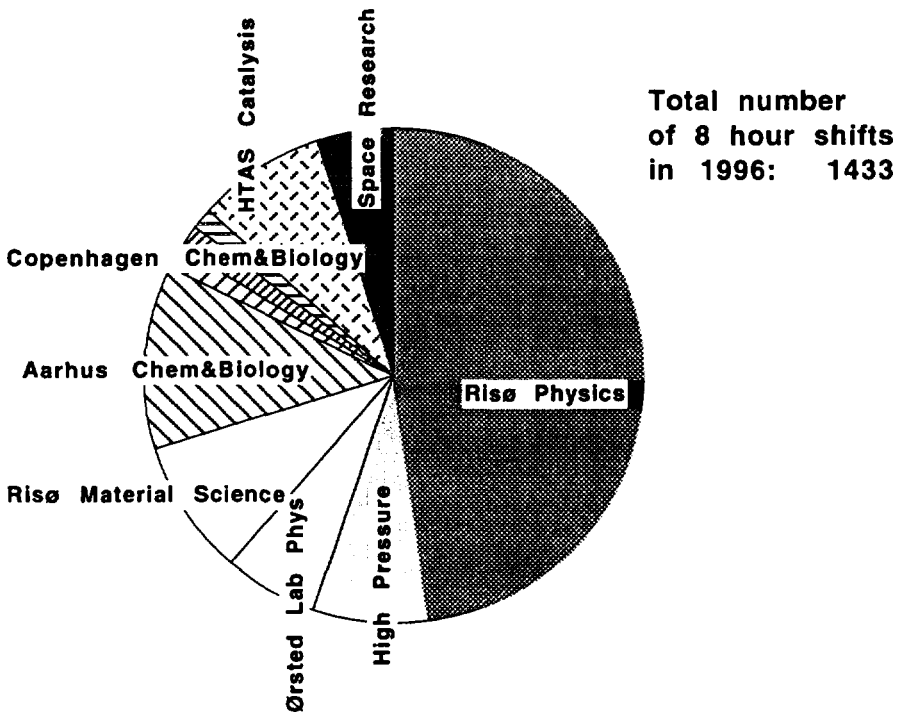


The danish synchrotron community is still growing, in 1996 in particular in the areas of materials science and biology. At Copenhagen University a general one semester synchrotron X-ray course for students in physics, biophysics and chemistry has been established, including a one week training at a bending magnet beam line at HASYLAB in Hamburg.

We do not have an X-ray synchrotron facility in Denmark, so all of this work is carried out at facilities abroad, represented in the pie diagram below:

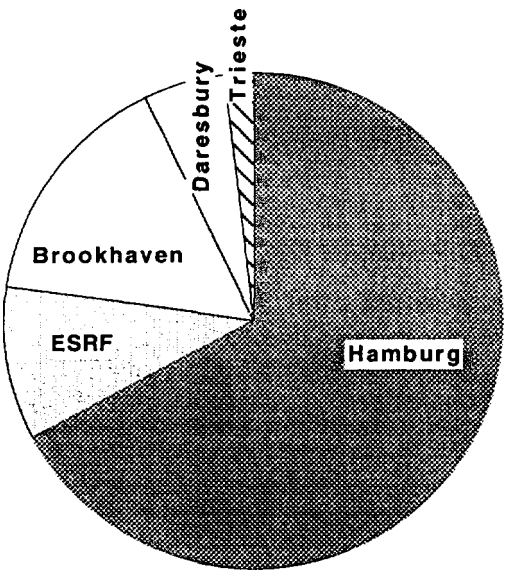


Clearly the facility at DESY in Hamburg (HASYLAB and EMBL) is of the greatest significance for danish synchrotron research.

You can on the following pages read about the many different kinds of research going on, and if you want to know more about DANSYNC please consult our homepage:

http://xray.fys.ku.dk/dansync/ (now)

http://www.dansync.dk/ (from around March 15 1997)

February 1997

Jens Als-Nielsen
Head of DANSYNC

# Content

## *In situ* XAFS studies of a V-Mg-O catalyst for oxidative dehydrogenation of propane

E. Törnqvist, G. Steffensen, A.M. Molenbroek*, and B. S. Clausen
*Haldor Topsøe Research Laboratories, DK-2800 Lyngby, Denmark*
**Center for Atomic-scale Materials Physics and Physics Department, Technical University of Denmark, DK-2800 Lyngby, Denmark*

There is considerable potential interest in industry to use oxidative dehydrogenation (with oxygen as the oxidative agent) instead of direct dehydrogenation, since there are no equilibrium limitations in the former process. The selectivity, however, of the existing catalysts is still unsatisfactorily, and in order to improve their performance it is necessary to gain detailed information about their function and structure. Therefore, we have initiated *in situ* XAFS studies of V-Mg-O catalysts used for oxidative dehydrogenation of propane to propene. The experiments were carried out at the EXAFS II beamline of HASYLAB at DESY. The catalyst samples were studied in an EXAFS *in situ* cell and exposed to different gaseous environments at 550 °C. The X-ray absorption spectrum at the vanadium K-edge with the catalyst exposed to air is recorded as the full drawn trace in Figure 1a together with the spectrum of a reference compound, $V_2O_5$, (dashed line). A comparison of the size of the pre-peaks and the position of the edges indicates that the vanadium in the catalyst is in oxidation state +5. When switching from air to a mixture of 1% $C_3H_8$ and 0.1% $O_2$ in He at 550 °C the spectrum of the catalyst changes to the full drawn trace shown in Figure 1b. The dashed line in this figure is the spectrum of a reference, $V_2O_3$. By similar arguments as before we conclude that the oxidation state of the vanadium in the catalyst is now changed to +3. More detailed structural analysis is now in progress and further work also including combined EXAFS/XRD studies is planned to elucidate the structural changes of the catalyst occuring during oxidative dehydrogenation conditions.

**Acknowledgments**
This work has been financed by the Danish Natural Science Research Council, the Danish National Research Foundation and the European Commission through the Joule program: Contract JOE3-CT95 0022.

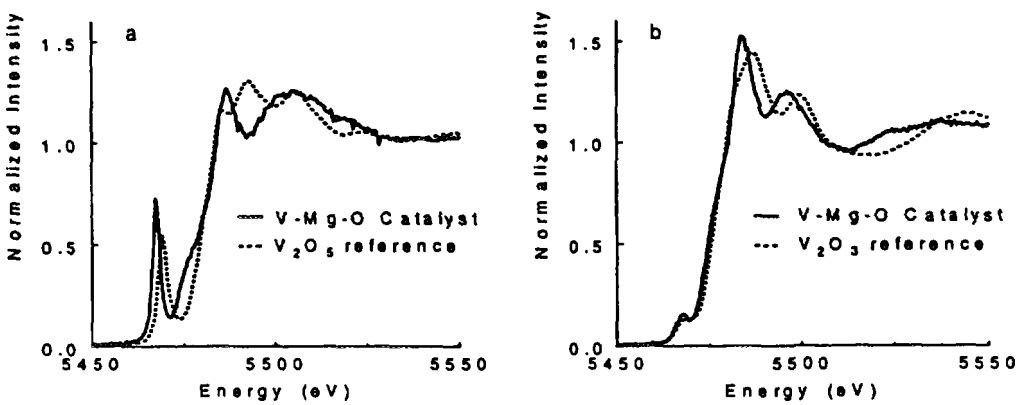


**Figure1.** Normalized XANES spectra at the V K-edge. a) Catalyst exposed to a flow of air at 550 °C. b) Catalyst exposed to a flow of 1% $C_3H_8$ and 0.1% $O_2$ in He at 550 °C.

# Surface alloying in Ni/Au nano-particle catalysts

A.M. Molenbroek, G. Steffensen*, J. Hyldtoft*, B.S. Clausen* and J.K. Nørskov
*Center for Atomic-scale Materials Physics and Physics Department, Technical University of Denmark, DK-2800 Lyngby, Denmark*
** Haldor Topsøe Research Laboratories, DK-2800 Lyngby, Denmark*

The synthesis of bimetallic alloy catalysts allows for the design of surfaces with specific chemical properties. In this study, we characterize the segregation behaviour of Ni/Au supported nano-particle catalysts. The Ni/Au bimetallic alloy is part of a new group of alloys for which the bulk metals are immiscible at low temperature, while STM studies on single crystals have shown that alloying does take place in the outermost atomic layer at the surface. By changing the atomic ratio of the metals, the surface composition and thus the chemical properties might be varied.

Ni/Au binary alloy nano-catalysts were prepared with several different atomic ratios of the constituents. A number of different synthesis methods and supports were used to prepare the supported alloys: surfactant stabilized colloid synthesis, coimpregnation and coprecipitation. The structure of the catalysts was determined by means of transmission EXAFS, carried out at the BW1 and RÖMO II beamlines at HASYLAB at DESY and at the BL18 beamline at the ESRF. The sample was loaded in an *in situ* cell which allowed for heating in different gas flows.

The Ni/Au samples were reduced in a flow of pure $H_2$ to 400-600°C, depending on the preparation method. Figure 1 shows EXAFS spectra at the Ni K-edge of the Ni:Au=20:1 and the pure Ni catalyst. The samples were synthesized by impregnating a silica support with $Ni(NO_3)_2$ and $Au(NH_3)_4(NO_3)_3$. Before reduction both spectra are indicative of oxidized Ni. After reduction in $H_2$ and cooling down to room temperature, both spectra resemble metallic Ni. Both samples were subsequently exposed to an oxygen flow. For the Ni sample a strong structural change of the spectrum is observed, while only small changes are seen for the Ni/Au catalyst. This strongly suggests that Au is alloyed in the surface of the Ni particles, preventing the Ni from being oxidized.

**Acknowledgments**
This work has been financed by the Danish Natural Science Research Council.
The Center for Atomic-scale Materials Physics is sponsored by the Danish National Research Foundation.

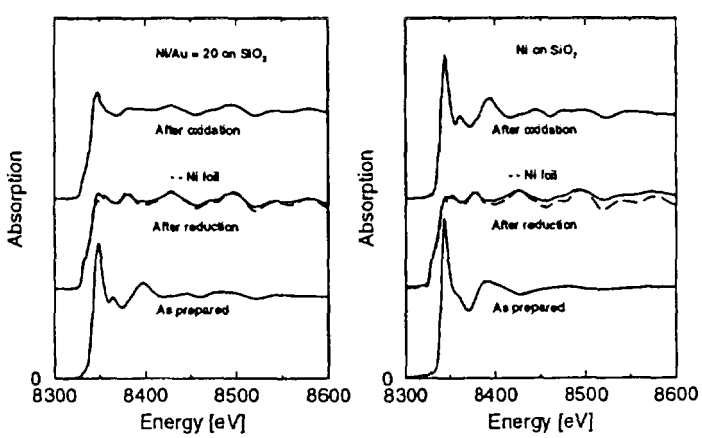


Figure 1: *Normalized EXAFS spectra at the Ni K-edge, before reduction, after reduction and after exposing to an oxygen flow.*

# Alloying in Cu/Pd nano-particle catalysts

A.M. Molenbroek, G. Steffensen*, J. Hyldtoft*, B.S. Clausen* and J.K. Nørskov
*Center for Atomic-scale Materials Physics and Physics Department, Technical University of Denmark, DK-2800 Lyngby, Denmark*
** Haldor Topsøe Research Laboratories, DK-2800 Lyngby, Denmark*

Bimetallic catalysts have long been of interest in heterogeneous catalysis. In this work we characterize the alloying and segregation behaviour in bimetallic Cu/Pd supported catalysts by means of EXAFS. Cu/Pd binary alloy nano-catalysts were prepared with several different atomic ratios of the constituents. A number of different synthesis methods and supports were used to prepare the supported alloys: surfactant stabilized colloid synthesis, coimpregnation, coprecipitation and atomic layer epitaxy.

The structure of the catalysts was determined by means of transmission EXAFS, carried out at the BW1 and RÖMO II beamlines at HASYLAB at DESY and at beamline BL18 at the ESRF. The sample was loaded in an *in situ* cell which allowed for heating in different gas flows. The EXAFS signals were extracted from the absorption spectra using standard background subtraction and normalization. After spline subtraction, the EXAFS spectra were Fourier transformed and the first shell shell backtransformed spectra at the Pd K-edge and the Cu K-edge are shown in figure 1 for a reduced Cu/Pd=1:1 supported catalyst. The Cu/Pd samples were reduced up to 230°C in pure hydrogen. The sample was synthesized by coimpregnation of a silica support with $Cu(acac)_2$ and $Pd(acac)_2$. The data are fitted with amplitude and phase functions obtained experimentally from Pd and Cu foils. It is clearly seen that fitting the data to a single metal does not describe the data, whereas a fit to a combination of Pd and Cu results in a good fit at both edges. This gives good evidence for the formation of a CuPd alloy.

**Acknowledgments**
This work has been financed by the Danish Natural Science Research Council.
The Center for Atomic-scale Materials Physics is sponsored by the Danish National Research Foundation.

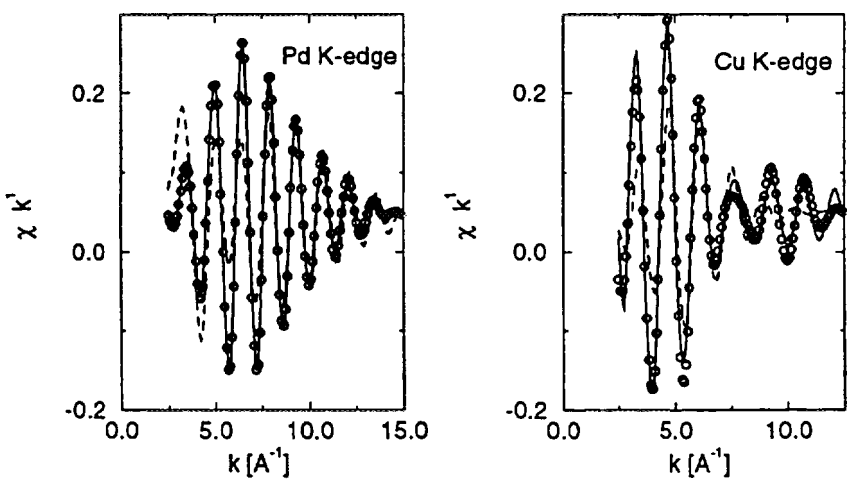


Figure 1: *First shell backtransformed EXAFS spectra obtained from the Pd K-edge (left) and the Cu K-edge (right) of a Cu/Pd supported catalyst after reduction in hydrogen. The data is shown by the circles. The dashed curves are best fits to the data using only a Pd resp. Cu amplitude and phase functions. The solid curves show best fits using a linear combination of Pd and Cu functions.*

# X-RAY DIFFRACTION ON PARCHMENT FIBRES

Kurt Nielsen & Kenny Ståhl
Department of Chemistry, Technical University of Denmark

Manuscript of parchment may be recognized among the most valuable objects of the European cutural heritage. Parchment is the bearer of some of the most essential parts of early written history, which today still constitutes the foundation, in terms of ideas, religion and policy, on which the modern European society is based. Parchment consists of the hide protein matrix composed by collagen molecules, small amounts of other organic and inorganic compounds and moisture. This complex matrix constitutes the very sensitive and unstable carrier of text and illustrations.

The deterioration of parchment has not, until now, been subject to systematic and detailed studies, and the present project is an attempt to use X-ray diffraction for obtaining information on the state of deterioration of the collagen molecule in parchment. The collagen molecule consists mainly of three peptide chains arranged as a triple helix, which are bundled into fibres. These helical structures give rise to a distinct X-ray diffraction pattern. On decay the helical structure is partly destroyed, and this leads to a change in the X-ray diffraction pattern. The major advantage of using synchrotron X-ray sources in this examination relates to the very high intensity. Because of this the sample size is small - one single fiber is sufficient. This is of particular importance, when the samples originate from rare historical documents such as the Dead Sea Scrolls.

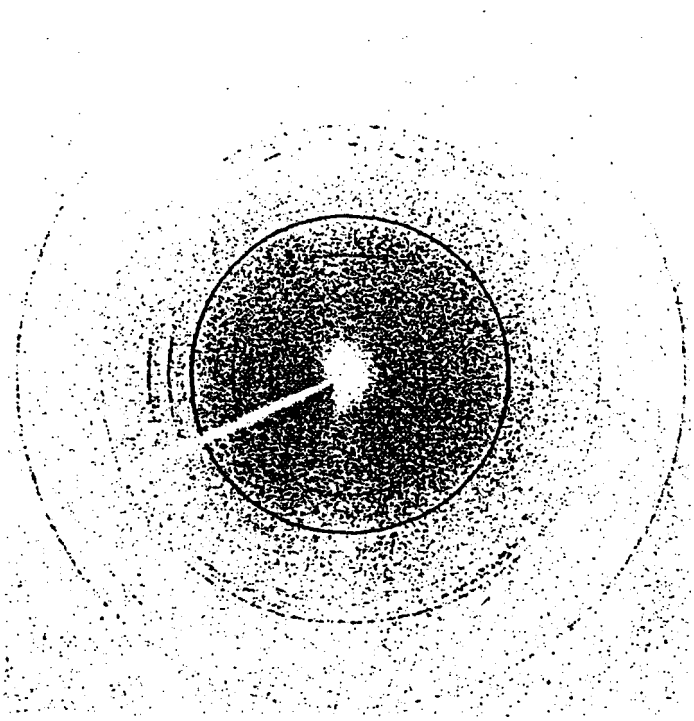

X-ray diffractogram of new parchment.
The circles originate from calcium carbonate.

# IN-SITU TIME RESOLVED SYNCHROTRON POWDER DIFFRACTION STUDIES OF THE AKAGANEITE - HEMATITE REACTION

Kenny Ståhl & Kurt Nielsen, Department of Chemistry, Technical University of Denmark

Akaganeite, $FeO_{1-x}(OH)_{1+x}Cl_x yH_2O$, is a commonly encountered corrosion product of iron. The compound is only formed, and is only stable in the presence of chloride ions. The chloride ions are, together with water molecules, enclosed in channels in the akaganeite structure, and may be liberated by washing, ion exchange or heating. In absence of chloride ions, iron may be stabilized to prevent further corrosion, but in presence of akaganeite, the loosely bound chloride ions may slowly be released, e.g. as hydrochloric acid. When heated to temperatures as low as 150°C, akaganeite liberates hydrochloric acid and the transformation to hematite, $Fe_2O_3$ starts to take place. In order to obtain information on the mechanism of hydrochloric acid release and a better understanding of the corrosion processes, time resolved studies have been carried out in the temperature range 150-250°C, covering the whole transformation region.

The X-ray examinations are accompanied by thermogravimetric and differential thermal analyses and Mössbauer spectroscopy.

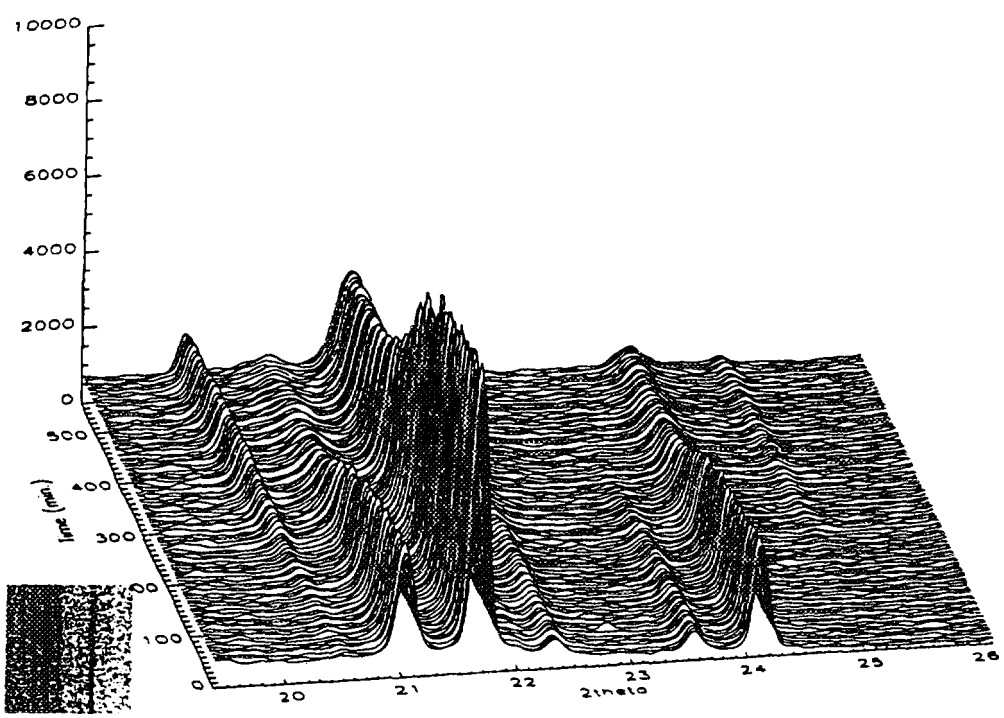


The change of the akaganeite powder pattern as a function of time and temperature.

**Studies of phase transitions. Molecular reorientations in tetraalkylammonium tetrafluoroborates.**

Finn Krebs Larsen,[a] Jesper Bager,[a] Thomas M. Schultz,[b] Poul Norby,[c] and Alex Darovsky.[d]

[a] Department of Chemistry, University of Aarhus, Denmark.
[b] Department of Sol.id State Physics, Risø National Laboratory, Denmark.
[c] Department of Chemistry, Brookhaven National Laboratory, New York, U.S.A.
[d] National Synchrotron Light Source, Brookhaven National Laboratory, New York, U.S.A.

Tetraalkylammonium tetrafluoroborates, $R_4N{\cdot}BF_4$, R = $CH_3$, $C_2H_5$, n = $C_3H_7$ and n = $C_4H_9$ are commonly used in electrochemistry as supporting electrolytes in aqueous and non aqueous solutions. In the solid state these compounds are built from cations and anions of tetrahedral symmetry, and thus they are representative for a substantial group of compounds known to possess rich pattern of phase transitions taken as function of temperature. The project aims at describing and explaining mechanisms for some of the presumably typical phase transitions of these compounds. So far we have carried out detailed single crystal data collections of $(CH_3)_4N{\cdot}BF_4$, also called TMT, using a scintillation detector and conventional MoKα radiation at 298, 160 and 9 K. Furthermore, complete data sets have been collected using imaging plate technique and synchrotron X-radiation with the sample crystal at 298, 240, 155, 145 and 15 K.

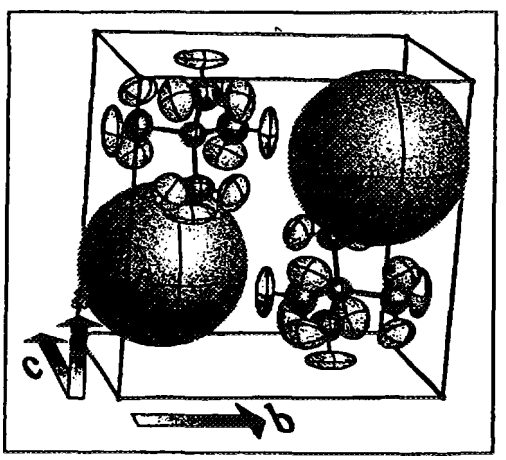


The tetragonal unit cell of TMT at 298 K, showing the ordered tetramethylammonium ions and the disordered tetrafluoroborate ions.

Analysis of the data shows that the $(CH_3)_4N^+$ ions sit ordered throughout this temperature range. Phase transitions are due to the $BF_4^-$ ions reorienting. At 298 K the symmetry of the structure is tetragonal, and the $BF_4^-$ ions can be described as randomly oriented over 16 orientations. By lowering the temperature to 160 K the number of orientations are halved. The eight orientations of lowest energy are frozen out. At 158 K a proper phase transition takes place, and the structure changes symmetry to probably monoclinic, and the unit cell volume doubles. Crystals hereby usually break up in twin components. It proved necessary to have well collimated synchrotron radiation and an area detector diffractometer at disposal for discerning the different components. The area detector data are also being explored to assess the intensity of the diffuse scattering in order to calculate the order parameter of the 158 K phase transition.

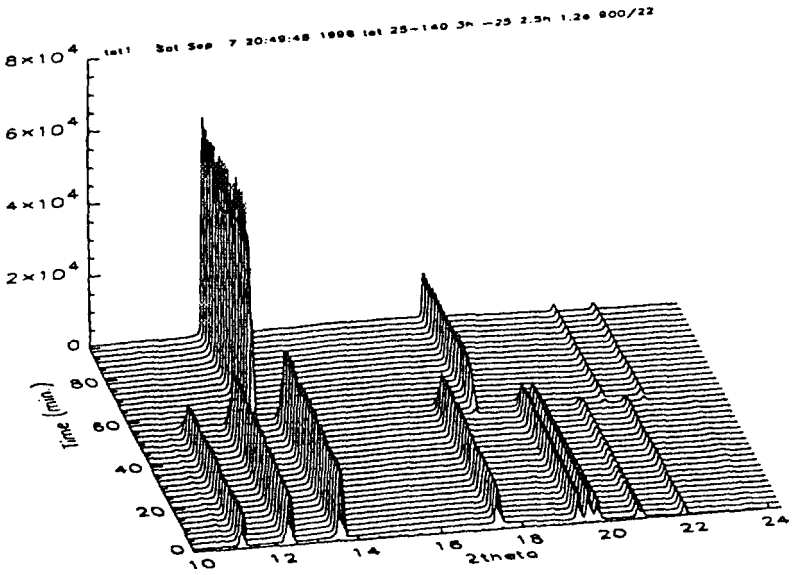


Powder diffraction studies of the row of tetralakylammonium tetrafluoroborates have been carried out at a range of temperatures to give a first survey of their phase transitions. The figure shows the high temperature phase transformation of tetraethylammonium tetrafluoroborate. The room temperature structure is monoclinic. The high temperature phase can be indexed as cubic.

NSLS, BNL, New York

| Beam line | # shifts | Week # | Dates |
|---|---|---|---|
| X3A1 | 30 | 34-35 | 21.8.-31.8. |
| X7B | 12 | 36 | 5.9.-8.9. |

**Studies of electron density distributions.**

Finn Krebs Larsen,[a] Claire Wilson,[a] Georg Madsen,[a] Bo Brummerstedt Iversen,[b] Tom Koetzle,[c] and Åke Kvick.[d]

[a] Department of Chemistry, University of Aarhus, Denmark.
[b] Department of Chemistry, University of California at Santa Barbara, U.S.A.
[c] Department of Chemistry, Brookhaven National Laboratory, New York, U.S.A.
[d] European Synchrotron Radiation Facility, Grenoble, France.

Much detailed information about ground state properties of molecules and crystals can be deduced from knowledge of their electron density distribution (EDD). Charge distribution, electric moments and electrostatic potentials can be calculated and f.inst. also in some approximation the d-orbital population in transition metal complexes. Topological analysis of the total EDD can give valuable insight in the chemical bonding and intermolecular interactions in crystals. Topological analysis is a promising tool for predicting chemical reactivity and for explaining reaction mechanisms.

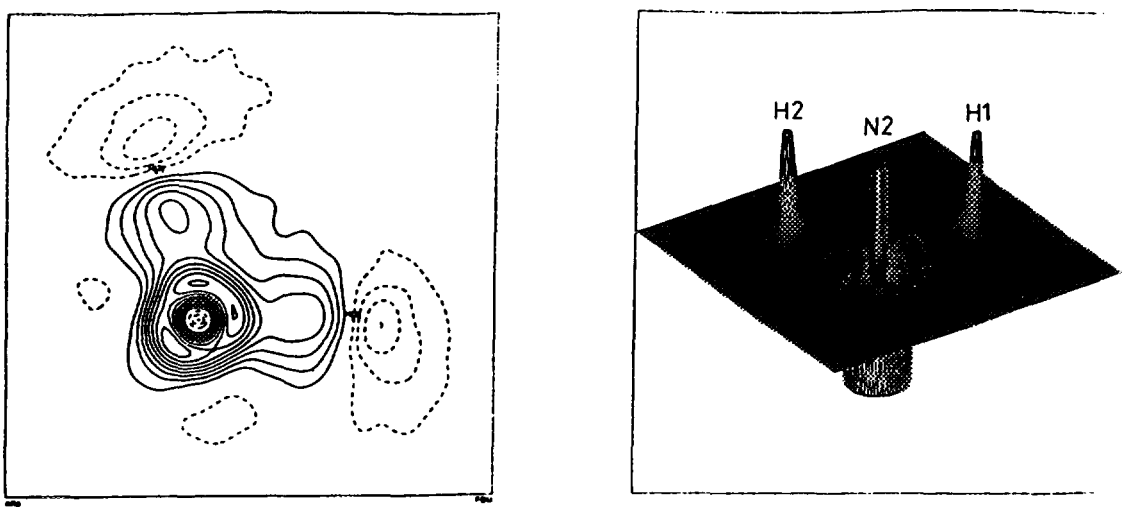


X-N study of the electron density distribution in trans-tetraammune dinitronickel(II) at 9 K. Deformation density in the $NH_2$ plane of $Ni(ND_3)_4(NO_2)_2$ is shown to the left. Contour interval 0.1 e/Å$^3$ and plot of $-\nabla^2\rho$ in the $NH_2$ plane is shown to the right.

Experimental determination of accurate, detailed EDD demands extensive, complete and accurate diffraction data set preferably measured at extremely low and stable temperature. This can be achieved for structures containing only light atoms when a conventional X-ray source is used for data collection. And for reason of intensity statistics relatively big single crystals (up to 0.5 mm diameter) must be used in this case, which usually means that low order strong reflections suffer from substantial absorption and extinction effects. Corrections are often difficult to calculate and are usually inaccurate for compounds containing atoms heavier than 1. row transition metals.

The high intensity available at synchrotrons makes it possible to use small crystals (< 0.1 mm diameter) for diffraction experiments. Absorption and extinction effects are highly reduced, especially when using very short (~ 2 Å) wave length radiation, which opens the possibility for the determination of the EDD of compounds containing heavy atoms. We have undertaken experiments of collecting and analysing complete sets of diffraction data using high-energy synchrotron radiation and area detector technique.
Presently we are working on three projects:
1. The critical point network of metallic Mg.
2. The EDD of $MoO(O_2)(HMPA)$ (dipic) at 15 k.
3. The EDD of $ReH_5(PPh_3)_3$ at 15 K.
As a first example of the promising advances we mention that for the rhenium hydride compound hydrogen atoms sitting next to the heavy rhenium atom were located unequivocally and accurately.

1. Iversen, B.B., Larsen, F.K., Figgis, B.N. and Reynolds, P.A. J.A.C.S. In press.

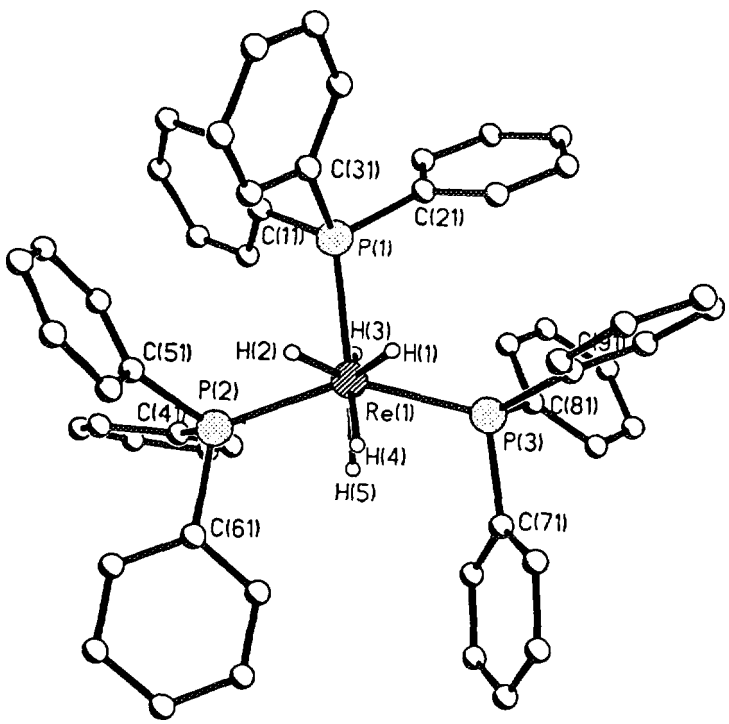


The atomic structure of $ReH_5(PPh_3)_3$.

ESRF, Grenoble

| Beam line | # shifts | # weeks | Dates |
|---|---|---|---|
| ID11-BL2 | 12 | 16 | 17.4.-21.4. |

NSLS, BNL, New York

| Beam line | # shifts | Week # | Dates |
|---|---|---|---|
| X3A1 | 27 | 42-43 | 17.10.-26.10. |

**Project title: On-line hydrothermal synthesis. In-situ powder diffraction studies of zeolite formation, chemical reactions and ion exchange.**

Axel Nørlund Christensen,[a] Poul Norby,[b] and Jon Hanson.[b]

a) Department of Inorganic Chemistry, Aarhus University, DK-8000 Aarhus C, Denmark.
b) Chemistry Department, Brookhaven National Laboratory Upton, New York 11973, U.S.A.

Zeolites and molecular sieves have framework structures with large holes and pores in which ions, water and organic molecules can be allocated. The molecular sieves have catalytic properties as molecules may react with each other in the pores of the framework structures. Aluminophosphate based molecular sieves are made at hydrothermal conditions from amorphous aluminophosphate gels containing organic molecules which size and shape direct the size and shape of the pore in the framework structures. In substitution of $Al^{3+}$ with $Me^{2+}$ ions in the framework greater acidity and stronger catalytic activity of the compounds are achieved.

Several papers have been published on the synthesis of aluminophosphate based molecular sieves, but little was known about the rate of formation in the hydrothermal reactions. In the present invesgigation[1] in-situ X-ray synchrotron powder diffraction has been used to follow the crystallization of the molecular sieves. It was possible to determine the formation of precursor phases and the rate of formation of different forms of the molecular sieves in dependence of temperature of reaction and concentrations of amorphous aluminiumphosphate and of the organic molecules in the reaction mixtures. The information obtained can be used to optimize the experimental conditions used in synthesis of the molecular sieves.

**References**

1. Christensen, A.N., Norby, P. and Hanson, J. Acta Chem. Scand. (submitted).

NSLS, BNL

| Beam line | # shifts | Week # | Dates |
|---|---|---|---|
| X7B | 21 | 7-8 | |

**Project title: Templates and metal cations in microporous materials. Crystal structure and time resolved in-situ studies of crystallization.**

Axel Nørlund Christensen[a] and Helmer Fjellvåg.[b]

a) Department of Inorganic Chemistry, Aarhus University, DK-8000 Aarhus C, Denmark.
b) Chemistry Department, University of Oslo, N-0315 Oslo 3, Norway.

Zeolite N is a synthetic molecular sieve with the composition $K_{12}Al_{10}Si_{10}O_{40}Cl_2.8H_2O$. It has a framework structure related to the zeolite mineral edingtonite and is obtained in hydrothermal synthesis as a fine powder. Details of the crystal structure can thus only be studied by the use of powder diffraction data.

A structure investigation of zeolite N by Baerlocher and Barrer[1] showed that zeolite N had the edintonite framework. However, it remained to be shown if the framework had an ordered arrangement of $AlO_4$ and $SiO_4$ tetrahedra, and the positions of the non-framework atoms, $K^+$, $Cl^-$ and the $H_2O$ molecules were not known in details.

These crystal structure problems were presently attached by means of high resolution synchrotron powder diffraction data. The results indicate an ordered arrangement of the $AlO_4$ and $SiO_4$ teteahedra in the structure with the distances Al-O 170.4-175.7 pm and Si-O 158.4-164.0 pm. The potassium chloride is arranged in deformed $ClK_6$ octahedra and the water molecules are arranged in two sites in the cavities of the framework. A manuscript describing the present investigation is submitted for publication.[2]

References

1. Baerlocher, C. and Barrer, R.M.
Z. Kristallogr. 140 (1974) 10
2. Christensen, A.N. and Fjellvåg, H.
Acta Chem. Scand. (submitted).

ESRF

| Beam line | # shifts | Week # | Dates |
|---|---|---|---|
| BM1 | 6 | 14 | |

**Project title: Triclinic type F structure of $Sm_2Si_2O_7$ and $Eu_2Si_2O_7$; geometry of the $Si_2O_7^{6-}$ ion in $La_2Si_2O_7$ at high pressure.**

## Part A: Investigation of the structure of $Sm_2Si_2O_7$.

Axel Nørlund Christensen,[a] Marie-Agnès Chevallier,[a] Anette Frost Jensen,[b] and Eric Dooryhee.[c]

a) Department of Inorganic Chemistry, Aarhus University, DK-8000 Aarhus C, Denmark.
b) Chemistry Laboratory IV, H.C. Ørsted Institute, Universitetsparken 5, DK-2100 Copenhagen Ø, Denmark.
c) ESRF, B.P. 220, F-38042 Grenoble Cedex, France.

The rare earth disilicates $RE_2Si_2O_7$ can exist in seven different crystalline phases of which four are high temperature phases. $Sm_2Si_2O_7$ exists in a low temperature phase, structure type A, and in a high temperature phase, structure type F, of which only the unit cell and space group are known. The goal of the present investigation was to obtain more information about the structure type F.

Synchrotron X-ray powder patterns were recorded with the wave length $\lambda$ = 0.4276 Å of samples of $Sm_2Si_2O_7$ and $Gd_2Si_2O_7$. The pattern of $Gd_2Si_2O_7$ was used as a test case for the structure analysis, as the structure of the compound is known.[1] The structure analysis showed acceptable agreement between the refined and published model but larger standard deviation of the refined positional parameters. The pattern of $Sm_2Si_2O_7$ was used in attempts to determine the structure of the phase F. Only the positions of the Sm and Si atoms could be located. The structure of $Sm_2Si_2O_7$ has later been determined in a single crystal X-ray analysis.

A manuscript describing the present investigation is in preparation.[2]

### References

1. Smolin, Yu.I. and Sepelen, Yu.F.
Acta Crystallogr. B26 (1970) 484.
2. Christensen, A.N., Jensen, A.F., Themsen, B.K., Hazell, R.G., Hanfland, M., and Dooryhee, E.
Manuscript in preparation.

ESRF

| Beam line | # shifts | Week # | Dates |
|---|---|---|---|
| BM15 | 6 | 21 | |

**Project title: Triclinic type F structure of $Sm_2Si_2O_7$ and $Eu_2Si_2O_7$; geometry of the $Si_2O_7^{6-}$ ion in $La_2Si_2O_7$ at high pressure.**

**Part B: Investigation of the structure of $La_2Si_2O_7$ at pressures up to 212 kbar.**

Axel Nørlund Christensen,[a] Brian Themsen,[a] Anette Frost Jensen,[b] and Michael Hanfland.[c]

a) Department of Inorganic Chemistry, Aarhus University, DK-8000 Aarhus C, Denmark.
b) Chemistry Laboratory IV, H.C. Ørsted Institute, Universitetsparken 5, DK-2100 Copenhagen Ø, Denmark.
c) ESRF, B.P. 220, F-38042 Grenoble Cedex, France.

The rare earth disilicates $RE_2Si_2O_7$ can exist in seven different crystalline phases of which four are high temperature phases. $La_2Si_2O_7$ exists in a low temperature phase, structure type A, and in a high temperature phase, structure type G. The present investigation concerns possible phase transitions of $La_2Si_2O_7$, structure type G, at 300 K and at pressures up to 212 kbar.

Two sets of experiments were performed with a diamond cell and an X-ray wave length $\lambda$ = 0.4664 Å. The powder patterns obtained in the investigated pressure range were used to follow the changes in the structure with increased pressure. The Si-Si distance in the $Si_2O_7^{6-}$ ion shows a significant decrease with pressure. With applied pressures at and over 166 kbar significant changes in the powder patterns were observed, and the sample becomes partly amorphous.

ESRF

| Beam line | # shifts | Week # | Dates |
|---|---|---|---|
| Bm3/ID9 | 6 | 44 | |

# Student Training Course at Diffractometer D4

J. Als-Nielsen and K. Joensen
Niels Bohr Institute, Copenhagen University, Denmark

Eight undergraduate students (6 in Physics, 1 in Biophysics, 1 in Chemistry) from Niels Bohr Institute in Copenhagen have spent one week in December at the bending magnet beamline D4 for an elementary training course in synchrotron radiation research. This concludes a one semester course in experimental X-ray physics given at the institute by us, partly as practical excercises in the rotating anode laboratory, partly as theoretical background lectures.

In HASYLAB experiments were carried out both in the white beam, in a beam reflected form a Au coated mirror, and in a monochromatic beam. In the white beam the natural opening angle of synchrotron radiation was determined by green paper exposures and the power density was determined by a calorimeter. The absolute flux and the energy spectrum in the beam reflected from the mirror was measured by $90^{o}$ vertical Compton scattering from a gas into a well defined aperture . The $90^{o}$ Compton scattering gas cell could be turned around the beam axis, so also the linear polarization of the radiation was verified. The monochromatic beam produced by symmetric Bragg reflection from a Si(111) crystal was energy calibrated using the K-edge fluorescence from a Cu foil and the fluorescent ESAFS wiggles were also observed. For comparison also the the fluorescence yield from Krypton gas at and above the K-edge was measured and the lack of EXAFS wiggles in the gas phase noted. The reflectivity, the Darwin width and the crystal truncation rod scattering from crystals used as samples were determined, for symmetric Si(111) in Bragg reflection, for Ge(111) at different energies around the Ge K-edge, and for Si(111) with an $8.8^{o}$ asymmetric cut surface at a number of Bragg angles both with the surface approaching the incident and scattered beam directions. Anomalous scattering from a GaAs(100) crystal at energies near the Ga and As K-edges were observed.

During the week the students, divided into a four-student+tutor day-shift and a four-student + tutor night shift, gained "hands-on" experience in the safety procedures, the line-up procedures and in the necessesary communication within the team to carry out a joint programme.

Financial support was provided by DANSYNC and the European Community Human Capital and Mobility Programme under contract no. ERBFMACCT 940002

## Bismuth-induced restructuring of the GaSb(110) surface

*van Gemmeren, T., Lottermoser, L., Falkenberg, G., Seehofer, L., and Johnson, R.L., II. Institut für Experimentalphysik, Universität Hamburg, Luruper Chaussee 149, D-22761 Hamburg, Germany, Gavioli, L., and Mariani, C., Dipartimento di Fisica, Universita di Modena, via G. Campi 213/A, I-41100 Modena, Italy, Feidenhans'l, R.., Landemark, E., Smilgies, D.-M., and Nielsen, M., Riso National Laboratory, DK-4000 Roskilde, Denmark*

Metal-semiconductor interfaces are of considerable interest for both fundamental and technological reasons. Most vapor-deposited metals react with III-V semiconductors to form complex, nonstoichiometric interfaces, however, it is generally believed that the semimetals Sb and Bi form nonreactive, ordered interfaces. Column-V metals on III-V semiconductors are frequently regarded as examples of ideal adsorbate-semiconductor heterojunctions. We present a new structural model which shows that this simple picture is generally not true and that column V elements can induce significant restructuring of the substrate.

The structure of the GaSb(110)(1×2)-Bi reconstruction was determined using surface x-ray diffraction, scanning tunneling microscopy and photoelectron spectroscopy. The x-ray diffraction experiments were performed at the wiggler BW2 beamline in HASYLAB. The ideal GaSb(110) surface is terminated with zigzag chains of anions and cations running in the [1 $\bar{1}$ 0] direction. In the Bi induced (1×2) reconstruction we find that every second zigzag chain in the uppermost substrate layer is missing. The surface is terminated by a full monolayer of Bi atoms which also form zigzag chains. The Bi atoms in the chains are alternately bonded to the first and second layer substrate atoms and the Bi chains are tilted 34.2° with respect to the (110) plane. We propose that the formation of the reconstruction is driven by the very favorable bonding geometry in the adsorbate chains.

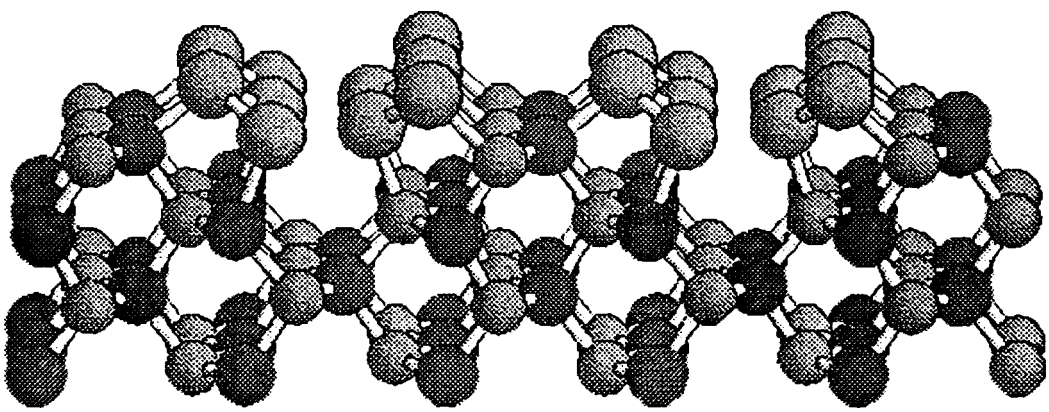

Fig. 1. The Bi induced 1x2 structure of the GaSb(110) surface. Bi atoms are shown as large light grey balls. Ga atoms as small light grey balls and Sb atoms as small dark grey balls.

## Surface X-ray Diffraction Study of the √3x√3 R 30° Structure of Sb on Cu(111)

J.M. Gay, G. Le Lay, *CRMC2, France,* R. Feidenhans'l, F.B. Rasmussen, J. Baker, T. Schultz, M. Nielsen, *Department of Solid State Physics, Risø National Laboratory, Denmark,* O. Bunk, G. Falkenberg, L. Seehofer, R.L. Johnson, *II. Institute for Experimental Physics, University of Hamburg, Germany*

Antimony is known to have a surfactant effect in epitaxial growth on both semiconductor and metal films. This property is closely related to its strong tendency to superficial segregation. The growth of Sb on Cu(111) has been recently studied by Auger Electron Spectroscopy (AES), Low Energy Electron Diffraction (LEED) and Photo Electron Spectroscopy (PES).

The dissolution kinetics at 400°C of 1 ML of Sb deposited on Cu(111) stops at a steady state with a √3x√3 R 30° structure. On the other hand, the segregation kinetics of Sb on the surface of a Cu(Sb)(111) solid solution (0.45 at%) gives similarly rise to the √3x√3 R 30° superstructure, as shown by LEED studies. The microscopic mechanisms of dissolution and segregation of Sb are still unclear. PES experiments have shown different binding states in the Sb monolayer deposited at room temperature and in the annealed layer. More precisely, two chemical states are observed after annealing when the √3x√3 R 30° structure appears. The purpose of the surface x-ray diffraction study was to investigate in detail the atomic structure of the Sb √3x√3 R 30° structure after annealing of a monolayer deposited at room temperature.

Integer and fractional order in-plane reflections have been measured, as well as rods. The analysis of the experimental data is in progress.

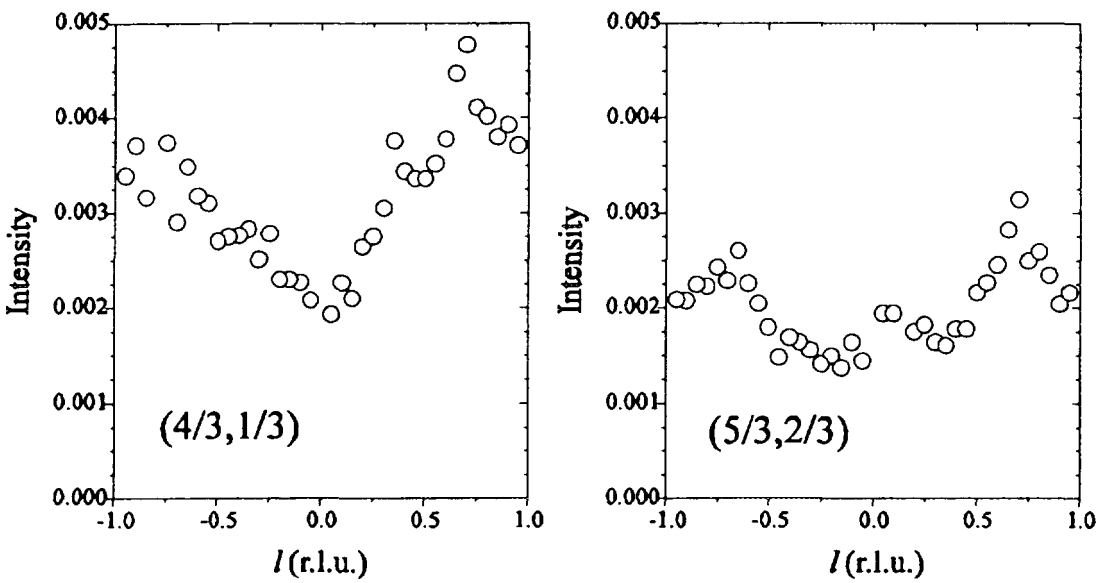


Fig. 1. Fractional order rods scan of the (4/3,1/3) and (5/3,2/3) reflections.

## Surface X-Ray Diffraction Studies of the Rb induced Ge(111)3x1 Structure

E. Landemark, M. Nielsen, R. Feidenhansl, *Department of Solid State Physics, Riso National Laboratory, Denmark,* L. Lottermoser, O. Bunk, L. Seehofer, G. Falkenberg, R.L. Johnson, *II. Institut für Experimentalphysik, Universität Hamburg, Germany*

There is currently a large interest for the metal induced 3x1 reconstructions of the Si(111) surface. Similar 3x1 reconstructions are induced by sub monolayer coverages of different adsorbates, such as Li, Na, K and Ag. Despite an extensive amount of studies presented during the last years, the atomic structure of these surfaces is still controversial. While the adsorbate coverage now generally is believed to be ~1/3 monolayer, the number of Si atoms per unit cell participating in the reconstruction is unknown and vary between 2 and 6 in recently proposed models.[1,2] Previously, we have studied the Si(111)3x1 Li, Na and Ag surfaces by XRD. In order to obtain more information of the 3x1 systems, we have now extended our studies to include the 3x1 reconstruction induced by Rb adsorption on the Ge(111) surface.

The contour maps of the 2D Patterson functions show similar interatomic vectors for the three Si surfaces (Fig. 1.). The variation in height of corresponding peaks can be explained by different Z values for the involved atoms and is an indication of ordered positions for the metal atoms. The Patterson function for the Ge(111) surface is more unlike. This might indicate a different surface structure but it might also be explained by the difference in Z and scattering factor between the two substrates.

The data analysis of the out of plane, rod scan, data sets is still in progress. We have not been able to reproduce the data by calculating the diffracted intensity from earlier proposed models. Instead we have found better agreement with a new model, consisting of four substrate atoms building up a "double zig-zag chain" structure. We are presently testing out our new data analyzes program that also includes minimization of the Keating energy. The idea is to use the Si/Li data, where the metal scattering can be neglected, to find the positions of the substrate atoms. The next step is then to find the positions of the metal atoms and completely determine the atomic structure for the four surfaces.

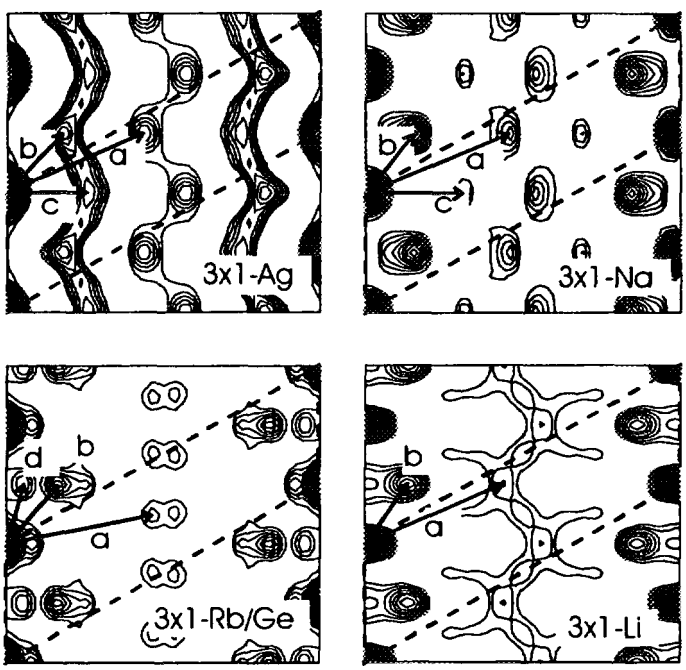


Fig. 1. Contour maps of the experimental Patterson functions for the Si(111)3x1-Ag, Si(111)3x1-Na, Ge(111)3x1-Rb and Si(111)3x1-Li surfaces.

[1] H.H. Weitering, N.J. DiNardo, R. Péres-Sandoz, J. Chen and E.J. Mele, Phys. Rev. B 49, 16837 (1994)
[2] Steven C. Erwin, Phys. Rev. Lett. 75, 1973 (1995)

## Surface X-Ray Diffraction Study of Ge(103) (1x1)-In

O. Bunk, J. Zeysing, L. Seehofer, G. Falkenberg, R.L. Johnson II. *Institut für Experimentalphysik, Universität Hamburg, Germany*, M. Nielsen, R. Feidenhans'l, *Department of Solid State Physics, Risø National Laboratory, Denmark*

The self-organisation of atoms on surfaces is of fundamental importance and has great potential as a method for producing highly regular three-dimensional nanoscale structures. We have found that very uniform clusters, similar in shape to the well-known "hut-clusters" produced by Ge deposition on Si(001), are formed after annealing an indium-covered Ge(001) surface.[1] The clusters are bounded by In-terminated {103} facets. A knowledge of the exact positions of the In and Ge atoms in the clusters would allow the strain relief in the cluster to be determined, which would provide insight into the fundamental mechanism driving the formation of the nanostructures. When In is deposited on a Ge(103) surface a stable (1x1) reconstruction with large domains[2] is formed. This surface is therefore a good starting point for determining the surface crystallography of the (103) facets. The sample was prepared at the photoemission system FLIPPER II and then transferred in a small portable UHV-chamber with a hemispherical Be window to the surface diffractometer on the wiggler beamline BW2 at HASYLAB in Hamburg. The recorded data consists of 297 measurements along 13 rods and 102 symmetry inequivalent in-plane reflections. A model for the reconstruction is shown in Fig. 1. A key aspect of this model is that the threefold-coordinated In atoms saturate all the surface dangling bonds and thereby minimize the surface free energy.

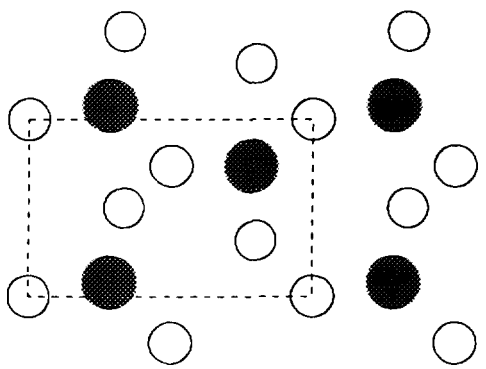

Fig. 1. A model of the Ge(103) (1x1)-In reconstruction. In atoms are represented by filled circles and the Ge atoms by open circles.

[1] M. Nielsen, D. Smilgies, R. Feidenhans'l, E. Landemark, G. Falkenberg, L. Lottermoser, L. Seehofer and R.L. Johnson, Surf. Sci. **430**, 352-354 (1996)

[2] L. Seehofer, G. Falkenberg and R.L. Johnson, Phys. Rev. B in press (1996)

## Surface X-Ray Diffraction Study of Ge(103)-(1x4)

O. Bunk, L. Seehofer, G. Falkenberg, R.L. Johnson *II. Institut für Experimentalphysik, Universität Hamburg, Germany*, M. Nielsen, R. Feidenhans'l, *Department of Solid State Physics, Risø National Laboratories, Denmark*

A new way of deriving a structural model for a complex high-index surface reconstruction has been successfully tested. The basic model for the reconstruction has been developed using a combination of an in-plane dataset with a small rod-scan dataset.[1] All the fractional order rods were calculated from this preliminary model. Using these theoretical calculations we were able to select rods with high intensity and distinctive features for the measurements which avoided wasting time measuring featureless rods.

The sample was prepared at the photoemission system FLIPPER II and then transferred in a portable UHV-chamber to the diffractometer on the wiggler beamline BW2 at HASYLAB in Hamburg. The recorded dataset for the final analysis consists of 237 measurements along 10 rods and 235 symmetry inequivalent in-plane reflections. The Patterson function is shown in Fig. 1a. The most important distance corresponding to the main feature of the reconstruction, a double step, is marked by "1", in Fig. 1. Two rod-scans are shown in Fig. 1b. The main features of these rods can already be explained with the model. Further structural refinements, now in progress, will reveal the exact atomic positions.

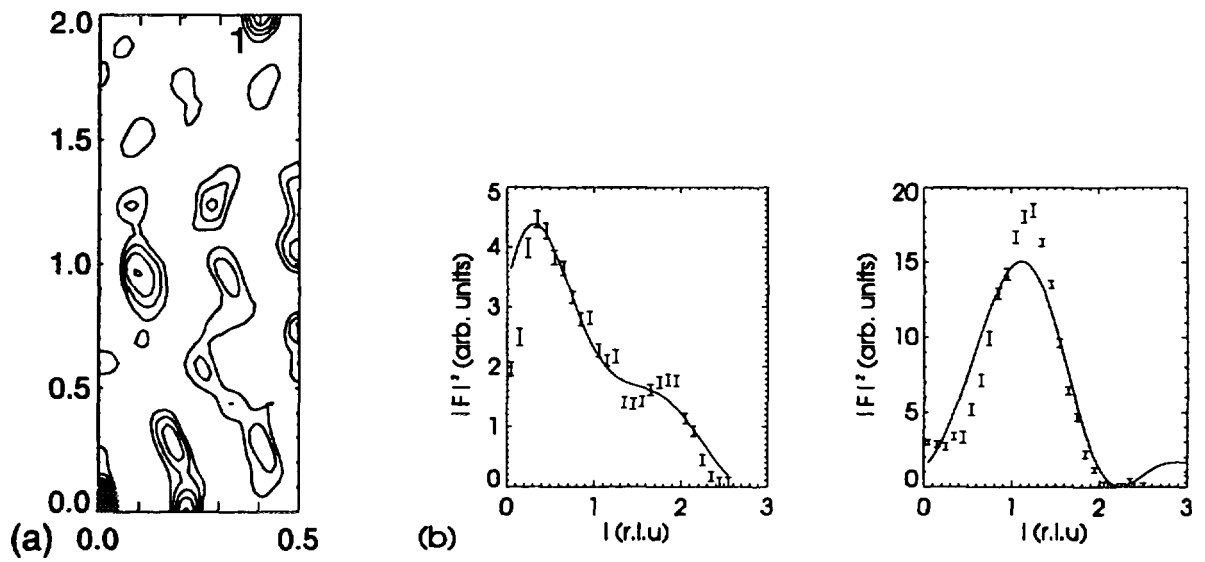


Fig. 1. a) Patterson function of the in-plane projected electron density calculated from the fractional order reflections (The asymmetric unit is shown. b) Rod-scans along (0,-4¼, *l*) and (4,- ½, *l*).

[1] L. Seehofer, O. Bunk, G. Falkenberg, L. Lottermoser, R. Feidenhans'l, E. Landemark, M. Nielsen and R.L. Johnson, submitted to Surf. Sci.

## Surface X-Ray Diffraction Study of Si(001)-(3x4)-In

O. Bunk, L. Seehofer, G. Falkenberg, R. L. Johnson, *II. Institut für Experimental-physik, Universität Hamburg, Germany*, M. Nielsen, R. Feidenhans'l, E. Landemark, *Department of Solid State Physics, Risø National Laboratory, Denmark*

A new structural model for the indium-induced 3x4 reconstruction on Si(001) has been derived from surface X-Ray diffraction measurements. Despite some previous studies on this system[1,2,3] there is still no established model for this surface reconstruction. The sample was prepared in a STM sytem under UHV (base pressure < $4x10^{-11}$ mbar) by the deposition of 0.5 ML In on the clean Si(001) (2x1) surface and annealing at 350°C. It was then transferred under UHV to the diffractometer on the wiggler beamline BW2 at HASYLAB in Hamburg. The recorded dataset consists of 235 symmetry inequivalent in-plane reflections, 133 measurements along six fractional order rods and 42 measurements along one crystal truncation rod. The Patterson function is shown in Fig. 1a. Within the radius of one unit-cell dimension there is no strong peak in the Patterson function. Therefore, In-In dimers are probably not a significant structural element in this reconstruction in contrast to the (2x2) reconstruction[4] and to some of the previously suggested models for the (3x4) reconstruction [3] The main distances (1-3 in Fig. 1.) can be found e.g. in a model which includes parallel rows of In-Si dimers. The basic structural model is shown in Fig. 1b. It includes six In atoms per unit cell, of which four replace Si atoms leaving two additional In atoms. This is in agreement with the STM measurements which revealed of 6±1 In atoms and some displaced Si atoms.

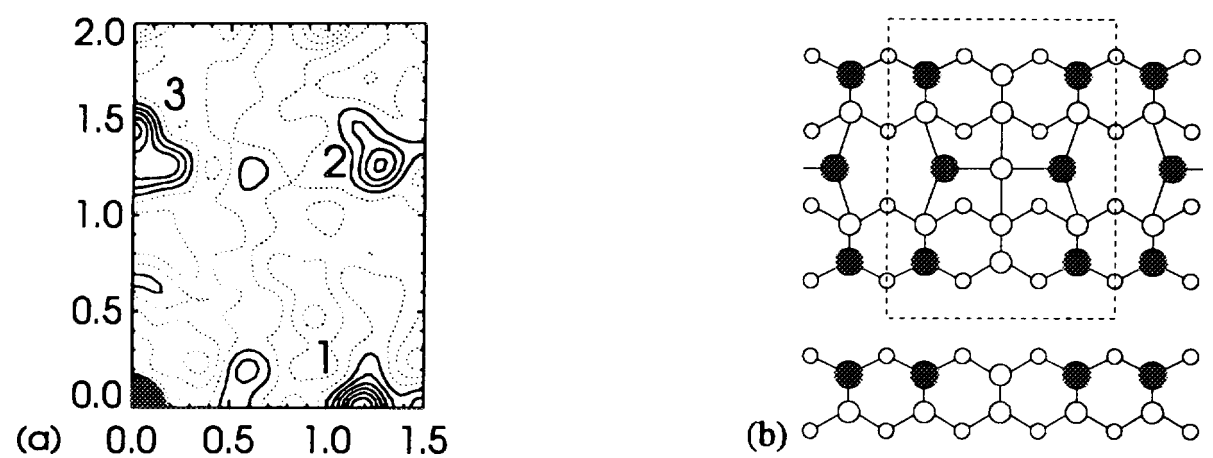


Fig. 1. a) Patterson function of the in-plane projected electron density calculated from the fractional order reflections. (The asymmetric unit is shown; the dotted lines are negative contour.) b) Structural model for the In on Si(001) (3x4) reconstruction with In-Si dimers and six In atoms. (Open circles represent Si atoms and filled circles In atoms.

[1] J. Knall, J.-E. Sundgren, G. V. Hansson and J. E. Green, Surf. Sci. **166** (1986)
[2] A. A. Baski, J. Nogami and C. F. Quate, Phys. Rev. B **43**, 9316 (1991)
[3] B. E. Steele, D. M. Cornelison, Lian Li and I. S. T. Tsong, Nucl. Instr. Meth. B **85**, 414 (1994)
[4] H. Sakama, K. Murakami, K. Nishikata and A. Kawazu, Phys. Rev. B **53**, 1080 (1996)

**Nanoclusters of the CWD Compound $Rb_{0.3}MoO_3$, Blue Bronze, Grown on $SrTiO_3$, Studied by Synchrotron x-ray Diffraction**

A.J. Steinfort, A.B. Smits, P.M.L. O. Scholte, A. Ettema, and F. Tuinstra, *Department of Applied Physics, Delft University of Technology, The Netherlands,* M. Nielsen and J. Baker *Department of Solid State Physics, Risø National Laboratory, Denmark*

Films of the compound $Rb_{0.3}MoO_3$ (blue bronze) are grown and characterized in anticipation of studies of their charge density related electronic behaviour. In these films interesting new mesoscopic phenomena are anticipated.

Blue bronze is grown by laser ablation on a substrate of $SrTiO_3$ (001). AFM and x-ray analysis of layers with an approximate thickness of 300 nm have shown that the film consists of elongated clusters with typical dimensions of 0.5 by 2 micron. The blue bronze is monoclinic with the b*-axis along the long direction of the clusters which in turn are oriented parallel to the principal axis of the substrate. The clusters have their $(\bar{2}01)$ direction parallel to the substrate normal.

X-ray diffraction measurements have been performed on the diffractometer at the BW2 wiggler beam line in HASYLAB, Hamburg, on both thin films of about 1.5 nm to establish the condition for initial growth and on thick films of about 300 nm to analyze epitaxy, facet structure and strain conditions of the clusters. The thin films show island growth with full orientational epitaxy and little or no strain.

For thicker films similar epitaxial behaviour is observed. Furthermore streak shaped satellite reflections are measured as illustrated in the figure below, and they signal a uniform morphology of the clusters. In this interpretation the satellite peaks are truncation rods from the cluster facets and their positions are determined by the slope of the facet surface to the substrate surface. However, analysis of the full data set reveals that final size effects, internal strains and possibly stacking faults are important. The data analysis is in progress.

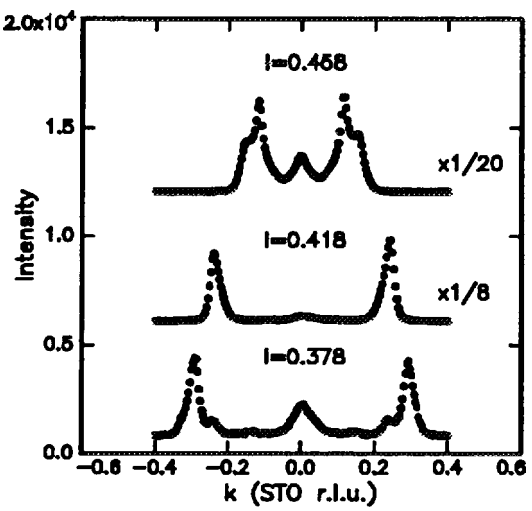


Fig. 1. Measured x-ray scattering profiles around the blue bronze ($\bar{2}01$) reflection perpendicular to the b*-axis at different heights in the reciprocal space above the substrate surface. The side peak positions are determined by the vertical momentum transfer l and they signal planar facets on the clusters. The upper curves are displaced by 600 and 1200 in intensity.

## Cu Films on Ni(100), Internal Faceting and Embedded Clusters Studied by Synchrotron x-ray Diffraction

M. Nielsen, J. Baker, F. B. Rasmussen and R. Feidenhans'l, *Department of Solid State Physics, Risø National Laboratory, Denmark.* R. L. Johnson, G. Falkenberg and L. Seehofer, *II Institut für Experimentalphysik, Universität Hamburg, Germany*

The formation of internal facets and nanoscale Cu-clusters on Ni(100) single crystal surfaces after deposition of Cu thin films were studied by x-ray diffraction. Cu atoms are 2.6 per cent larger than Ni atoms and the first 20 monolayers (ML) of Cu were thought to grow pseudomorphically on Ni(100), with the Cu atoms simply extending the Ni lattice despite the misfit. It was recently discovered[1] using scanning tunneling microscopy that stripes are formed on the surface, where the Cu atoms protrude about 0.6 Å above the level of the surface. The authors concluded that the strain associated with the misfit is partly relaxed by the formation of wedges as illustrated in panel (a) beneath. The atoms inside the wedges are displaced half a lattice spacing in the long direction of the clusters and a little, 0.4-0.6 Å upwards. The buried surfaces of the clusters are (111) facets. This internal faceting model may be quite general in epitaxial crystal growth.

At the wiggler beamline BW2 in HASYLAB, Hamburg, we have studied the wedge-shaped clusters in 9 ML and in 20 ML Cu films by x-ray diffraction. The clusters are regular and monodispersed and give a very distinctive scattering response at the positions of the truncation rods from the facets as illustrated in panels (b) and (c). Due to the half lattice spacing shift of all atoms inside the wedge, these will scatter either in phase or out of phase with the Cu atoms outside, when the proper scans are chosen. The mechanism driving the cluster formation is strain relaxation, and from the diffraction results we can determine the inhomogeneous strain fields both inside and outside the wedges. Panel (c) illustrates the sensitivity of x-ray scattering to the strains. The asymmetry of the profiles arises from the inhomogeneous strain.

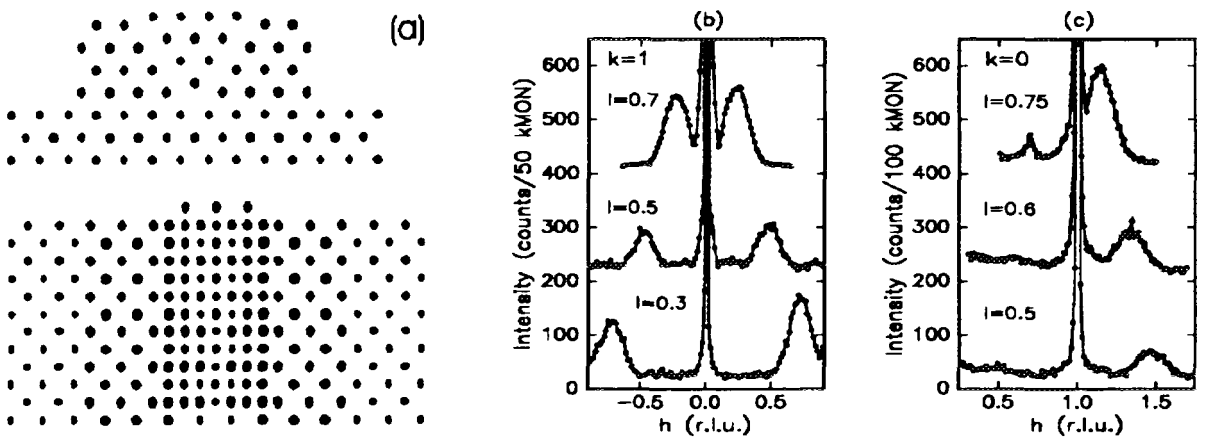


Fig. 1. (a) The wedge-shaped cluster, red atoms, are displaced half a nearest neighbour distance along the wedge axis and about 0.6 Å upwards. The Cu atoms outside the wedge, green atoms, are pseudomorphic with the Ni-substrate, black atoms. (b) "Transverse" x-ray scans. The side-peak scattering is from clusters with the long axis along the k-direction. (c) "Longitudinal" x-ray scans. The side-peak scattering is again from clusters lying along the k-direction. The asymmetry is due to inhomogenous strain.

[1] B. Müller, B. Fischer, L. Nedelmann, A. Fricke and K. Kern, Phys. Rev. Lett. **76**, 2358 (1996)

## X-ray Surface Structure Studies on Organic Crystals of Benzamide

R. Edgar, *Department of Materials and Interfaces, Weissmann Institute, Israel*, R. Feidenhans'l, T. Schultz, *Department of Solid State Physics, Riso National Laboratory, Denmark*, L. Leiserowitz, *Department of Materials and Interfaces, Weissmann Institute, Israel*

Probing the surface structure of organic crystals arises many questions which were addressed to semiconductor and other inorganic surfaces only. The complexity and diversity of organic matter make this new field exciting for both pure and applied studies.

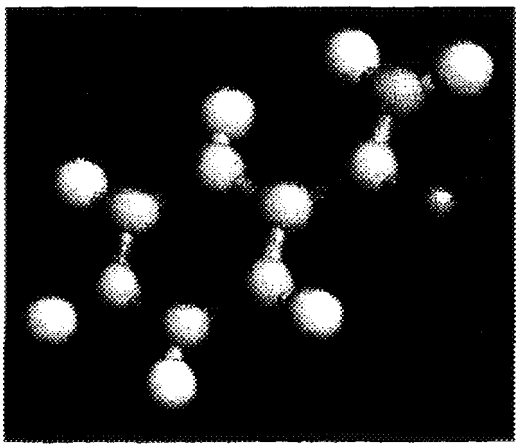

Figure 1: One benzamide molecule, visualized using the Rasmol 2.6 programme

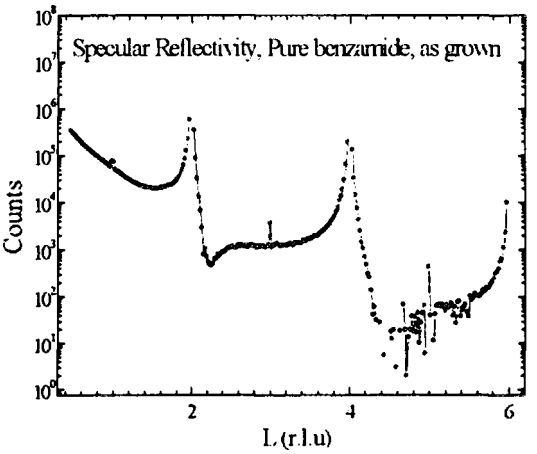


Figure 2: Specular reflectivity curve for pure benzamide, as grown.

Benzamide (see fig. 1) is a simple organic molecule which packs in a triclinic space group $P2_1/c$ with four molecules in the unit cell. Dry single crystals of benzamide, grown from alcoholic solution to yield large (001) surface areas of ca. 12x12 mm and thicknesses of about 5mm, were mounted on the 6 circle surface diffractometer at BW2. The crystals were measured as grown (se specular rod fig.2) or freshly cleaved along the (001) face (see fig. 3). In addition crystals grown from solutions containing acetamide and trifluoroacetamide were measured.

The results presented here are so recent, that no data analysis has been perfomed yet. The data from the surface X-ray scattering experiment are of a very high quality, and therefore we aim to determine and refine the suface structure of benzamide, and thereby gaining knowlegde on the differences between the bulk and surface structure. If we succed in that, it will be the first time the surface structure of a organic crystal has been determined and refined.

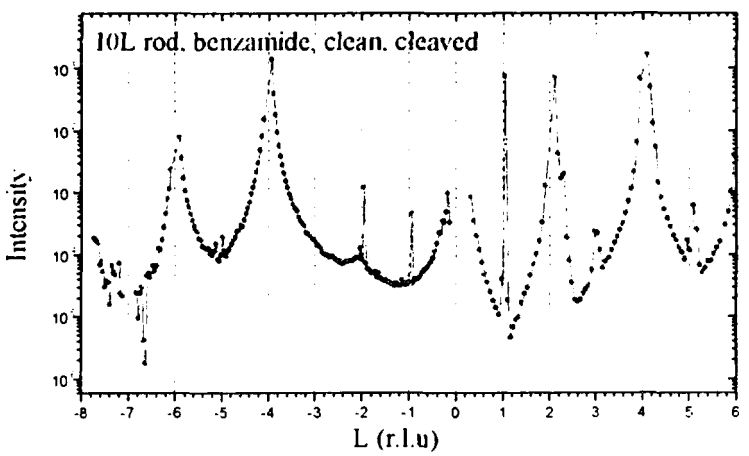


Figure 3: 10*l* crystal truncation rod from pure, cleaved benzamide.

## Surface X-Ray Diffraction at the n-GaAs(001)/Electrolyte Interface

G. Scherb, A. Kazimirov, J. Zegenhagen, *MPI-FKF Stuttgart, Germany*, T. Schultz, R. Feidenhans'l, *Risø National Laboratory, Denmark*, D.M. Kolb, *University of Ulm, Germany*

In-situ surface x-ray diffraction (SXD) has shown to be a powerful method for getting atomic scale structural information from the metal/electrolyte interface. We have extended the application of this technique to the challenging field of semiconductor/ electrolyte interfaces, and the first system under study is n-GaAs(001) in acidic aquous electrolytes ($H_2SO_4$, HCl). The experiments were performed at beamline BW2 at HASYLAB, Hamburg, using a thin layer electrochemical cell equipped with a 6 μ mylar window and working in the classical three-electrode configuration.

Whereas in-plane scattering yields details about the atomic arrangement in the interfacial plane, information on surface roughness, facetting and also on the electron density at the electrolyte side of the interface can be derived from the intensity distribution along the crystal truncation rods (CTR). Measuring the potential dependence of the (11*l*) rod intensity, we monitored the roughness transitions at the GaAs(001)/$H_2SO_4$ interface associated with anodic oxidation (increase in roughness) and cathodic reduction (decrease in roughness).[1] Our measurements of the specular (00*l*) rod at the n-GaAs(001)/HCl interface have clearly shown that surface roughness is not the only factor contributing to the rod shape (Fig. 1). While around $l = 4$ the intensity profile can be fitted using only a roughness parameter, the rod at $l = 2$ shows a remarkable broadening that is not described in terms of roughness. This peak, being much weaker in intensity than the (004) reflection, is rather sensitive to electron density variations, and the ions in the electrochemical double layer present at the interface have to be considered. In terms of a simple model for additional electron density due to chloride ions, the fit of the specular rod was greatly improved. Best agreement was achieved for ~ 1ML chloride. However, these preliminary results are derived from a real simple model which has to be refined on the basis of further measurements.

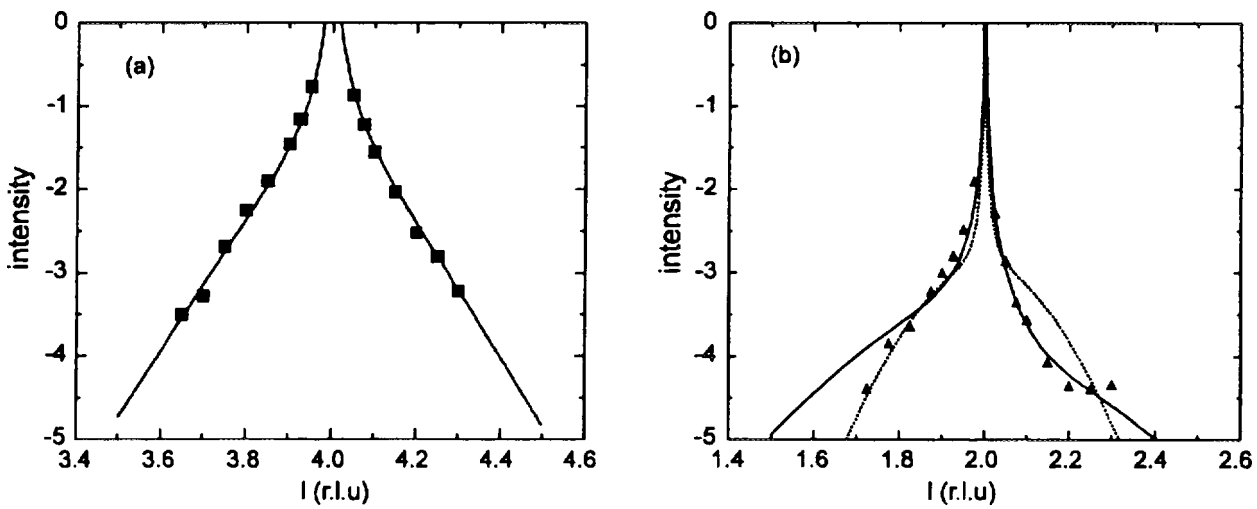


Fig .1: Specular (00*l*) rods at the n-GaAs(001)/HCl interface at -1.0V. (a) Rod at (004), fitted with rms = 4.3 A. (b) Rod at (002), fitted for roughness only (broken line, rms = 6.4 Å) and for the roughness obtained from (004) and 1ML of chloride (solid line).

[1] J. Zegenhagen, A. Kazimirov, G. Scherb, D.M. Kolb, D.-M. Smilgies, and R. Feidenhans'l, Surf. Sci **352-354**, (1996) 346

## Structure and Orientation of Sn Precipitates in Epitaxial Layers of $Si_{1-x}Sn_x$

M.F. Fyhn, J. Chevallier, S.Y. Shiryaev, A.N. Larsen, *Institute of Physics and Astronomy, University of Aarhus, Denmark.* R. Feidenhans'l and J. Als-Nielsen, *Niels Bohr Institute, University of Copenhagen, Denmark*

Binary group IV alloys have gained considerable interest during the last decade. These alloys can be used to make devices, compatible with conventional Si technology, which are faster than structures based on Si alone. The research has primarily been devoted to $Si_{1-x}Ge_x$, and $Si_{1-x}C_x$ while $Si_{1-x}Sn_x$ only recently was grown of high structural quality.[1] $Si_{1-x}Sn_x$ has a smaller bandgab than Si and is expected to have electrical properties suitable for heterostructure devices.[2]

We have grown $Si_{1-x}Sn_x$, x~5.5% by molecular beam epitaxy on Si <001> and $Si_{1-x}Ge_x$ substrates.[3] Due to the large difference in lattice constant between Si and Sn (20%) and the low solubility of Sn in Si (~0.1%) the $Si_{1-x}Sn_x$ layers are metastable, and we are currently studying the relaxation of $Si_{1-x}Sn_x$ at different temperatures. The relaxation channels have been found to be precipitation and generation of misfit dislocations. The Sn precipitates in epitaxial $Si_{1-x}Sn_x$ layers have been studied by transmission electron microscopy, and the figure below shows a plan-view micrograph of the diffraction pattern from $Si_{1-x}Sn_x$, x=5.3% annealed at 950°C for 1 hour. The additional spots seen between the ones related to the diamond-structure of $Si_{1-x}Sn_x$ are due to precipitates, which have lattice constants different from the surrounding matrix. X-ray diffraction measurements at Risø National Laboratory and at DESY, Hamburg have been performed to measure the lattice constants in a more precise way and to determine the orientation of the precipitates. These measurements confirm the texture seen by TEM (as figure) and verifies that two different solid phases of Sn (α-Sn and β-Sn) are present.

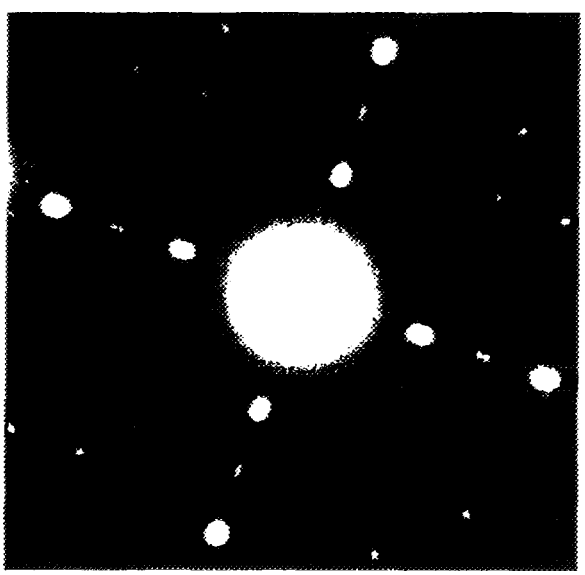

Figure 1. TEM pattern of a $Si_{1-x}Sn_x$, x=5.3% sample annealed at 950°C for 1 hour

[1] S. Yu. Shiryeav, J. Lundsgaard Hansen, P. Kringhøj and A. Nylandsted Larsen, Appl. Phys. Lett. 67, 2287 (1995)

[2] A. T. Khan, P. R. Berger, F. J.Guarin and S. S.Iyer, Appl. Phys. Lett. 68, 3105 (1996)

[3] M. F. Fyhn, S. Yu. Shiryaev, J. Lundsgaard Hansen and A. Nylandsted Larsen, Appl. Phys. Lett. 69, 394 (1996)

# HIGH-PRESSURE X-RAY DIFFRACTION

In 1996 our group has performed experiments at 4 different experimental stations at Hasylab. At F3 powder diffraction with energy dispersive method has taken place. At BW4 a new powder diffraction method with image plate detector has been used at the monochromatic Wiggler line. At D3 we have performed single crystal diffraction at high pressure, and at F2 (MAX 80) we have used the multi anvil equipment to make experiments at both high pressure and high temperature.

## *Small particles of ceramic oxides*

J. Staun Olsen[1], S. Steenstrup[1], L. Gerward[2], J.Z. Jiang[2], B. Palosz[3], F. Ferrall[1]

1. Niels Bohr Institute, Oersted Laboratory, Copenhagen, Denmark
2. Physics Department, Bldg 307, Technical University of Denmark, Lyngby, Denmark
3. High Pressure Research Center UNIPRES, Polish Academy of Science, Warszawa, Poland

Nanostructured materials, consisting of small crystallites of diameters
1 - 100 nm, often have novel physical and chemical properties, which differ from those observed in bulk materials. The existence of these unique properties opens up the general question of the effects of crystallite size on structural stability in these materials, i.e. how the relative stability of different possible solid structures will change for nanostructured materials as compared with bulk materials. A promising approach to this problem is to force nanostructured materials to convert from one solid structure to another by applying high pressures. Therefore we are performing *in-situ* high pressure synchrotron x-ray diffraction measurements for a wide range of nanostructured materials, addressing a number of important questions related to the understanding of first order solid-solid phase transitions. Recent studies on nanostructured semiconductors Si, CdSe and CdS indicates, that the transformation pressure increases with decreasing particle size. However, our experiments show, that this is no general result. Thus for nanometer-sized $\gamma$-$Fe_2O_3$ particles, the phase transition pressure for the $\gamma$-$Fe_2O_3$ to $\alpha$-$Fe_2O_3$ transition is lower than in bulk material, and no big difference in transition pressure has been observed in nanostructured and bulk $SnO_2$ , for the t-$SnO_2$ to o-$SnO_2$ transition. The phase transitions are also studied as functions of both pressure and temperature at the MAX 80 station of beamline F2 at Hasylab. With UNIPRES in Warsaw we have studied the behaviour of SiC at increasing pressure. We found, that the free surface is important, and has to be compared with the importance of the grain size.
The Danish Technical Research Council has approved an application with a 2 year grant to the project "High pressure behaviour of

nanostructural materials". The money per year, 468000 DK, is for VIP salary, expenses and overhead. Ph.D. J.Z. Jiang will start in october 1997 with the grant.

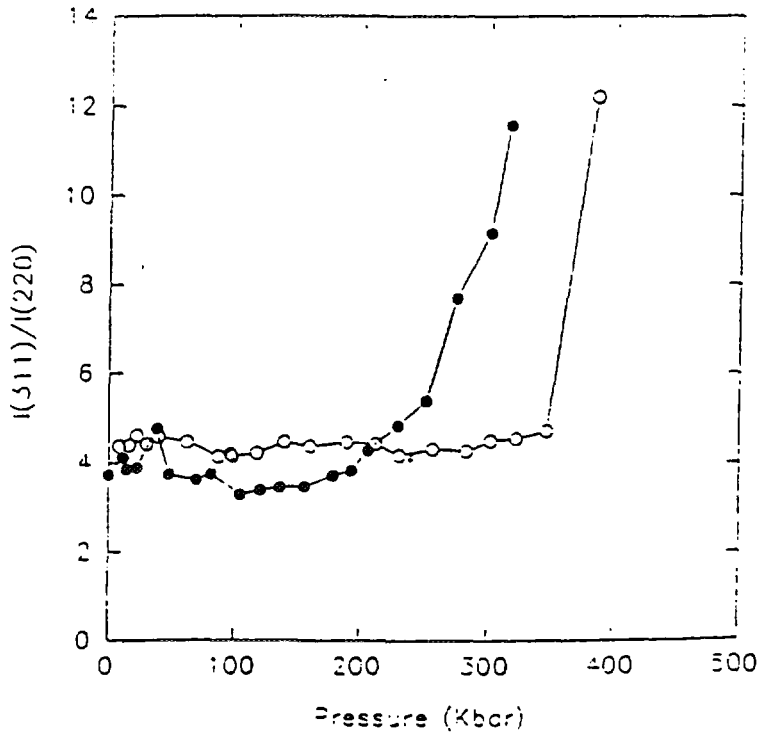


$\gamma$ - $\alpha$ transformation in $Fe_2O_3$.

- Small particles ( 7 nm )
- Large particles ( 1 µm )

The disappearance of $\gamma$- phase at increasing pressure, measured by decreasing intensity of the (220) reflection

*Image plate set-up for monochromatic beam*

J. Staun Olsen[1], S. Steenstrup[1], L. Gerward[2], F. Ferrall[1], S. Cunis[3]

1. Niels Bohr Institute, Oersted Laboratory, Copenhagen, Denmark
2. Physics Department, Bldg 307, Technical University of Denmark, Lyngby, Denmark
3. Hasylab, Hamburg, Germany

Energy-dispersive diffraction methods have limited resolution and generally give unreliable intensities. The situation has been transformed recently by the introduction of the image plate detector, which allows angle-dispersive, monochromatic methods to be used with greatly improved resolution and powder averaging. Instrumental studies have been performed at the beamline BW4. We expect to have an improved set-up ready in 1997, to be used by different groups making high pressure diffraction experiments.

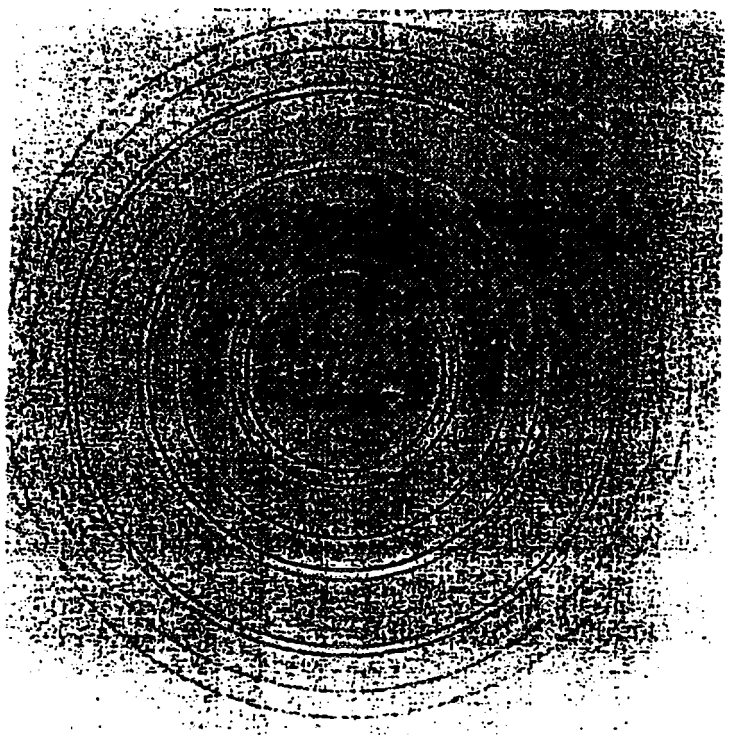

Image plate picture of Au foil, obtained by 24.609 keV x-rays in 15 min.

*$Mn\ Ni_2\ O_4$ spinel*

J. Staun Olsen[1], S. Steenstrup[1], L. Gerward[2], A. Waskowska[3], S. Åsbrink[4], F. Ferrall[1]

1. Niels Bohr Institute, Oersted Laboratory, Copenhagen, Denmark
2. Physichs Department, Bldg 307, Technical University of Denmark, Lyngby, Denmark
3. Institute of Low Temperature and Structure Research, Wroclaw, Poland
4. Dept. of Inorganic Chemistry, Arrhenius Laboratory, Stockholm, Sweden

The 3d transition metal oxide $NiMn_2O_4$ belongs to the group of cubic spinels; the structure of which consists of tetrahedrally and octahedrally coordinated metal cations, distributed in the fcc configuration of oxygen anions. High-pressure x-ray powder diffraction has shown, that there is a structural phase transition at 11 GPa. The unit cell of the high-pressure phase is tetragonal with c/a = 0.9, which is comparable with the corresponding structure of $Cr_2CuO_4$ . Powder diffraction has been compared with single crystal high pressure experiments on the material. S. Åsbrink received a Norfa grant in 1996 and spent 1 month together with our group. A. Waskowska from Wroclaw, Poland also spent 1 month together with our group.

*Single crystal, high-pressure studies of critical effects in $V_3O_5$*

J. Staun Olsen[1], S. Steenstrup[1], L. Gerward[2], A. Waskowska[3], S. Åsbrink[4], F. Ferrall[1]

1. Niels Bohr Institute, Oersted Laboratory, Copenhagen, Denmark
2. Physics Department, Bldg 307, Technical University of Denmark, Lyngby, Denmark
3. Institute of Low Temperature and Structure Research, Wroclaw, Poland
4. Dept. of Inorganic Chemistry, Arrhenius Laboratory, Stockholm, Sweden

In the mixed-valency oxide $V_3O_5$ a first-order phase transition occurs at $T_t$ = 155° C. The accurate crystal structures of the two phases have been determined from x-ray single crystal data at room temperature and at 185° C, respectively. The main result of the phase transition was found to be a redistribution of the vanadium valency electrons. Even if the phase transition is of first order, there are changes in the low-temperature phase, preparatory to the phase transition, commencing several tens of degrees below $T_t$ . Similarily, upon lowering the temperature, there are preparations for the transition in the high-temperature phase several tens of degrees above $T_t$ . A particular feature is, that the strong x-ray reflections show a strong increase in peak intensity just at the phase transition. Furthermore, two new but weaker critical intensity effects have been recorded just below $T_t$ .

The wavelength dependence of the anomalous intensity increase at $T_t$ was studied by us, using white-beam, energy-dispersive x-ray diffraction, and disclosing some new and challenging problems. For that purpose we built an oven, capable of changing the temperature in steps of 0.01° C. The anomalies of the strong *h00* Bragg reflections were also correlated with x-ray topographic observations of the $V_3O_5$ crystals, using syn-chrotron radiation. Thus, an unexpected decrease in crystal perfection was observed a few hundredths of a degree below $T_t$ . The photon-energy dependence of the intensity maxima at $T_t$ for the strong reflections was explained semi-quantitatively on the basis of extinction theory.

The experiences from the experiments described above have led us to the conclusion, that it also should be very interesting to study the same phase transition as a function of pressure. We expect to observe critical effects close to the transition pressure $P_c$ = 6.3 GPa (= 63 kbar) for $V_3O_5$ . A first study was made at beamline D3 using the four-circle diffractometer. The results are promising and they are now being evaluated.

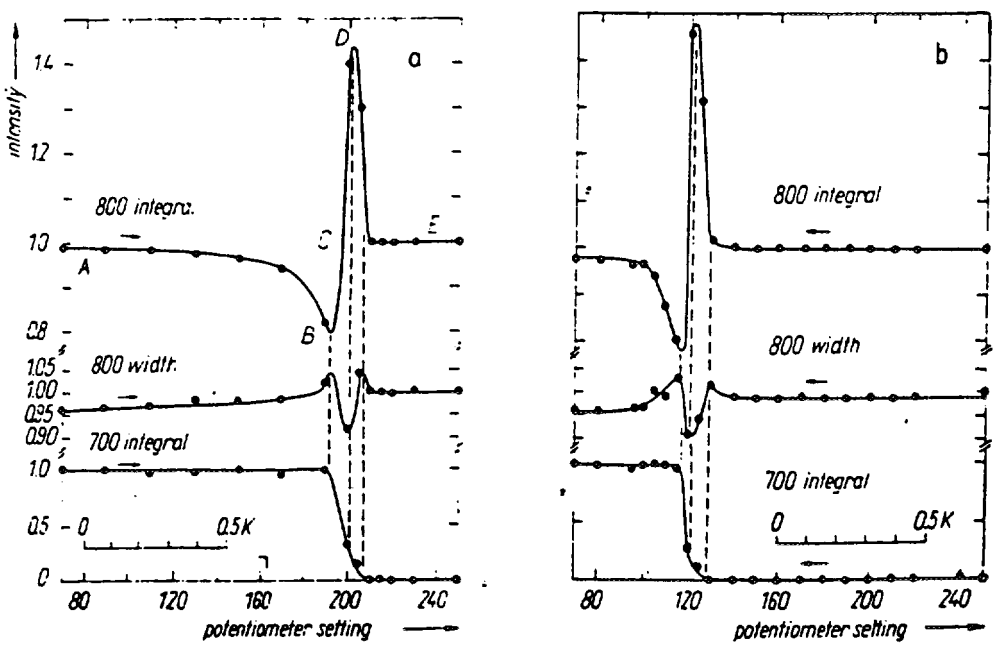


Integrated intensities of the 800 and 700 reflections and the integral width of the 800 reflection at 32.8 keV versus temperature in the phase transition region: *N.b.* reflections with $h + k + l = 2n + 1$ are absent in the high-temperature region. All variables have been normalized to unity outside the phase transition region. The 700 and 800 intensities 1 K below $T_t$ are related as about 1:80. Observations for a) increasing temperatures and b) decreasing temperatures

$V_3O_5$ at increasing temperature. Transition at 155°C

*High pressure and high temperature*

J. Staun Olsen[1], S. Steenstrup[1], L. Gerward[2], T. Peun[3], T. Steenberg[4], P. Olesen[4], F. Ferrall[1]

1. Niels Bohr Institute, Oersted Laboratory, Copenhagen, Denmark
2. Physics Department, Bldg 307, Technical University of Denmark, Lyngby, Denmark
3. GeoForschungsZentrum Potsdam, Potsdam, Germany
4. Institute for chemistry, Technical University of Denmark, Lyngby, Denmark

By use of MAX 80 (multi anvil cell) we have studied, by energy-dispersive methods, the behaviour of $Zn_3(PO_4)_2 4H_2O$ and $Ca_xZn_{3-x}(PO_4)_2$ at pressure up to 7 GPa and at temperature up to 1000° C. Both materials are used by Danfoss at about 6 GPa and 600° C as lubricant at the massive shaping of stainless steel. The first material is in crystalline form at ambient pressure and temperature, and changes to an amorphous form, while the other one starts in an amorphous form, and changes to a crystalline form at the extreme pressure and temperature used in our experiment.

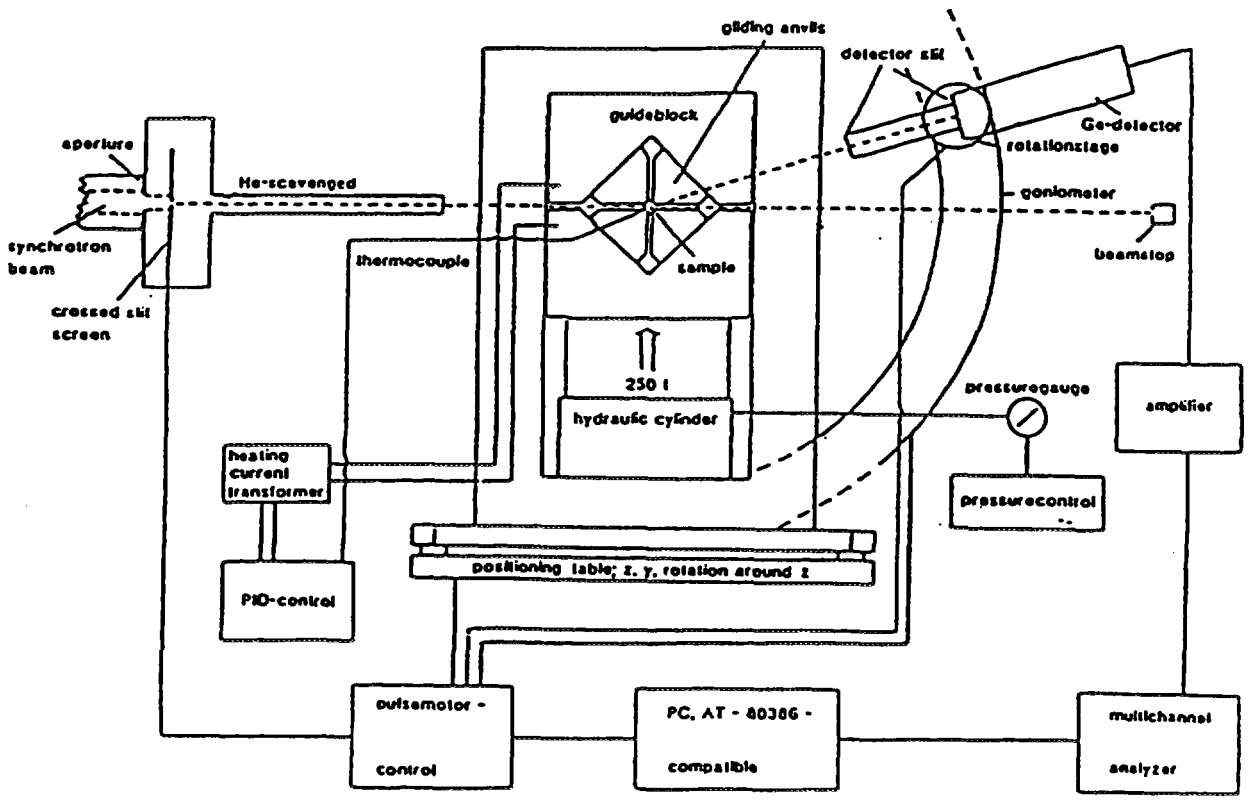


Schematic set-up

NEXT PAGE(S) left BLANK

## Resonant X-ray Magnetic Scattering at the K-edge from NiO

J.P. Hill, *Department of Physics, Brookhaven National Laboratory, USA*, C.-C. Kao, *National Synchrotron Light Source, Brookhaven National Laboratory, USA*, D.F. McMorrow, *Department of Solid State Physics, Risø National Laboratory, Denmark*

Resonant x-ray magnetic scattering exploits enhancements in the cross-section occurring when the incident photon energy is tuned through an atomic absorption edge. Large enhancements were first observed at the L edges in Ho and explained in terms of electric multipole transitions. In addition to the L edges much larger enhancements are expected, and observed, at the M edges of the actinides for which the dipole excitation is to the highly polarized 5f levels. Conversely, resonant scattering at a K-edge is expected to be considerably weaker because the strong (dipole) transitions involve *s* and *p* levels for which there is no spin-orbit correlation of either the core level or the intermediate state. Nevertheless, K-edge studies would be of some interest because of the window they would provide on transition metal compounds.

We report the observation of K-edge resonant magnetic scattering in the antiferromagnet NiO, for which an approximately two-fold increase in the scattering is observed at an energy corresponding to a *quadrupolar* feature in the absorption spectrum (Fig.1). Quadrupole excitations couple to *d*-like states at a K-edge and for transition metals these are the magnetic states. Thus, the high degree of polarization of the localized $3d^8$ states compensates for the small size of the quadrupolar matrix elements and an observable enhancement results. From the ratio of the non-resonant to resonant magnetic scattering, we estimate that the first order quadrupolar resonant scattering amplitude is $0.016r_0$, which is of the same order of magnitude as similar terms in the rare earths. These studies provide for the possibility of element specific magnetic diffraction in such notable transition metal oxides as the high $T_c$ cuprates and colossal magnetoresistance manganites.

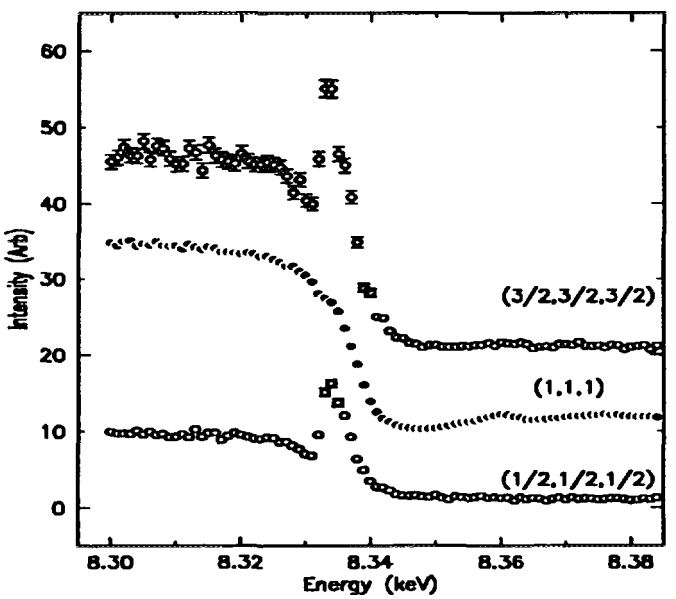


Fig. 1. The energy dependences of the (1,1,1) charge peak, and the (1/2, 1/2, 1/2) and (3/2 3/2 3/2) magnetic peaks from NiO at room temperature.

## An X-ray Magnetic Scattering Study of $DyFe_4Al_8$

S. Langridge, *ESRF, France and European Commission, JRC, Institute for Transuranium Elements, Germany*, J.A. Paixão, *Department of Physics, University of Coimbra, Portugal*, S.Aa. Sørensen, *Department of Solid State Physics, Risø National Laboratory, Denmark*, C. Vettier, *ESRF, France*, G.H. Lander, *European Commission, JRC, Institute for Transuranium Elements, Germany*, D. Gibbs, *Physics Department, Brookhaven National Laboratory, USA*, A. Stunault, D. Wermeille and N.B. Berhoeft, *ESRF, France*, E. Talik, *Institute of Physics, University of Silesia, Poland*

The magnetic structure of the $ThMn_{12}$-structure compound $DyFe_4Al_8$ is complicated and not yet fully understood. The general features of the magnetic ordering determined mainly from neutron scattering experiments are summarized in 2.2.14. A central problem has been to establish whether the Dy-moments when ordering below approximately 25 K are forming a transverse amplitude modulated structure in the basal plane of the *bct* crystal structure or the moments are rotating in some helical or cycloidal structure. An X-ray resonant magnetic scattering experiment was performed on the ID20 beamline of the European Synchrotron Radiation Facility. As shown in Fig. 1, the intensities of the first order magnetic satellites around (*hh*0) reciprocal lattice points were measured at the Dy $L_{III}$-edge at the temperature 12 K. In the figure, the intensity is shown as a function of the Bragg-angle, θ with the $DyFe_4Al_8$ single crystal sample in two different orientations. In orientation (A), the reciprocal lattice [110]-[$\bar{1}$10] plane is parallel to the diffractometer plane defined by the incident wavevector, $\boldsymbol{k}_i$ and the outgoing wavevector, $\mathbf{k}_f$. In the orientation (B), the sample has been rotated by 90 degrees around the [110] relative to the first orientation, thus bringing the basal plane of the crystal perpendicular to the diffractometer plane. From the angular dependence of the satellite intensities in the two orientations it is concluded, that the Dy moments must rotate in the basal plan. In the experiment, the intensity of the (330) + $\boldsymbol{q}$ and (440) + $\boldsymbol{q}$ satellites were measured at the Dy $L_{III}$-edge as a function of temperature. A steep drop in the intensity was observed in the temperature range between 11 K and 20 K corresponding to the disordering of the Dy 4f-moments. However, a weak signal was detected all the way up to the temperature of disordering of the Fe-moments. This is a sign of the importance of hybrydization of the Dy-5f and Fe-3f bands in mediating the interaction between the two magnetic sublattices.

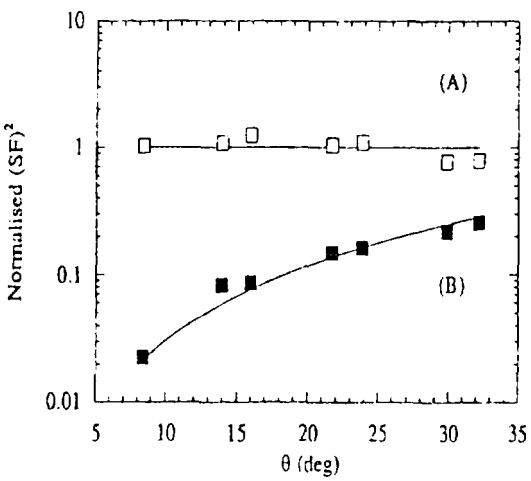


Fig. 1. Lorentz-corrected intensity of the 1st order magnetic satellites measured in the σ→π channel.The average intensity of all satellites measured in orientation (A) has been normalized to unity. For orientation (B), the solid curve has been drawn to predict the intensities with no adjustable parameters.

## Magnetic Resonant X-ray Scattering of Samarium Thin-Films

J.-G. Lussier, A. Madsen, R. Feidenhans'l, D.F. McMorrow, *Department of Solid State Physics, Risø National Laboratory, Denmark,* J.P. Hill and D. Gibbs, *Department of Physics, Brookhaven National Laboratory, USA*

The magnetism of Sm cannot be well studied by neutron scattering. In its natural form, Sm has several isotopes which contribute to the large absorption cross-section and give a large incoherent background. Historically, the magnetic structure of Sm was discovered on single isotope samples.[1] Another, more modern approach, which is not sensitive to isotopic differences, is to use an atomic absorption edge to enhance the magnetic X-ray cross-section (magnetic resonant X-ray scattering). We performed a series of measurements at the X-22c beamline, Brookhaven National Laboratory on two thin-films grown at the MBE facility, Risø National Laboratory. The films were grown with the sequence: Nb(1000Å) / Y (200Å) / Sm(5000Å) / Y(375Å) / Nb (1000Å) / Sapphire and Nb(1000Å) / Y (500Å) / Sm(10000Å) / Y(250Å) / Nb (1000Å) / Sapphire. Bulk-Sm has a rhombohedral crystal structure and one of the complication in the growth of Sm thin-films is the possible formation of HCP-Sm. Our study has shown that, although the rhombohedral structural phase of Sm is observed, Fig. 1 a) and b), the films failed to reveal any magnetic Bragg peaks using the $L_{II}$- and $L_{III}$-edge radiation of Sm. The mosaic spread (≈0.4°) and strains in the film (Fig. 2) may have prevented the magnetic order to develop or to be observable. A soft annealing procedure has been applied on the 10000Å-film and will be studied again in a near future.

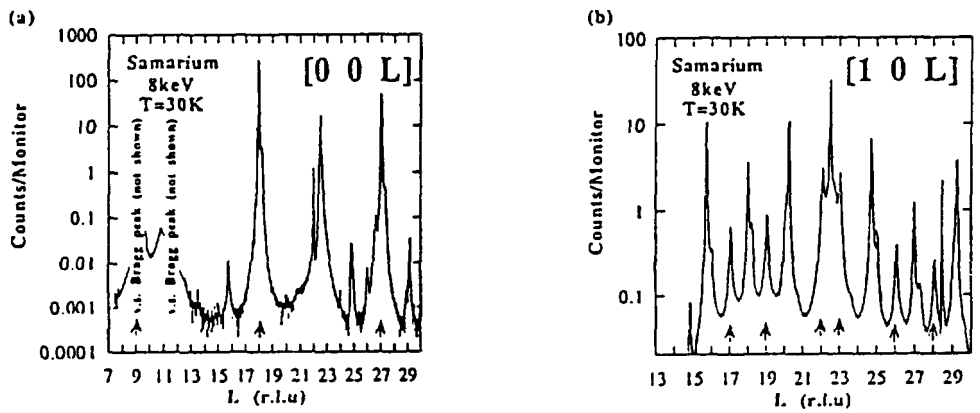


Fig. 1. X-ray scattering scans: a) along the (00L) and b) along the (10L) direction at 8keV. Both labeling refer to the hexagonal representation of the rhombohedral structure. The expected peaks for RH-Sm are shown by the arrows. The other peaks are due to the substrate and other components of the films.

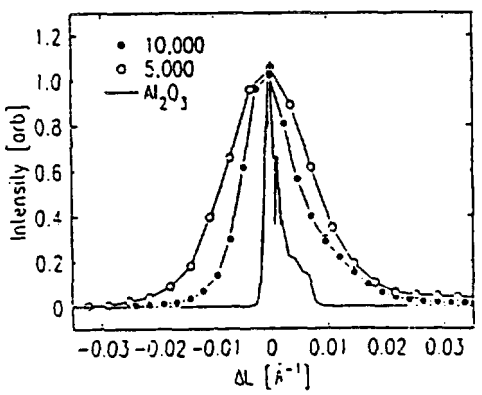


Fig. 2. The lineshape broadening, which reveals the level of strains in the films, is an order of magnitude larger in the Sm-films than what was found in Ho films previously studied at the X-22c beamline.

[1] W.C. Koehler and R.M. Moon, Phys. Rev. Lett. (1972) 29, 1468

# Heparin Binding Protein

*Lars Fogh Iversen, Jette Sandholm Kastrup og Ingrid Kjøller Larsen.*
*Institut for Medicinalkemi, Danmarks Farmaceutiske Højskole.*

Heparin binding protein (HBP) betegnes som et multifunktionelt protein, da det besidder en række egenskaber, der alle er rettet mod immunforesvaret og bekæmpelse af bakterielle infektioner. HBP er et glykosyleret protein fra de hvide blodlegemer (lymfocytter), og bliver frigivet, når disse skal bekæmpe en infektion. I samarbejde med Hans Flodgaards gruppe på Novo Nordisk A/S arbejder vi på at undersøge sammenhænge mellem struktur og funktioner af HBP (1, 2).

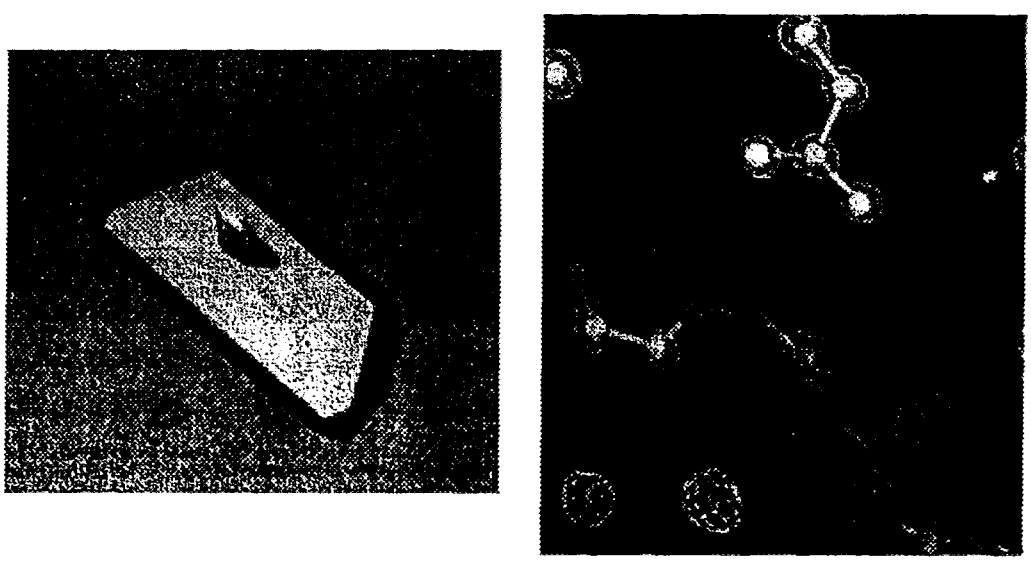

Figuren viser en krystal af human HBP samt et 1.1 Å data elektrontæthedskort.

Strukturen af glykosyleret og af deglykosyleret HBP er blevet bestemt ved hjælp af proteinkrystallografi. Ved brug af synkrotron stråling har vi omsamlet diffraktionsdata til 1.1 Å opløsning, dvs. af en detaljeringsgrad der hidtil var forbeholdt mindre organiske molekyler. Proteinstrukturene vil blive anvendt som skabelon for design af nye lægemiddelstoffer, der kan stimulere immunforesvaret. Desuden har vi udfra proteinstrukturerne opnået yderligere forståelse for proteinets biologiske funktion.

1. Iversen, L.F., Kastrup, J.S., Larsen, I.K., Bjørn, S.E., Rasmussen, P.B., Wiberg, F.C. and Flodgaard, H.F. (1996). Crystallisation and molecular replacement solution of human heparin binding protein. Acta Cryst. D52, 1222-1223.

2. Iversen, L.F., Kastrup, J.S., Bjørn, S.E., Rasmussen, P.B., Wiberg, F.C., Flodgaard, H.F. and Larsen, I.K. (1997). The three-dimensional structure of HBP/CAP37/azurocidin, a multifunctional protein with a serine protease fold (accepted).

# Peptide Nucleic Acid (PNA) komplekser.

Hanne Rasmussen og Jette Sandholm Kastrup
Institut for Medicinalkemi, Danmarks Farmaceutiske Højskole

PNA (Peptide Nucleic Acid) er en oligonukleotid-analog, hvor phosphat-ribose backbone er substitueret med en pseudopeptid backbone. På trods af denne drastiske kemiske ændring i forhold til DNA er PNA strukturelt homomorf til denne. Eksperimenter har vist, at PNA hybridiserer med såvel DNA og RNA som med PNA selv, under dannelse af en dobbelthelix [1].

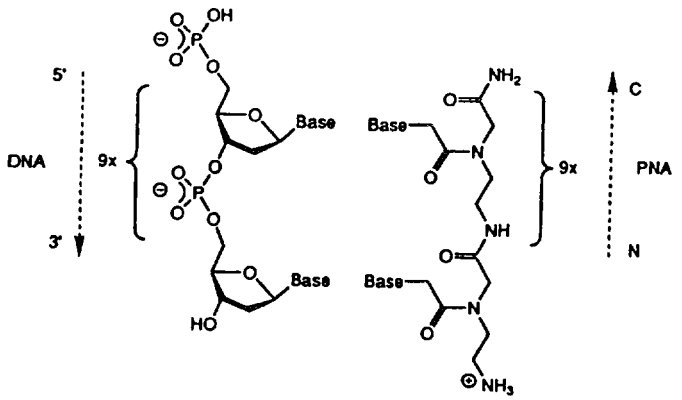


*Skematisk repræsentation af PNA-DNA dobbelthelix*

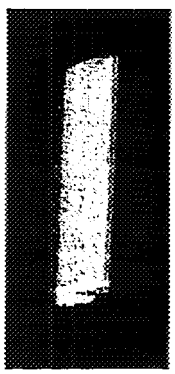

*Krystal af PNA-PNA duplex*

Ved binding til mRNA griber PNA ind i ribosomernes funktion og virker herved som en antisense inhibitor af translationen, ligesom en binding til DNA inhiberer RNA polymerasens transkription. PNA besidder således mange af de ønskede egenskaber for en antisense/antigen lægemiddelkandidat, inklusiv stabilitet overfor nukleaser, proteaser, peptidaser og humant serum, samt en høj grad af specificitet overfor det ønskede oligonukleotid.

Et kendskab til den tre-dimensionelle struktur er essential for forståelsen og videreudviklingen af disse analoger. Desuden kan dette kendskab føre til en øget viden om DNA og RNAs struktur og funktion. For detaljerede studier er diffraktionsdata til høj opløsning nødvendige. Disse data opnås ved hjælp af synkrotronståling. Vi har fornylig bestemt strukturen af en PNA-PNA duplex ved hjælp af røntgen-krystallografi [2]. Denne struktur har afsløret en ny helix-form (P-form), som bl.a. tilfører viden om mekanismen for helix-dannelsen af oligonukleotider. Til at belyse helix-formens afhængighed af henholdsvis basen, backbone eller sekvensen har vi krystalliseret flere forskellige analoger med forskellige modifikationer. Projektet foregår i samarbejde med Forskningsprofessor Peter E. Nielsen og medarbejdere, Center for Biomolekylær Genkendelse.

*1. M. Egholm, O. Buchardt, L. Christensen, C. Behrens, S. M. Freier, D. A. Driver, R. H. Berg, S. K. Kim, B. Norden & P.E. Nielsen. PNA hybridizes to oligonucleotides obeying the watson-Crick hydrogenbonding rules. Nature **365**, (1993)565-568*

*2. H. Rasmussen, J.S.Katrup, J. N. Nielsen, J. M. Nielsen og P. E. Nielsen. Crystal structure of a peptide nucleic acid (PNA) duplex at 1.7 Å resolution. Nature Struct. Biology vol 4. (1997)*

## Makromolekylær Krystallografi.

Projekterne på Laboratoriet for Makromolekylær Krystallografi er grupperet om protein biosynthesen og om proteinerne i familien.

I protein biosynthesen har vi igennem mange år arbejdet på strukturen af elongeringsfaktor Tu (EF-Tu). EF-Tu er en central komponent i protein biosynthesen idet den transporterer aminoacyleret-tRNA (aa-tRNA) til ribosomet hvor aa-tRNA bidrager med endnu en aminosyre til den voksende peptidkæde.

EF-Tu tilhører G-protein familien, som har det fællestræk at de binder enten GDP eller GTP. Når GTP er bundet kan EF-Tu binde aa-tRNA. Når komplekset EF-Tu:GTP:aa-tRNA bliver bundet til ribosomet hydrolyseres GTP til GDP og EF-Tu:GDP frigøres. For at EF-Tu kan binde aa-tRNA igen skal GDP udskiftes med GTP. Denne reaktion katalyseres af elongeringsfaktor Ts (EF-Ts). Den cycklus EF-Tu gennemgår kan inhiberes af antibiotikaet kirromycin (Kir). Kirromycin virker sandsynligvis ved at fastholde EF-Tu i en struktur der minder om EF-Tu:GTP således at EF-Tu forbliver bundet til ribosomet selv efter hydrolyse af GTP til GDP.

Vi har tidligere løst strukturen af E.coli EF-Tu:GDP i en trypsineret form(1), T.aquaticus EF-Tu:GDPNP ( en analog til GTP) (2), T.aquaticus EF-Tu:GDPNP:phe-tRNA$^{Phe}$ (3). Disse strukturer viste en drastisk ændring i konformationen af EF-Tu:GDP og EF-TU:GDPNP. Således ændres den relative position af domæne 1 i forhold til domæne 3 med ca 90°. Derved opstår der et bindings site til aa-tRNA i EF-Tu:GDPNP. Strukturen af T.aquaticus EF-Tu:GDPNP:phe-tRNA$^{Phe}$ (3) viste hvordan aa-tRNA binder i dette bindings site og hvorledes EF-Tu er istand til at diskriminere mellem aminoacyleret og ikke-aminoacyleret tRNA.

I 1996 publicerede vi strukturen af T.aquaticus EF-Tu:GDP (4).Data til bestemmelse af denne struktur blev indsamlet ved synchrotronen i Daresbury i 1995 og 1996. Strukturen viste at den ændring af konformationen der er mellem trypsineret EF-Tu:GDP (1) og EF-Tu:GDPNP (3) ikke var et resultat af trypsinering men derimod en reel del af EF-Tu's funktion. I 1996 har vi desuden indsamlet data ved synchrotronbesøg på krystaller af EF-Tu:GDPNP:Kir:phe-tRNA$^{Phe}$ (5), EF-Tu:GDPNP:Cys-tRNA$^{Cys}$ og EF-Tu:EF-Ts. Alle tre strukturer forventes publiceret i 1997. Specielt strukturen af komplekset med kirromycin er interessant idet kendskab til antibiotika binding muligvis vil gøre os istand til at designe andre typer af antibiotika med en tilsvarende virkningsmåde.

Proteinerne i Alpha-2-makroglobulin familien kan opdeles i to grupper protease inhibitorerne og complement proteiner. Protease inhibitorerne virker ved at danne et covalent compleks med proteasen. Når dette kompleks er blevet dannet eksponeres et receptor bindende domæne således at det kovalente kompleks kan binde til receptorer på leverceller og siden nedbrydes i leveren. Det receptor bindende domæne af bovint Alpha-2-makroglobulin er blevet krystalliseret (6) og adskillige datasæt er blevet indsamlet i 1996 for det native protein og af tungt atom derivater ved synchrotronen i Hamburg. Strukturen er netop blevet løst og forventes publiceret i løbet af 1997.

Complement proteinerne C3, C4 og C5 tilhører også Alpha-2-makroglobulin familien. Disse medvirker i immunresponsen ved bl.a andet at binde til immunoglobuliner bundet til overfladen af fremmede celler. Når C5 er bundet til overfladen af en celle bliver cellen genkendt som mål for yderligere complement proteiner C6-9 som er istand til at lysere cellen. Vi har tidligere løst strukturen af Alpha-2-makroglobulin til 10Å opløsning og beskrevet krystaller af C3 som viste diffraktion til 8 Å. Vi har nu indgået et samarbejde med Dr. R.G.DiScipio, la Jolla, Californien, som har krystalliseret C5. Disse krystaller har vist diffraktion til 3.3 Å ved synchrotronen i Trieste. Vi forventer at indsamle diffraktionsdata fra både native og tung-atom derivat krystaller i løbet af 1997.


1. Kjeldgaard,M. & Nyborg, J., J.Mol.Biol, 223, 721-742, (1992)
2. Kjeldgaard,M., Nissen,P., Thirup,S. & Nyborg, J., Structure, 1, 35-50, (1993)
3. Nissen, P., Kjeldgaard, M., Thirup, S., Polekhina, G., Reshetnikova, L., Clark, B.F.C. & Nyborg, J. Science 270, 1464-72 (1995).
4. Polekhina, G., Thirup, S., Kjeldgaard, M., Nissen, P., Lippmann, C. & Nyborg, J. Structure 4, 1141-1151, (1996)
5. Kristensen, O., Reshetnikova, L., Nissen, P., Siboska, G., Thirup, S. & Nyborg, J. FEBS Letters 399, 59-62 (1996).
6. Dolmer, K., Jenner, L.B., Jacobsen, L., Andersen, G.R., Koch, T.J., Thirup, S., Sottrup Jensen, L. & Nyborg, J. FEBS Letters 372, 93-5 (1995).

**Center for Krystallografiske Undersøgelser**

**Rapport over eksperimenter udført med synkrotronstråling i 1996**

Anvendelsen af synkrotronstråling til diffraktionseksperimenter indgår i et stadigt stigende omfang i centrets forskningsaktiviteter. Det er strålingens store intensitet og muligheden for at måle med meget lave bølgelængder, som vi drager fordel af i de projekter, der beskrives i det følgende.

*Undersøgelse af den eksperimentelle ladningstæthed i* $[Co(NH_3)_5CH_3]\ S_2O_6$ .

I samarbejde med Pauli Kofod, Kemisk Institut, RUC har vi undersøgt en række klassiske co-ordinations forbindelser af Co, der indeholder en methyl gruppe som ligand [1]. I disse forbindelser kunne det observeres, at methylgruppen udøver en kraftig *trans* effekt. Den viser sig ved, at den Co-$NH_3$ binding, der er *trans* til methyl gruppen, er ca. 0.15Å længere end Co-$N(H_3)$ afstandene i det equatoriale plan of den oktaedriske $[Co(NH_3)_5CH_3]^{+2}$ cation.

Vi har fornyligt vist, at en topologisk analyse, analog med den Richard Bader har anvendt på teoretisk beregnede ladningstætheder, også kan benyttes til at studere interatomare vekselvirkninger i krystaller ud fra eksperimentelle ladningstætheder. Den topologiske analyse viste, at den korte symmetriske O-H-O hydrogenbinding mellem carboxylat gruppen og carboxylsyre gruppen i methylammonium hydrogensuccinat monohydrat har covalent karakter [2].

De unikke interatomare vekselvirkninger, der eksisterer i $[Co(NH_3)_5CH_3]\ S_2O_6$ gør dens ladningstæthed til et attraktivt mål for en topologisk analyse. Intensiteterne målt med konventionelle Røntgenstrålingskilder vil for forbindelser, der indeholder tungere atomer, være påvirket af fysiske fænomener som absorption, anomal spredning og extinction. Effekten af disse kan reduceres kraftigt, hvis en meget kortere bølgelængde kan anvendes til diffraktionseksperimentet.

Af den grund søgtes om måletid på beamline for materials science ved ESRF. Den tildelte måletid på 48h blev udnyttet 5-6. februar 1996. Et nyligt anskaffet kommercielt CCD detektor system (Siemens SMART) blev benyttet til målingerne, som blev gennemført med en bølgelængde på 0.4Å. Selv om der blev registreret 100.000 refleksioner, faldt eksperimentet desværre ikke så heldigt ud, som vi havde håbet, d.v.s. de målte intensiteter var ikke af den ønskede nøjagtighed. Det skyldes primært indkøringsproblemer med det nye udstyr. Når de

målte data er færdiganalyseret, vil vi vurdere om en Siemens CCD detektor kan give data af tilstrækkelig kvalitet til at gennemføre en ladningstæthed. Hvis dette er tilfældet, vil vi søge om ny måletid.

[1] Kofod, P., Harris, P. & Larsen, S. Inorg. Chem. In the press.
[2] Flensburg, C., Larsen, S. and Stewart, R.F. J. Phys. Chem. 99 (1995) 10130-10141

*Undersøgelser af struktur/funktions sammenhænge for enzymer, der indgår i nucleotidstofskiftet.*

Anvendelsen af synkrotronståling har haft en revolutionerende effekt på den proteinkrystallografiske forskning. Således har vores gruppe i 1996 gennem adskillige eksperimenter erfaret, at vi har kunnet opnå en kraftig forbedring af kvaliteten af de målte diffraktionsdata fra proteinkrystaller ved anvendelse af synkrotronstråling. De to måleperioder på henholdsvis 63 og 64 timer, som vi fik tildelt ved EMBL's beamlines i Hamburg i 1996, har primært været udnyttet til indsamling af data for enzymer, der spiller en central rolle i cellers nucleotidstofskifte. De proteiner, som vi har studeret er alle af bakteriel oprindelse og katalyserer processer i *de novo* og salvage reaktioner for nucleosider og nucleotider.

Dihydroorotatdehydrogenaser

Dihydroorotat dehydrogenaser (DHOD) er enzymer, der inderholder flavinmononucleotid (FMN) som cofactor. De katalyserer oxidationen af (*S*)-dihydroorotate til orotat, det fjerde trin og den eneste redox reaktion i *de novo* biosynthesen af pyrimidin nucleotider. *Lactococcus lactis* er den eneste organisme som indeholder do forskellige DHOD's, DHODA og DHODB. Den ene af disse DHODA findes som en dimer, der indeholder en FMN per subunit. Det andet enzym, DHODB, er en heterotetramer opbygget af to forskellige polypeptider. I modsætning til DHODA kan DHODB benytte $NAD^+$ som elektron acceptor. Det heterotetramere protein kompleks indeholder to FMN, to FAD og to (2Fe-2S) jern-svovl klynger som cofactorer. Krystallerne af DHODA var både tilstrækkeligt store og af en kvalitet, som gjorde det muligt at bestemme strukturen af DHODA til en opløsningseevne på 2.0 Å ud fra data indsamlet med en konventionel Røntgenkilde (1).

Krystallerne af DHODB er generelt af langt ringere kvalitet. Kun lejlighedsvis er det lykkedes at finde en krystal af det tetramere protein kompleks, der diffrakterer til en opløsningsevne, der

er højere end 4.0 Å med vores "in house" dataindsamlingsfacilitetet. Dataindsamlingen med synkrotronstråling med en bølgelængde på 0.96 Å på beamline X11 på EMBL viste en kraftig forbedring af opløsningsevnen til 2.2 Å. Disse data har dannet basis for bestemmelsen af DHODB strukturen.

Phosphoribosyl pyrophosphat synthetase (PRPPsase).

5-Phosphoribosyl-alfa-1-phosphate (PRPP) indgår som sukker-phosphat delen i alle ribonucleotider. I den biosynthetiske fremstilling af PRPP sker der en usædvanlig overførsel af en pyrophosphat gruppe fra ATP til ribose 5-phosphat, samtidig virker ADP hæmmende på enzymets funktion.

Oprindeligt blev de hexagonale krystaller af PRPPsase fremstillet ved fældning med ammonium sulfat under tilstedeværelsen af ATP, ribose-5 phosphat og ADP. Krystalstrukturbestemmelsen viste dels at PRPPsase findes som den funktionelle hexamer i krystallen dels at der var bundet sulfationer til proteinet i stedet for de foventede nucleotider. Derfor søgte vi at ændre krystallisationsbetingelserne, så man undgik tilstedeværelsen af sulfat. Det lykkedes at fremstille krystaller fældet med citrat men disse var af langt ringere kvalitet end de tidligere krystaller og diffrakterede kun til 2.8 Å opløsningsevne med vores lokale dataopsamlingsudstyr.

Vi opnåede en kraftig forbedring af opløsningsevnen (2.2Å) ved at benytte synkrotronstråling. Data indsamlet på beamline X11 i Hamburg er blevet benyttet til en færdigforfining af strukturen, hvor det er muligt at identificere og få et detaljeret billede af proteinets katalytiske og allosteriske nucleotid bindnings sites.

(1) Rowland, P., Nielsen, F.S., Jensen, K.F. and Larsen, S. Structure 5 (1997) 239-252.

# *In-situ* studies of air electrodes in Solid Oxide Fuel Cells at 850°C using hard x-rays at BW5.

F.W. Poulsen, L. Sörby*, H.F. Poulsen and S. Garbe
Materials Department, Risø Nat. Lab.,
DK-4000 Roskilde Denmark
Kemiska Institutionen*, Uppsala University,
S-75121 Uppsala Sweden

Purpose. The kinetics of oxygen reduction at high temperature in solid oxide fuel cells is currently under discussion. Oxygen from the gas phase, as well as oxygen from the air electrode material itself, may be involved. The air electrode is typically a Sr-doped lanthanum manganite perovskite (LSM) deposited on yttria stabilised zirconia ceramics (YSZ).

Experimental details. A versatile vertical furnace with quarts windows (max. operating temperature 1000°C), housing a plug-in sample holder system has been developed and successfully tested. The transmission through windows and the electrochemical cell at BW5, using 0.124Å radiation, is approximately 50%. In a conventional two-axis set-up we used a CCD 2D detector (Photonic Science) at a distance of 3.6 m from the sample, allowing inspection of the 2-theta range from 2-4°. Images were acquired at 1 to 10 min intervals, with corresponding exposure times. A total of approx. 2000 images were recorded from 6 different electrochemical cells. The cells had silver foil/net current collectors on both sides - a silver painted counter electrode and a 5-50 μm LSM layer on a 150 μm thin YSZ ceramic plate.

Results. Integration of sections of the Debye-Scherrer pictures allows conventional powder diffractograms to be obtained. Systematic changes in lattice parameters, integrated intensities and FWHM's of the LSM phase are observed, when the LSM air electrode is polarised electrochemically in reducing or oxidizing direction, cf. the figure below. The peak positions from YSZ are unchanged. This is the first experimental proof that the oxygen stoichiometry of LSM is strongly influenced by the electrochemistry taking place. The lattice expands under reducing conditions due to a decrease in the oxygen content in LSM. Rietveld refinement on the data are in progress.

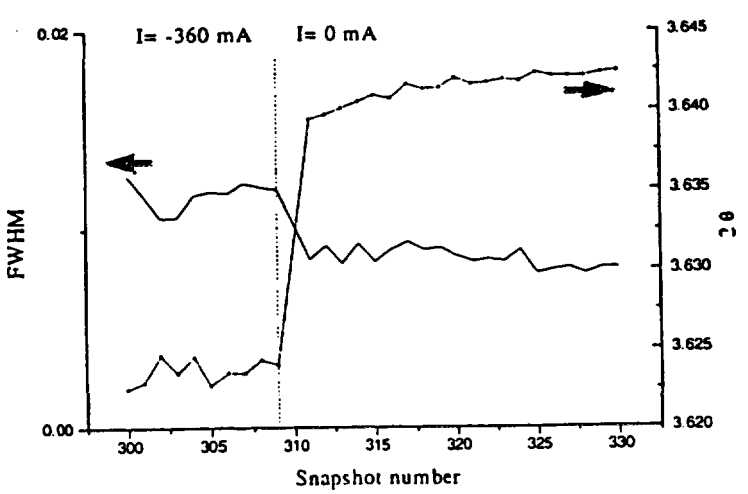


Figure 1. Analysis of diffraction data from a Ag/YSZ/LSM/Ag electrochemical cell under cathodic ( -360mA) and no polarisation. Cell at 850°C in air. Transmission experiment at BW5 with 0.124Å radiation. Snapshot number on x-axis equals minutes after start.

# Local Strain around Inclusions in Wire Drawn Cu/W Composites

T. Lorentzen [1], A.P. Clarke[1], H.F. Poulsen[1], S. Garbe[1] and H. Graafsma[2]
[1] Materials Department, Risø National Laboratory, DK-4000 Roskilde, Denmark
[2] ESRF, F-38043 Grenoble CEDEX, France

Purpose To study the local strain field around embedded inclusions in composite samples.

Experimental 8 cylindrical specimens of diameter 3 mm were investigated. Samples were produced by casting copper around long, single-fibre inclusions of tungsten and subject them to drawing and various heat treatments. Measurements were performed at beamline ID11, ESRF, operating at 80 keV. The radial and axial strain components, $\varepsilon_r$ and $\varepsilon_a$, were mapped in three dimensions with a spatial resolution of 20x20x270 $\mu m^3$ and with a precision of $\Delta\varepsilon = 1\times10^{-4}$.

Results Typical results are shown in Fig. 1. The variation in radial strain along a given diameter was small - of the order of $\pm3\times10^{-4}$. The axial lattice strains, however, showed a very strong variation with radial position showing a strong shift towards compression near the fibre interface. The strain variation was independent of axial position even when measurements were made far from the end of the fibres. A 'knee' in the axial lattice strains at mid-radius was observed. This is related to strong variations in texture (measured simultaneously). The observed strain variations are not consistent with standard theory based on the strains being related to thermal expansion, plastic or elastic mismatch between the W-fibre and Cu matrix. In stead we propose, the observed compressive shifts to be caused by the deformation of the Cu matrix by the W-fibre segments as they slipped relative to the matrix during wire drawing. This would result in a uniaxial compressive stress in the core of the Cu matrix balanced by tensile stresses towards the sample surface similar to the process of inducing biaxial stresses by grinding.

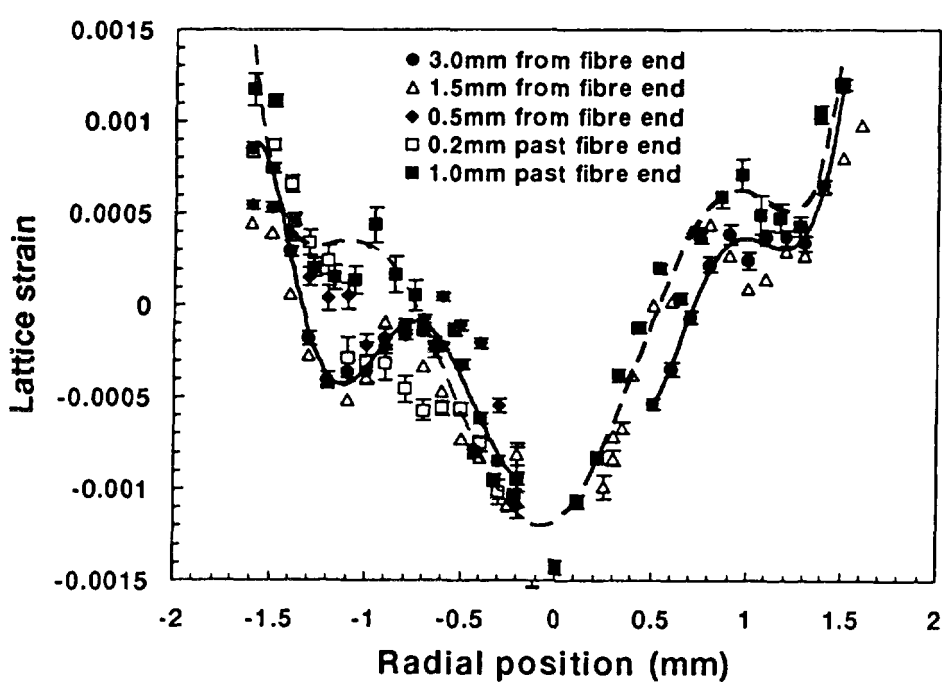


Fig. 1. (111) axial lattice strain as a function of radial position at several axial positions in a sample with a 4.5 mm long, 0.5 mm diameter W-fibre along the axis. The solid line is a polynomial fit to the closed circles and the dashed line a fit to the closed squares.

# Characterization of point defect clusters in n-irradiated Cu

H.F. Poulsen, S. Garbe, M. Eldrup, and B.N. Singh
Materials Department, Risø National Laboratory, DK-4000 Roskilde

Purpose Within the field of radiation damage it is well established that small clusters of self-interstitial atoms and vacancies may be formed during neutron irradiation in addition to larger voids. The interstitials form dislocation loops while the vacancies form loops as well as stacking fault tetrahedra. At present it is very difficult by any technique to quantify the concentration of the two types of clusters, due to their size (1-5 nm). A feasibility study is performed to learn whether such a quantification may be done by means of diffuse x-ray scattering.

Experimental A set of identical disk shaped Cu single crystals were irradiated for 2500 h in the DR3 reactor at Risø. One was used for synchrotron measurements at the 3-axis diffractometer at beamline BW5, HASYLAB using 100 keV X-rays. Others will be investigated by positron annihilation and TEM techniques, which will provide data on concentration of voids and defect clusters.

Results The diffuse scattering around the Cu (200) reflection was mapped out in 2 dimensions - in the (100)/(110) plane - before and after *in-situ* annealing at 700 °C in vacuum. The peak width (FWHM) along <100> was observed to narrow from 0.005 $Å^{-1}$ to 0.002 $Å^{-1}$ with the center shifted towards lower Q-values, cf. Fig. 1. At the same time a broad plateau situated at $-0.025\ Å^{-1} < Q_{<100>} < -0.01\ Å^{-1}$ and $-0.012\ Å^{-1} < Q_{<110>} < 0.012\ Å^{-1}$ disappeared after annealing. The two effects are attributed to interstitials and vacancies, respectively. The acquirement of larger data-set (with a 2D detector) and modeling of results are planned for 1997.

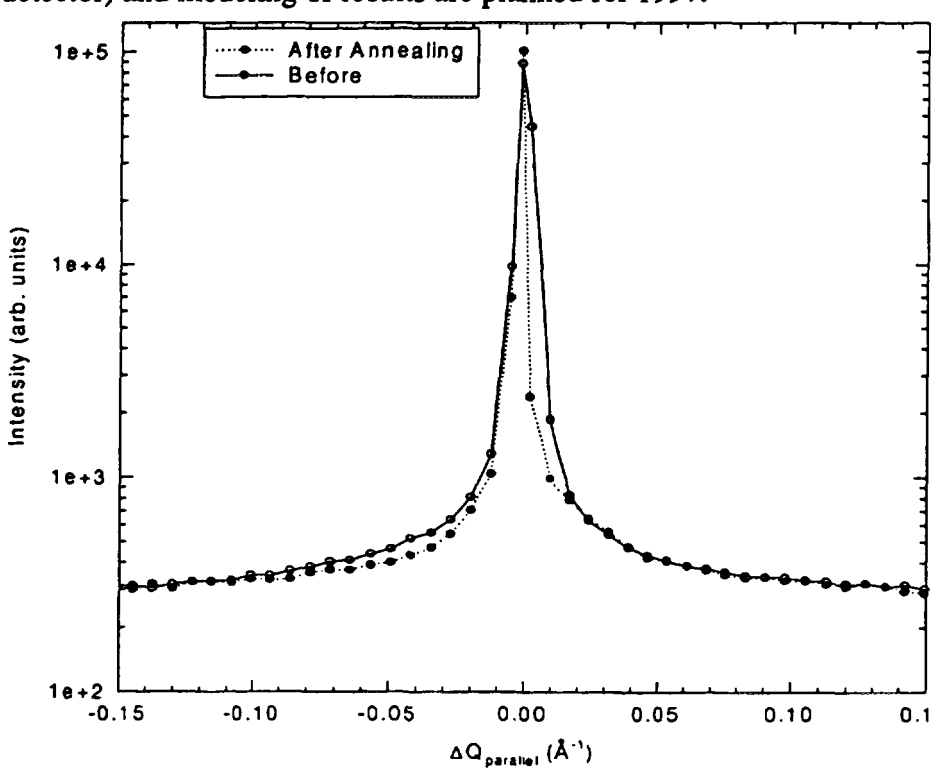


Fig. 1. Scan along <100> through the center of the Cu (200) peak. The instrumental resolution is $4x10^{-4}$ $Å^{-1}$. The plateau on the low Q side is obscured in this figure by a rod of diffuse scattering along <100> going through the center of the peak.

# Characterization of local texture in Aluminium

S.Garbe[1], J.Falk[2], D. Juul Jensen[1] and H.F.Poulsen[1]
[1]Risø National Laboratory, Materials Department, DK-4000 Roskilde
[2]Technical University of Denmark, DK-2800 Lyngby

Depending on process parameter, the texture in a rolled plate may be homogeneous or inhomogeneous through the thickness of the plate. Knowledge about such possible through-thickness texture variation allows optimization of process parameters. By standard techniques the texture in a layer in a given depth from the surface can only be determined destructively. The most commonly used technique is laboratory X-rays and for such measurements the sample has to be serial sectioned or polished to the given depth. A new measurement technique using high energy X-rays have been developed. The penetration power is in the cm-range. In comparison to sectioning measurements are fast, non-destructive, and provides higher spatial resolution as well as better quality texture data.

A broad band (10 x 500$\mu m^2$) monochromatized incident synchrotron beam is defined by a slit system. Thereby, textures in 10$\mu$m thick layers can be determined. Measurements are done layer by layer, while rotating the sample only from 0° to 90° at every layer. The specific diffraction pattern (Debye-Scherrer-cones) are registered in a high resolution 2D-CCD-camera.

The first series of measurements were carried out at the beam line BW5 of HASYLAB at DESY in Hamburg. An example of the results are given in the figure. This particular sample was inhomogeneous rolled to a strain $\varepsilon$ of 0.2. Large texture variations from the surface to the center of the rolled plate is observed.

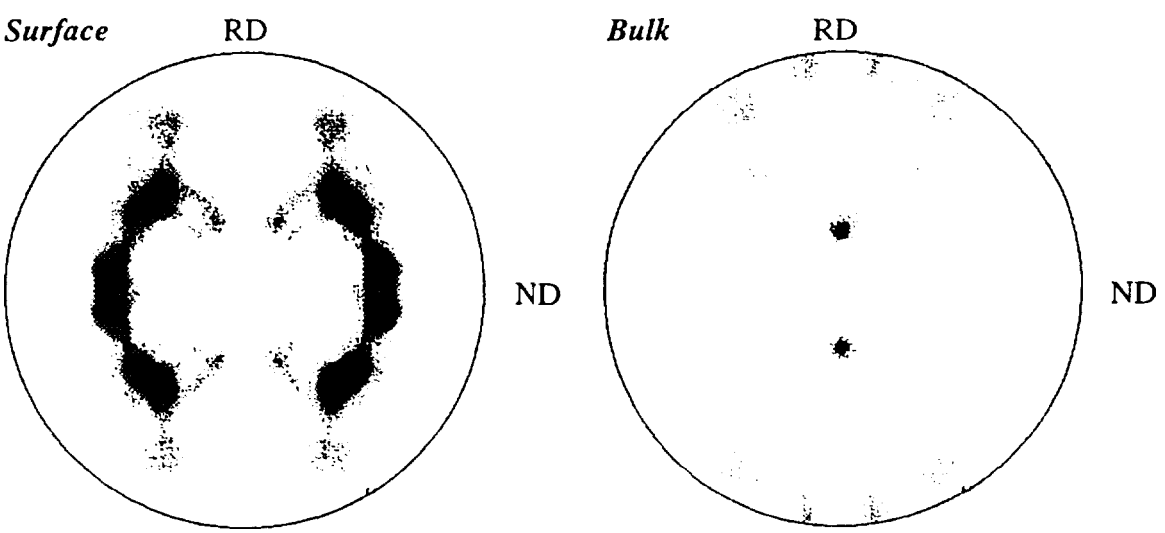


Figure 1: The texture expressed in terms of a (200) pole figure of an inhomogeneous rolled aluminium sample at the surface (50$\mu$m) and in the bulk (3000$\mu$m) (RD = Rolling Direction, ND = Normal Direction).

# Characterization of Grain Boundaries in Copper

S.Garbe[1], D.Juul Jensen[1], U.Lienert[1], H.F.Poulsen[1]and H.Graafsma[2]
[1]Risø National Laboratory, Materials Department, DK-4000 Roskilde
[2]ESRF, F-38043 Grenoble CEDEX, France

The three-dimensional conglomeration of grains and grain boundaries is a fundamental characteristic of polycrystalline materials. The topology of the boundaries is governed by an interplay between spatial and crystallographic parameters. In order to establish the underlying growth-laws, a need is identified for a non-destructive experimental technique, which allows for simultaneous determinations of the crystallographic orientations of the individual grains and 3D mappings of the positions of the associated boundaries. The experiment was a feasibility study of the use of hard X-rays for such purposes. In order to compare with conventional technique selected local volumes within the surface of a 5 x 5 x 3 $mm^3$ sample of 99.99% pure Copper were investigated.

In order to achieve a sufficient penetration power the measurement were performed at 88.08 keV at the material science beam line ID11 at the ESRF. The diffraction pattern were registered on a 2D CCD-camera. The local volume information was obtained by a novel cross-beam technique, involving the use of a conical collimator. The incoming beam was confined by a pin-hole to 20 μm x 20 μm. The diffracted beam was collimated by the conical collimator, cf. Fig. 1. The collimator has two sets of cone shaped openings orresponding to the <311> and <200> Debye-Scherrer cones in an FCC system. It is made of 5 mm thick Ta material with a width of the cone openings of 20 μm leading to a gauge volume of 20 x 20 x 400$\mu m^3$.

On the surface reflections from the individual grains were found. The intensities of the reflections were then mapped two-dimensionally with a step size of 50 μm x 200μm. Based on these data the grain boundaries were determined after a suitable correction for the spatial resolution function. From a set of reflections belonging to the same grain, the crystallographic orientations of the individual grains were determined with an accuracy of the order 1°. This accuracy is comparable to the conventional electron microscopy technique (EBSP). The resulting map of all grains and their surroundings are shown in Fig. 2. Microscopy work on the same sample is presently being done using EBSP.

The present experiment demonstrates the potential of synchrotrons radiation for non-destructive grain mapping in the $\mu m^3$-scale.

There are several options for substantial improvements of the spatial resolution and the speed of data collection, including the use of conical slit-systems with a reduced gap (presently being designed), software that couples data collection and motor control, and the use of broad-band focusing at the high energies (multilayers, imperfect monochromator crystals). Still, the present set-up enables various *in-situ* growth studies of fundamental interest to recrystallization.

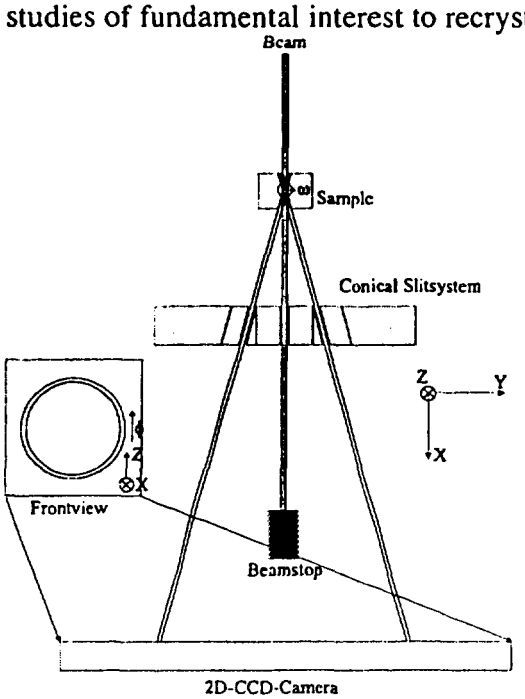


Fig. 1: Schematical view of the novel cross beam technique.

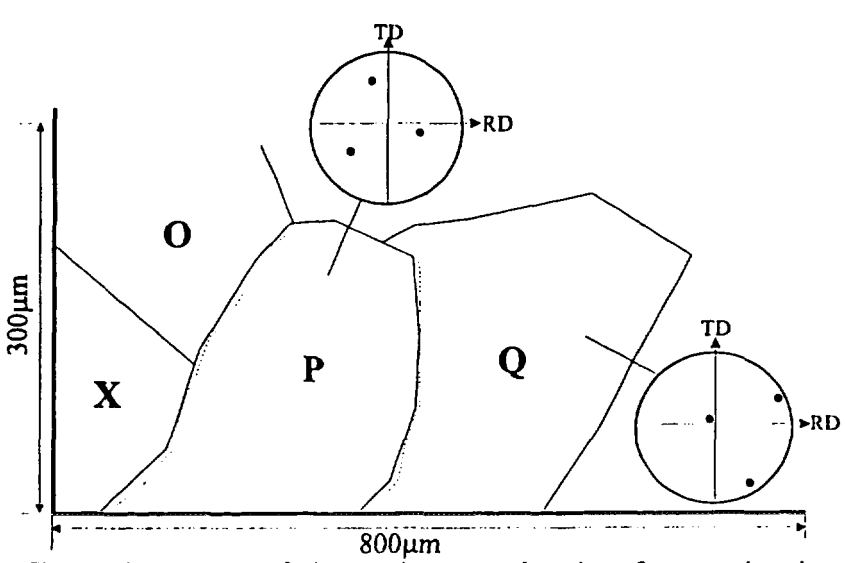


Figure 2: A part of the grain map showing four grains in the Copper sample describing their orientations in terms of a pole figure (RD = Rolling Direction, TD = Transverse Direction). The grain boundaries are determined in two ways scanning one reflection of the P-grain (solid line) and of the Q-grain (dashed line).

# SYXRF measurements on $(Pb,Bi)_2Sr_xCa_yCu_zO_w$ /Ag superconducting tapes

S.Garbe[1] and F.Lechtenberg[2]
[1]Risø National Laboratory, Materials Department, DK-4000 Roskilde
[2]Röntgen-Analytik-Service, Klingenberg 16a, D-25451 Quickborn

Risø National Laboratory is involved in the design and optimisation of High Tc superconducting tapes and cables of the $(Pb,Bi)_2Sr_xCa_yCu_zO_w$ /Ag type in collaboration with other Danish institutes and the industrial partner NKT Research Center. The spatial variation of the various chemical phases within the Ag sheet of the tapes has recently attracted much attention. A need has been identified for a technique that determines the elemental distribution more accurately than what presently is obtainable with the electron microscope (EDAX). The aim of the experiment is to determine the suitability of SYXRF for such measurements and to determine the degree of inhomogeniety within selected samples.
The measurements were performed at beam line L using the SYXRF set-up. The beamsize was collimated by an ordinary slit-system to 10 x 10 $\mu m^2$. The samples were 9 sectioned parts of tapes each consisting of a layer of 5 μm superconducting material on a 60 μm Ag-layer. In addition a $Bi_{1.8}Pb_{0.3}Sr_{1.8}$ $Ca_1Cu_2O_x$-standard from Hoechst was investigated. Acquisition times are 1800 sec. The elemental distribution in the standard was also was also determined with an electron-microprobe (EMS) (Cameca SX-50)[2].

| Sample | Method | O (x=10) | | Bi | | Ca | | Cu | | Pb | | Sr | |
|---|---|---|---|---|---|---|---|---|---|---|---|---|---|
| | | cert. | exp. | cert. | exp. | cert. | exp. | cert. | exp. | cert. | exp. | cert. | exp. |
| Reference | EMS | 17.17 | 14.08 | 40.36 | 40.23 | 4.30 | 4.24 | 13.64 | 14.53 | 6.67 | 6.78 | 19.07 | 17.86 |
| Ref W90PW96 | SYXRF | | 15.18 | | 39.43 | | 5.13 | | 14.14 | | 6.90 | | 18.20 |
| F69A1W68PW69 | SYXRF | | 16.71 | | 38.43 | | 5.20 | | 14.67 | | 7.12 | | 14.67 |

Table 1:
Experimental results of the SYXRF and the EMS-measurements of the reference $Bi_{1.8}Pb_{0.3}Ca_1Sr_{1.8}Cu_2O_x$ sample compared to certificate values (above). SYXRF for one of the tape sections (below).

As a first result the SYXRF and EMS data for the standard are compared with the certificate values in table 1. The agreement at most of the elements is within 2%. The discrepancies may be explained in terms of observed inhomogenities in topography and in the elemental distribution of the reference. In conclusion, the SYXRF method needs further development and the use of better standards.
Also shown in the table are the experimental data for one of the tape sections. The data analysis for the 9 samples is still on-going, but preliminary results point to variations of up to 5% within some of the samples.
We acknowledge the staff from beam line L, especially M. Radtke, for their support. Furthermore we would like thank NKT Research Center for providing the samples.

**Annealing of Silver-clad BiSCCO Wires Studied in-situ by High-Energy Synchrotron X-ray Diffraction.**

T. Frello, H.F. Poulsen, N.H. Andersen, S. Garbe, A. Abrahamsen, *Risø National Laboratory, Denmark*, M.D. Bentzon, *NKT Research Center, Brøndby, Denmark*, M. von Zimmermann, *HASYLAB, Hamburg, Germany.*

Much effort is put into the development of superconducting wires for power transmission.. A key point in obtaining a high critical current density $j_c$ in the tapes is the optimisation of the heat-treatment of the wires. During annealing at ≈840 °C the BiSCCO-2212 phase ($T_c$=85 K) is transformed into the BiSCCO-2223 phase ($T_c$=110 K) inside the silver cladding. The influence of the silver on the phase transformation as well as the texture development is not yet well understood. We have used High-Energy Synchrotron X-ray Diffraction for an *in-situ* study of the solid state transformation and texture formation of the BiSCCO powder inside the silver cladding during annealing. The photon energy used was 100 keV, having sufficient penetration power to allow for X-ray diffraction in a transmission geometry. To our knowledge, this is the only technique suitable for such *in-situ* measurements. The diffraction patterns were recorded by a two-dimensional CCD detector, enabling us to obtain simultaneous information of both phase development as well as texture formation, see Fig. 1. Experiments were performed for single- and multi-filament wires with annealing temperatures of 820, 835 and 850 °C for up to 26 hours. We find that the texture improvement takes place almost exclusively for the 2212 phase, starting already during the initial heating before the final annealing temperature is reached. The 2223 phase is created from the 2212 crystallites, thus the 2223 texture is strongly dependent on the 2212 texture. We also see a melt phase appearing between 837 and 850 °C, apparently related to a degradation of the superconductor compound. Both heating and cooling ramps have a great influence on the development of the BiSCCO phases as well as secondary non-superconducting phases. The solid state transformation generally runs faster for the multi-filament wires and the optimum annealing temperature also seems to be lower than for the single-filament wires.

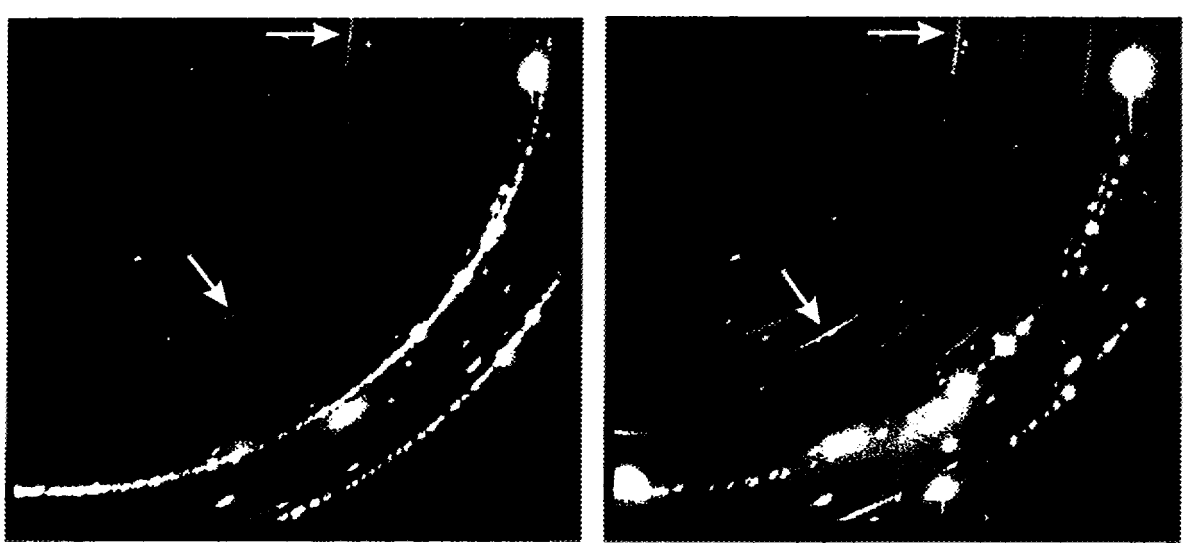

a) b)

Fig. 1. Diffraction images from the CCD detector for a single-filament wire annealed at 835 °C for a) 0 hours and b) 26 hours. The ring segments indicated by arrows on the figure are diffracted signals from the BiSCCO. The full rings and bright spots originate from the silver cladding. The images show that the 2212 phase in a) is totally transformed into the 2223 phase in b). Furthermore, the texture of the 2223 phase is considerably more narrow than that of the 2212 phase. The annealing also leads to a recrystallisation of the silver.

## Phase Behaviour of Hydrocarbon-poly(dimethylsiloxane) Diblock Copolymer Melts Related to Temperature and Their Volume Fraction of Hydrocarbon

M.E. Vigild, S. Ndoni, and K. Almdal, *Department of Solid State Physics, Risø National Laboratory.* I.W. Hamley, *School of Chemistry, University of Leeds, UK*, J.P.A. Fairclough, and A.J. Ryan, *Manchester Materials Science Centre, UMIST, UK*

In this study we present the first promising results showing the features of the phase diagramme for an asymmetrically composed poly(ethylene-alt-propylene)-poly(dimethylsiloxane) (PEP-PDMS) copolymer system. Samples are very carefully synthesised by "living" anionic polymerisation (please see K.Almdal et al. elsewhere in this report). Di-block copolymers are known to form different phases under conditions given by the molar mass and the strength of interaction between the chemically distinct units of the polymer. This dependence is summarised in the variable $\chi N$ (the Flory-Huggins interaction parameter $\chi$ times the molar mass $N$) as is illustrated along the y-axis in Fig. 1. $\chi N$ is inversely related to the temperature. Individually synthesised block copolymers are mapped along the x-axis in Fig. 1 as a function of the volume fraction of hydrocarbon. This constitutes a semi-phase diagramme of the PEP-PDMS system falling in the two ranges of the volume fraction: 0.3 to 0.5 and 0.6 to 0.7.

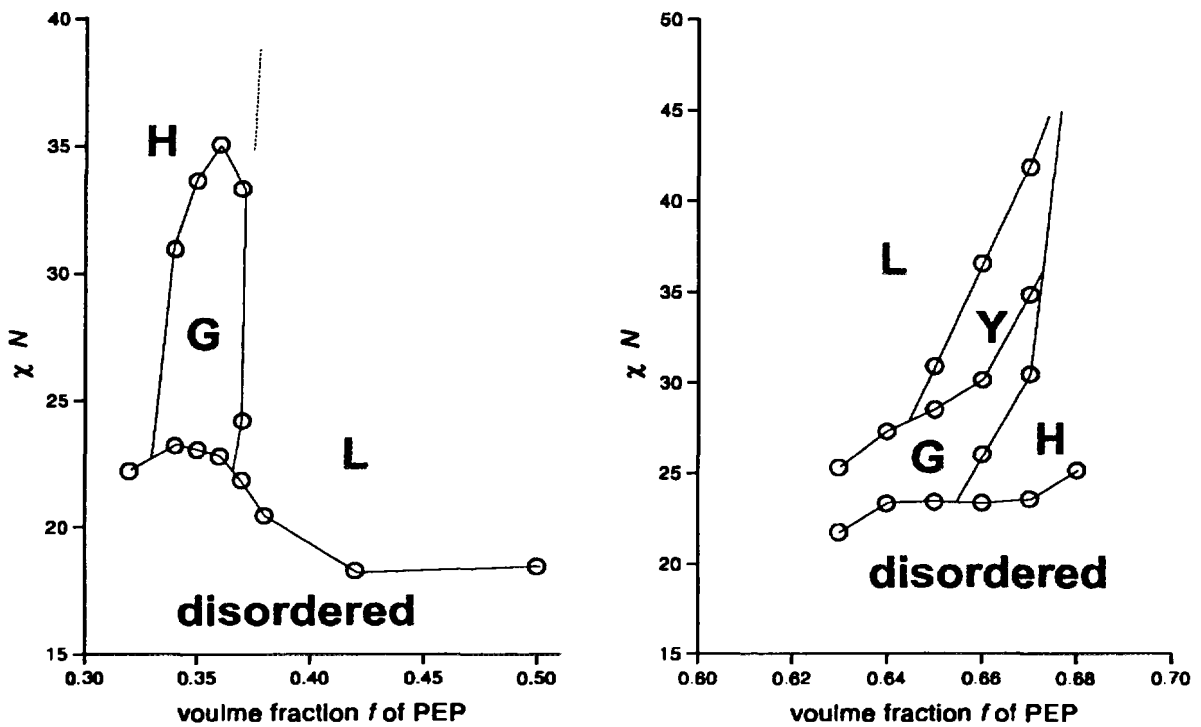


Fig. 1. Semi-phase diagrammes of PEP-PDMS falling in the volume fraction ranges of 0.3 to 0.5 and 0.6 to 0.7.

Phase transition temperatures between ordered states, $T_{OOT}$, and from ordered to disordered states, $T_{ODT}$, are determined by dynamical mechanical spectroscopy measuring the value of the elastic shear modulus G' as a function of temperature. The phase structures in the ordered states are analysed by using small angle x-ray scattering (SAXS). Our investigation shows that especially the asymmetrically composed PEP-PDMS system transforms through a series of morphologies as the temperature rises until, eventually, the polymer disorders. The phases identified are lamella (L), hexagonal (H), gyroid (G), and at the present an unidentified metastable phase (Y).

## An X-ray Photon Correlation Spectroscopy Experiment on a Diblock Copolymer System

C.M. Papadakis and K. Mortensen, *Department of Solid State Physics, Riso National Laboratory, Denmark*, D. Posselt, *Institute of Mathematics and Physics, Roskilde University, Denmark*, D.-M. Smilgies, D.L. Abernathy, and G. Grübel, *European Synchrotron Radiation Facility, Grenoble, France*

The dynamic processes in block copolymer systems in the bulk are still under intensive discussion.[1] Photon correlation spectroscopy (PCS) using laser light has been the most important technique for investigations of the dynamics.[1] X-ray photon correlation spectroscopy (XPCS) using synchrotron radiation constitutes a new method to study these processes on a time-scale between milliseconds and ca. 100 sec and covering larger $q$-values than is possible with PCS.[2]

We have studied the dynamics of a low molar mass, symmetric polystyrene-polybutadiene diblock copolymer sample in the disordered state using XPCS. In previous PCS-experiments, four processes had been identified, two of which are related to the diblock structure: one related to single chain diffusion and another attributed to chain relaxation and chain stretching.[3] However, the time-dependent correlation function of the scattered intensity, $g_2(t)$, is dominated by a slow process (~100 s), attributed to long-range heterogeneities (~100 nm), which hampers the characterization of the other modes.[3] As the relative amplitude of the mode related to the long-range heterogeneities decreases with increasing $q$, XPCS may allow more detailed studies of the other modes.

The XPCS-experiment was conducted at the TROIKA beamline at the ESRF. In order to achieve a transversally coherent beam, an 8 $\mu$m pinhole was inserted into the beam. $g_2(t)$ was measured at two different temperatures in a $q$-range between 0.0036 and 0.011 Å$^{-1}$. The curves display a fast decay in the millisecond range. However, the decays are obscured by oscillations having a period of 60 ms, which are attributed to mechanical instabilities in the set-up. In order to extract the relaxation times of the fast decay, the sum of a fast exponential decay and a damped sine-function have been fitted to the data (Fig. 1):

$$g_2(t) = 1 + b(1 + a_1 e^{-t/\tau_1})^2 + a_2 \sin\left(\frac{2\pi}{T_2} t + \varphi\right) e^{-t/\tau_2} \qquad (1)$$

The relaxation times of the fast decay, $\tau_1$, are found to be between 1.5 and 7.0 ms, in accordance with the relaxation times of the mode related to chain diffusion observed in PCS-experiments. However, in order to investigate the sample dynamics closer, the origin of the oscillations should be located and eliminated.

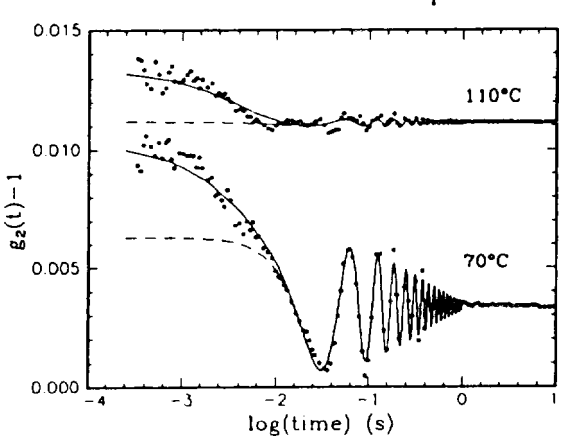


Fig. 1: Time-dependent intensity autocorrelation functions of a polystyrene-polybutadiene sample measured using XPCS (q = 0.0036 Å$^{-1}$). The full lines are the fits of Eq. 1 and the dashed lines of the oscillating part alone. For clarity, the curves are shifted.

[1] P. Stepanek and T. P. Lodge, in "Light Scattering. Principles and Development". Oxford 1996.
[2] *E.g.* I. K. Robinson *et al.*, Phys. Rev. B, **52**, 9917 (1995).
[3] C. M. Papadakis, W. Brown, R. M. Johnsen, D. Posselt, and K. Almdal, J. Chem. Phys., **104**, 1611 (1996).

## X-ray Diffraction from Curved Thin Films

P. B. Howes and K. Kjær, *Department of Solid State Physics, Risø National Laboratory, Denmark*

X-ray diffraction has proved to be a powerful technique in the study of Langmuir monolayers. It is well known that diffraction from a flat, two-dimensional, crystalline monolayer leads to rods of scattering in reciprocal space which are sharp in the directions parallel to the surface, $q_{xy}$, but extended perpendicular to the surface: along $q_z$. A number of experiments on amphiphilic mono- or multi-layers have given rise to diffraction which, instead of exhibiting the expected Bragg rod (see Fig. 1a), are additionally extended along a curved line[1] which follows the Scherrer ring of constant $(q_{xy}^2 + q_z^2)^{1/2}$ (see Fig. 1b). Such scattering can be explained by a mosaic spread in the normals of flat crystallites.[2] Another possible explanation is that the individual crystallites may be curved (Fig 1c); however it is not immediately obvious if this would give rise to the observed peak profile, or whether an X-ray diffraction experiment could distinguish the two cases. To investigate this phenomenon, we have performed numerical simulations of the X-ray scattering from both curved crystallites and mosaic distributions of flat crystallites. The simulations were performed on one-dimensional crystals (Fig 1c). The electron density of the long, linear molecules was taken to be a Gaussian ellipse for simplicity. For the curved domains, the scattered intensity was calculated as the coherent sum in reciprocal space of the Fourier transforms of $N$ molecules on a circularly curved line with radius $R$. For the case of a mosaic spread of flat crystallites the Fourier transform of the density of a single crystallite was first calculated then added incoherently to that from other crystallites with different tilts.

It was found that the two different kinds of surface gave broadly similar scattering. In both cases the Bragg rod was extended along the Scherrer ring (Fig 1b). However, whereas the mosaic crystallites lead to a constant $q_{xy}$-width, the curved layer diffraction becomes broader with increasing diffraction order. Thus it is, in principle, possible to distinguish the two cases experimentally.

Fig. 1. Calculated diffraction peak profiles for a flat monolayer (N=30) (a) and a curved monolayer (N=30, R=120 intermolecular spacings) (b). Real space electron density of the curved monolayer is shown in (c).

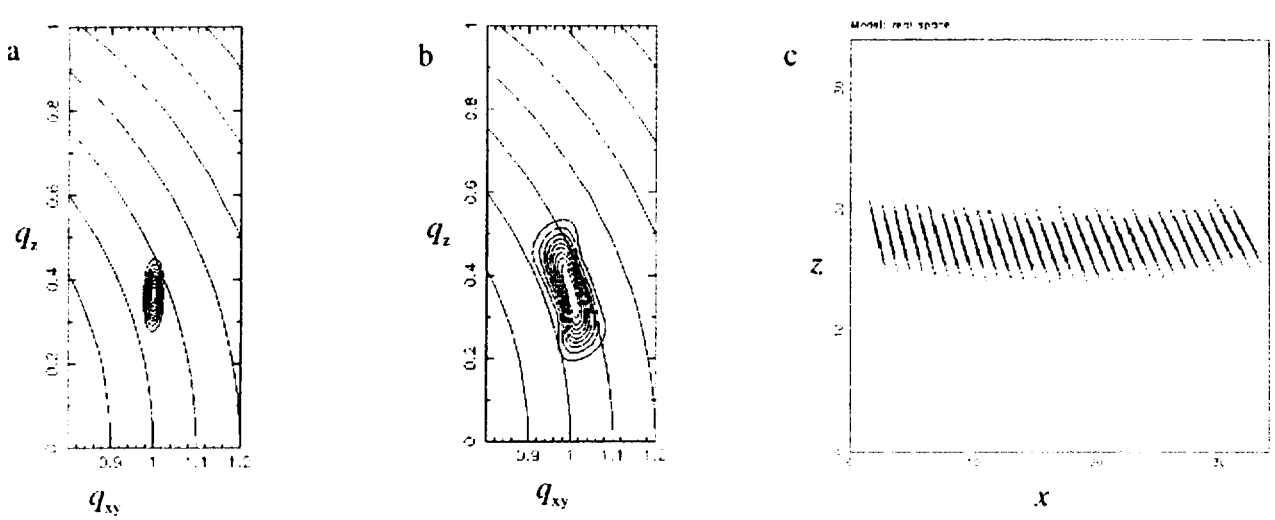


[1] S. P. Weinbach *et al.*, Ann. Rep. Solid State Physics Dept., Risø, 1994, 2.6.12 and Adv. Mater. **7**, 857 (1995)
[2] W. Bouwman and K. Kjær, Ann. Rep. Solid State Physics Dept., Risø, 1994, 2.6.1

## Studies of Phase Transitions in Langmuir Monolayers of a Triple Chain PE

F. Bringezu, G. Brezesinski, H. Möhwald, *Max-Planck-Institute for Colloids and Interfaces, Germany*, P. Howes and K. Kjær, *Department of Solid State Physics, Risø National Laboratory, Denmark*

Branched-chain phospholipid monolayers provide interesting model systems for the study of the interplay between the polar head group region and the hydrophobic chains. We have investigated condensed phases of a triple chain 1($2C_{16}$-18:0)-2H-PE (**a**, *cf.* Fig. 1) by means of Grazing-Incidence X-ray Diffraction (GIXD), using the liquid surface diffractometer at the undulator beamline BW1 in HASYLAB at DESY, Hamburg. The lipid consists of three hydrocarbon chains and one glycerophosphoethanolamine head group. In this case the molecular area is influenced by two factors. First, three chains require more space in the monolayer than the small head group. Second, regardless of the large hydrophobic part of the molecules interactions between the hydrophilic head-groups must be taken into account.[1]
The pressure ($\pi$) *vs.* molecular area ($A$) ,isotherm at 20°C indicates a phase transition at $\pi \cong 9$ mN/m (Fig. 1). $\Delta A$ yields a transition enthalpy of 16.7 kJ/mol (Clausius-Clapeyron equation). GIXD experiments were performed between 0 and 37 mN/m at 20°C. At $\pi \cong 0$ a centred-rectangular lattice with chains tilted in a symmetry direction towards nearest neighbours (NN) was observed with in-plane area *per molecule* $A_{xy} \cong 42$ Å$^2$. With increasing $\pi$ the tilt decreases from 13.5° ($\pi \cong 0$ mN/m) to 5.7° ($\pi \cong 11$ mN/m). At $\pi \cong 15$ mN/m only one sharp diffraction peak with a $d$-spacing of 4.86 Å appears, indicating a hexagonal lattice of upright oriented chains. Further increase of $\pi$ leads to decreasing $d$- and $A_{xy}$-values (4.82 Å, 40.8 Å$^2$ at $\pi \cong 37$ mN/m). Fig. 1 compares the isotherm and the $A_{xy}$ -values from the GIXD-measurements. The change in the molecular area in the isotherm is apparently not only due to a change in the lattice of the hydrocarbon chains. The phase transition from centred-rectangular to hexagonal occurs between 11 and 15mN/m and not at $\pi \cong 9$ mN/m as inferred from the isotherm. Brewster angle microscopy studies showed that, on expansion, monolayer inhomogeneities, resulting from an anisotropy contrast due to the tilting of the chains, appear between 13 and 11 mN/m. At around $\pi \cong 10$ mN/m inhomogeneities resulting from unoccupied areas in the monolayer are observed for parallel polarizers as well. In previous work[2] with DPPE a model of head group ordering was deduced from analysis of Bragg rod profiles. Possibly, the tilting of the triple-chain PE leads to an analogous orientational ordering of the head group dipoles. Thus, the surprising behaviour of (**a**), showing large differences between the molecular areas derived from isotherm and X-ray measurements below 10 mN/m, could be due to electrostatic repulsion between condensed phase domains.

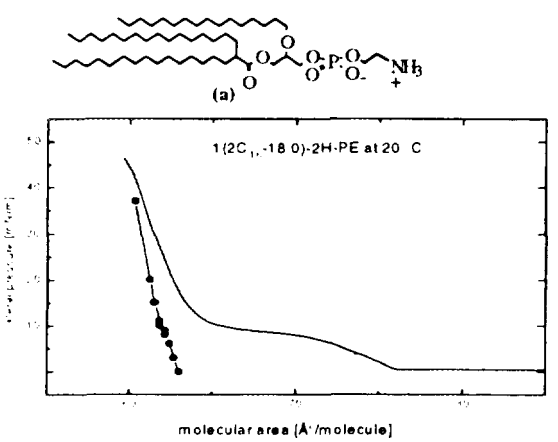


Fig. 1. Isotherm (_) and $A_{xy}$ per molecule calculated from GIXD data (•).

[1] F. Bringezu, G. Brezesinski, H. Möhwald, B. Struth, W.G. Bouwman, K. Kjær, Annual Report for 1995
[2] C. Böhm, H. Möhwald, L. Leiserowitz, J. Als-Nielsen and K. Kjær, Biophys. J., **64**, 553 (1993)

## Influence of Head Group Methylation on the Phase Behaviour of Lipid Monolayers

F. Bringezu, G. Brezesinski, H. Möhwald, *Max Planck Institute for Colloids and Interfaces, Germany* and K. Kjær, *Department of Solid State Physics, Risø National Laboratory, Denmark*

In phospholipid monolayers the interaction between adjacent head groups is one of the basic factors which influences the arrangement of the hydrophobic chains. The present investigations focus on the effect of systematic changes in head group methylation in triple- chain phospholipids on the structure of monolayers formed at the air-water interface. Therefore we have studied monolayers of the racemic 1-($2C_{14}$-16:0)-2H-PE($CH_3$)$_n$ [n=0 (**a**), 1 (**b**), 2 (**c**), 3 (**d**)] (*cf.* Fig. 1). From isotherm measurements we conclude that with increasing number of methylene groups the characteristic temperatures of the monolayers change systematically. *E. g.*, the temperature $T_0$ (at which the liquid-expanded phase appears) decreases from **a**: 16°C to **b**: 13°C, **c**: 11°C and **d**: 6°C. Grazing-incidence diffraction (GIXD) measurements (performed at the liquid surface diffractometer on the undulator X-ray beamline BW1 at HASYLAB, DESY, Hamburg) show that at 5°C and $\pi \cong 0$ mN/m monolayers of **a** exhibit 2 diffraction peaks indicating a rectangular unit cell. The molecules are tilted in symmetry direction towards nearest neighbours (NN). Increasing pressure leads to a phase transition from rectangular to hexagonal symmetry with vertical chains. On introduction of methyl groups at the nitrogen the area per head group increases continuously. The diffraction patterns of **b**, **c** and **d** at 5°C and low pressures are very similar to that of **a**, however the tilt angles are increased (see Fig.1). Methylation of the head group increases the transition pressures to the hexagonal phase. This corresponds to increasing differences of space requirement between head and tail region in the monolayer. At 15°C **a** shows only one sharp diffraction peak, indicating hexagonal packing of upright chains, even at ≅ zero pressure. Tilted phases were observed for **c** and **d** only (see Fig.1).

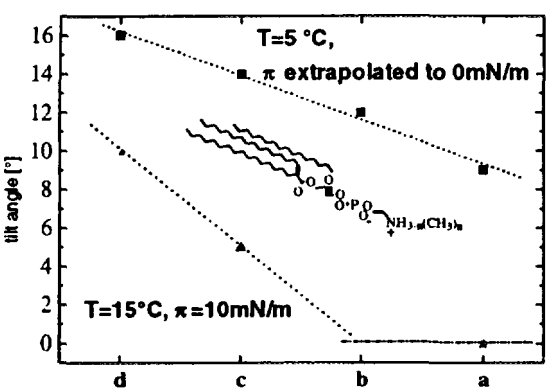


Fig.1. Tilt angle as function of methylation degree.

For further discussion it is interesting to note that for all these triple-chain lipids the phase transition from NN to hexagonal is characterised by a pressure region where the in-plane components $Q_{xy}$ of the two peaks coincide while the out-of-plane components $Q_z$ differ (see

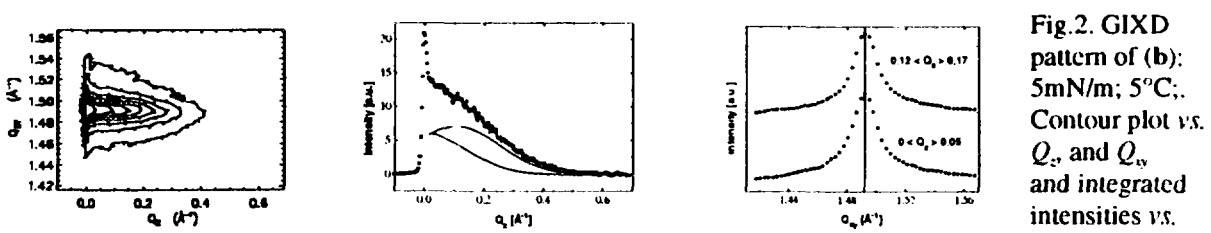

Fig.2. GIXD pattern of (**b**): 5mN/m; 5°C;. Contour plot *v.s.* $Q_z$, and $Q_{xy}$ and integrated intensities *v.s.* $Q_z$, resp. $Q_{xy}$

Fig.2). This indicates an undistorted hexagonal lattice even though the symmetry is broken by the tilted chains. Despite the large cross-sectional area of the chains one observes an influence on the phase behaviour of triple-chain phospholipids of head group size and their resulting ability to form hydrogen bonds.

## Binary Phase Diagram of Monolayers of Simple 1,2-Diol Derivatives

G. Brezesinski, F. Bringezu, H. Möhwald, *Max-Planck-Institute for Colloids and Interfaces, Germany*, P. Howes and K. Kjær, *Department of Solid State Physics, Risø National Laboratory, Denmark*

In order to obtain information about the interplay in Langmuir films between polar head groups and hydrophobic tails it is helpful to resort to simple model systems. Therefore, the phase behaviour of monolayers of several amphiphilic 1,2-diol derivatives has been characterised in recent years. Here we report on the miscibility behaviour of 1-palmitoylglycerol (1) with 1-hexadecylglycerol (2) (*cf.* Fig. 1). The different chemical linkage of the chain to the glycerol (via an ester bond in (1) and an ether bond in (2)) leads to different molecular conformations and different interactions between the hydrophilic head groups. Because of the similarity of the transition pressures of (1) and (2) we investigated the miscibility behaviour by comparing the lattice structures measured by means of Grazing Incidence X-ray Diffraction (GIXD). At all pressures up to 44 mN/m monolayers of compound (1) exhibit a rectangular lattice with chains tilted in a symmetry direction towards nearest neighbours (NN). On increasing lateral pressure the parameters *a* and *b* of the rectangular unit cell decrease continuously. For (2) the tilt direction changes towards next nearest neighbours (NNN) at a lateral pressure of 18 mN/m. This transition is connected with an increase of *b* and a decrease of *a*. Further pressure increase leads to a drastic decrease of *b* (long axis of the unit cell along the tilt direction) but a small change of *a*. Comparing the tilt angles of (1) and (2) one observes that at low lateral pressures (1) has a lower tilt angle than (2), and *vice versa* at high pressures. For a 1:3 mixture of (1) and (2) the measurements indicate a NN tilted phase between 10 and 30 mN/m. At 35 mN/m the tilt direction changes towards NNN. For a 1:1 mixture this phase transition is shifted to a lateral pressure between 40 and 45 mN/m. Since the transition pressure is higher the increase of *b* during the NN-NNN transition is smaller (see Fig. 1). The dependence of this transition pressure on the mixing ratio points to complete miscibility of (1) and (2) in all phases, so that a theoretical pressure of 67 mN/m for the transition NN-NNN of (1) can be extrapolated. The smaller *a*-values of compound (1) than of (2) at low pressures may indicate an orientation of the polarised carbonyl group along the *a*-axis. The NN-NNN transition seems to be connected with a reorientation of these carbonyl groups and therefore a higher energy (higher pressure) is needed for this transition in case of (1). The carbonyl groups stabilise the NN-tilted rectangular phase obviously not only by dipole-dipole interactions: Different molecular conformations of (1) and (2) must be assumed.

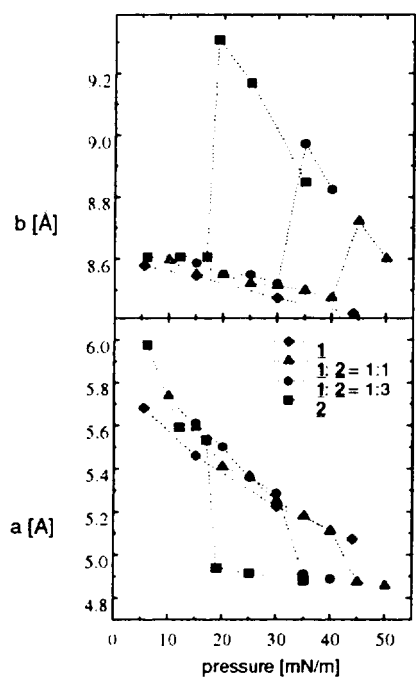


Fig.1. Lattice parameters *a* and *b* of the rectangular unit cell vs. pressure at 20 °C.

**Influence of Polyelectrolyte Coupling on the Structure of Charged Monolayers**

K. de Meijere, G. Brezesinski, H. Möhwald, *Max Planck Institute for Colloids and Interfaces, Germany* and K. Kjær, *Department of Solid State Physics, Risø National Laboratory, Denmark*

Langmuir monolayers of charged lipids coupled to polyelectrolytes of opposite charge are of interest for understanding the importance of different interactions on the structure of the monolayer. The present investigations focus on structural changes, shifts of phase transitions and the phase diagram of negatively charged 1,2-dipalmitoyl phosphatidic acid (DPPA) at the air/water interface at normal *pH*, bound to the positively charged polyelectrolyte PDADMAC (see Fig. 1, left) using pressure/area isotherms, fluorescence microscopy and Grazing-Incidence X-Ray Diffraction (GIXD) at the liquid surface diffractometer on the undulator beamline BW1 at HASYLAB, DESY, Hamburg, Germany.

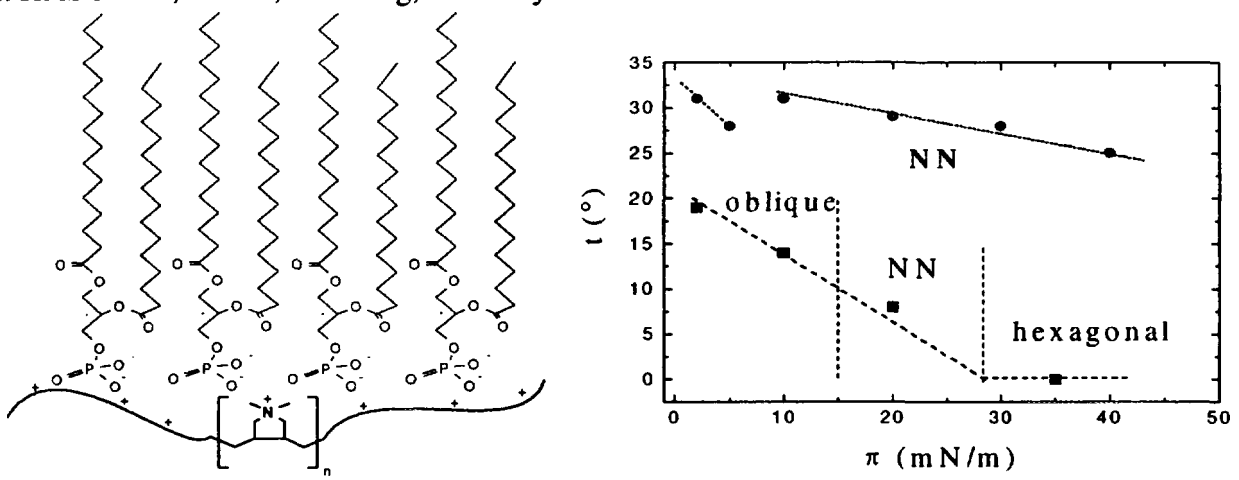


Fig. 1. Left: Chemical structures of the lipid DPPA and the polyelectrolyte PDADMAC (poly-[$CH_2CHCH_2N^+(CH_3)_2CH_2CHCH_2$]). Right: phase diagram of DPPA on water (■) and DPPA on PDADMAC (•).

The isotherms show that binding to the polymer causes an expansion of the DPPA monolayer. At low lateral pressure coexistence of ordered and disordered regions, with possible protrusion of polymer into the disordered monolayer regions, is observed by fluorescence microscopy. On increase of pressure, the inhomogeneities are gradually removed. At high lateral pressures (>20 mN/m) polymer insertion into the film can be excluded by comparing the molecular areas derived from isotherm and GIXD measurements. Fig. 1 (right) shows a schematic phase diagram (tilt angle t versus lateral pressure $\pi$) deduced from GIXD. At all pressures investigated the film of the coupled system exhibits two X-ray diffraction peaks, indicating a rectangular structure with uniform chain tilt. The tilt angle decreases only slightly with increasing lateral pressure while on pure water DPPA has a much lower tilt angle at all pressures, decreasing to zero for $\pi >$ 28 mN/m. Binding to the polyelectrolyte leads to a decrease of the lateral lipid density, and to optimise van der Waals interaction the lipid responds by an increase of the tilt angle. The pure acid film has the phase sequence oblique-rectangular-hexagonal. The removal - for DPPA bound to PDADMAC - of the oblique phase at low pressure is apparently due to destruction of the head group lattice by the polyelectrolyte. The well-defined rectangular structure of the DPPA monolayer coupled to the polyelectrolyte may be due to the 1:1 stoichiometry of the complexes[1] where the packing constraints are determined by the polymer because of its strong entropic forces.

[1] H. Dautzenberg, J. Hartmann, S. Grunewald, F. Brand, Ber. Bunsenges. Phys. Chem. **100**, 1024 (1996)

## Superlattices of Crystalline Copper Complexes of α-Amino Acid Amphiphiles at the Air-Aqueous Solution Interface

I. Weissbuch, M. Berfeld M. Lahav, L. Leiserowitz, *Department of Materials & Interfaces, The Weizmann Institute of Science, Israel*, J. Als-Nielsen, *Niels Bohr Institute, H.C. Ørsted Laboratory, Denmark*, P. Howes and K. Kjær, *Department of Solid State Physics, Risø National Laboratory, Denmark*

The reaction between insoluble amphiphiles and soluble ions from the subphase can lead to the formation of self-assembled crystalline monolayers of complex systems in 2D superstructures involving several molecules.[1] The present study describes the effect of the length and nature of the hydrocarbon chain of zwitterionic α-amino acid amphiphiles, R-CH($NH_3^+$)$CO_2^-$, on the packing of their crystalline copper complexes, self-assembled at the air-aqueous solution interface. Fig. 1 (left) shows the grazing-incidence X-ray diffraction (GIXD) pattern for a monolayer of the amphiphile with R=$C_{15}H_{31}$-CONH-$(CH_2)_4$ (enantiomerically pure) spread on a 1mM copper acetate aqueous solution at normal *pH*. Assignment of all the Bragg peaks yielded a cell ($a_s$=14.40Å, $b_s$=12.77Å $\gamma_s$=103°) that can be interpreted as a superstructure ($a_s$=3*a*-*b*; $b_s$ =2*b* ) of a subcell (*a*=4.79Å, *b*=6.38Å, γ=77.4°, *A*=29.9Å$^2$) *i. e.* with one molecule per subcell. The reflections of this subcell, presumably with contribution mainly from the hydrocarbon chains, are marked with arrows in Fig. 1. By contrast, the copper complex with a longer amphiphile, R=$C_{21}H_{31}$-CONH-$(CH_2)_4$, yielded a GIXD pattern showing only the contribution from the chains (see Annual Report for 1994). Fig. 1 (right) shows the GIXD pattern obtained from a monolayer of the enantiomerically pure amphiphile with R=$C_{16}H_{33}$ spread on a 1mM copper acetate aqueous solution. Assignment of all the Bragg peaks yielded a cell ($a_s$=15.65Å, $b_s$=14.63Å $\gamma_s$=104.74°) that can be interpreted as a superstructure ($a_s$=3*a*; $b_s$=3*b*-2*a* ) of a distorted-hexagonal subcell (*a*=5.22Å, *b*=5.22Å, γ=64.66°, *A*=24.6Å$^2$; one molecule per cell). The GIXD pattern of the racemic counterpart (not shown) gave a cell (*a*=8.06Å, *b*=6.10Å, γ=92°, *A*=49.14Å$^2$) corresponding to a complex unit in which the copper is linked to two ligand molecules, presumably of opposite handedness. Thus the racemic amphiphile forms a racemic copper complex monolayer.

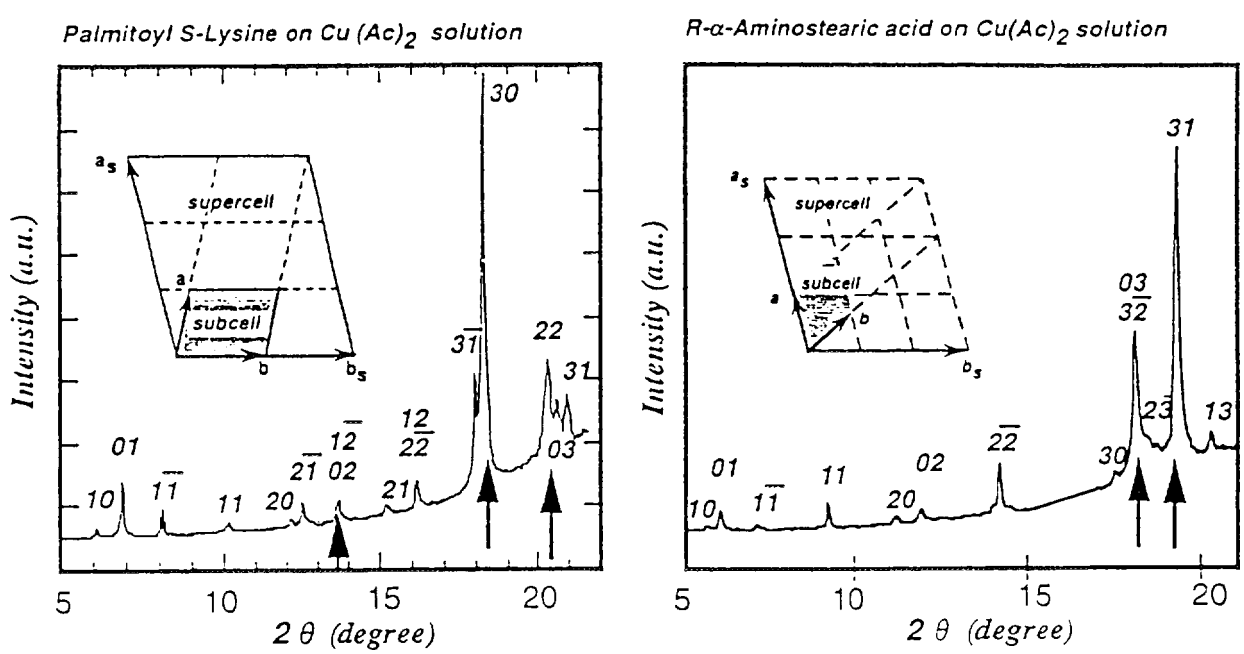


[1] F. Leveiller *et al.* Langmuir **10**, 819 (1994); C. Böhm *et al.*, Langmuir **10**, 830 (1994)

## Supramolecular Architecture Prepared *in-situ* at the Air-Aqueous Solution Interface; Thin Films of a 3x3 Grid Silver Complex

I. Weissbuch, L. Leiserowitz, M. Lahav, *Department of Materials & Interfaces, Weizmann Institute of Science, Israel,* P. Howes, K. Kjær, *Department of Solid State Physics, Risø National Laboratory, Denmark,* J. Als-Nielsen, *Niels Bohr Institute, Denmark* and P. Baxter, J.-M. Lehn, *Laboratoire de Chimie Supramoléculaire, Université Louis Pasteur, France*

We report on self-assembled crystalline domains of a 3x3 silver grid complex with a specific orientation at the interface, as determined by grazing incidence synchrotron X-ray diffraction (GIXD). Evidence is provided for the self-assembly process of a complex between nine silver(I) metal ions and six ligands, $[Ag_9L_6]^{9+}$ $\bullet 9CF_3SO_3^-$, where *L* is 6,6'-bis[2-(6-methylpyridyl)]-3,3'-bipyridazine, (Fig. 1, left). The process of film preparation, involving spreading a ligand solution in chloroform onto the surface of a 1mM aqueous solution of silver triflate ($Ag^+CF_3SO_3^-$) in the dark, could be monitored by the surface pressure *vs.* area isotherm which showed a significant difference in shape from that of the ligand spread on water. The GIXD pattern measured for the ligand on water, (Fig. 1, mid) yields a rectangular 2-D unit cell of dimensions $a$=8.12Å, $b$=20.01Å and molecular area of 81.2Å$^2$. Bragg rod intensity profiles exhibit maxima that occur at $q_z$ values of 0, 0.6 and 1.2Å$^{-1}$ indicating an orthorhombic unit cell a vertical spacing of 10.5Å ($\cong 2\pi/\Delta q_z$). Indeed, analysis of powder synchrotron X-ray data from 3-D material confirmed the orthorhombic unit cell. In the packing arrangement obtained (space group *Pcab* ) the long molecular axis is parallel to the *ab* plane. Since this crystalline plane of the multilayers is parallel to the water surface according to GIXD data, we conclude that the nucleation was initiated by molecules lying flat on the water surface. The GIXD pattern obtained from the ligand spread on a silver triflate aqueous solution, Fig. 1 right, is significantly different. Given the known 3-D crystal structure of the 3x3 silver grid complex ($a$=28.58Å, $b$=31.494Å, $c$=22.45Å, β=116.36°, space group $P112_1/n$, *c* unique axis) all the Bragg peaks can be easily assigned (*hk*) Miller indices. Such an assignment implies that the crystalline domains adopt a structure akin to that of the 3-D crystal and are oriented with their (001) plane parallel to the liquid surface. Other preferred orientations of the complex crystals would imply the appearance of a strong reflection at $q_{xy}$ of ~0.372Å$^{-1}$ not observed in our measured pattern. Hence the crystallites must be oriented with their *ab* plane parallel to the water surface. The crystalline domains are ~20Å thick, in agreement with the estimate from scanning force microscopy. This value corresponds to an (001) bilayer of the complex units which are related by centers of inversion within each layer, and make interlayer contact by twofold screw symmetry along the vertical *c* axis.

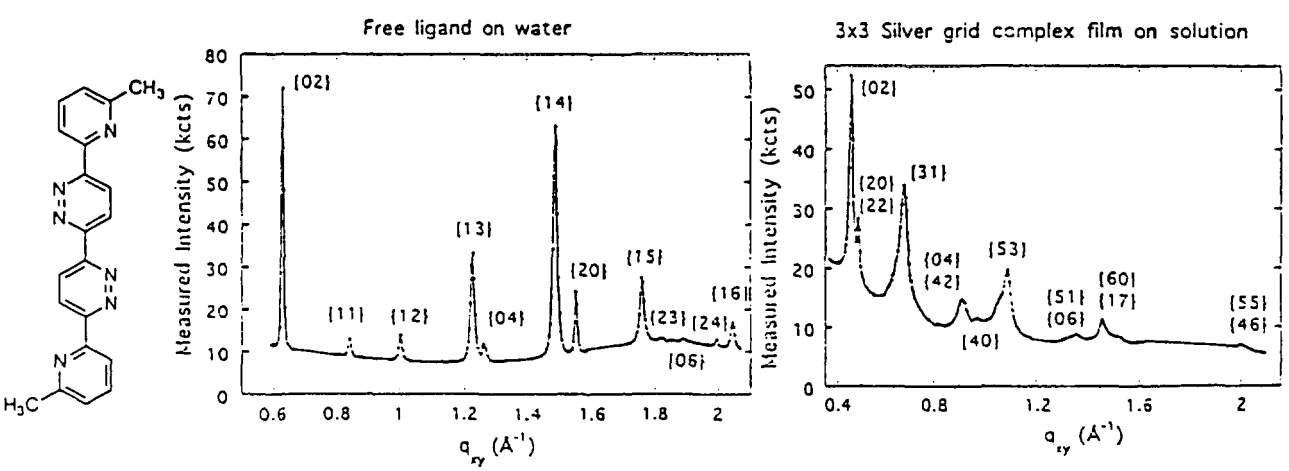

## Oriented Crystalline Multilayers of Metal Dicarboxylic Acid Salts Self-Assembled at the Air-Aqueous Solution Interface

I. Weissbuch, M. Lahav, L. Leiserowitz, *Department of Materials & Interfaces, Weizmann Institute of Science, Israel,* J. Als-Nielsen, *Niels Bohr Institute, H.C. Ørsted Institute, Denmark,* P. Howes and K. Kjær, *Department of Solid State Physics, Risø National Laboratory, Denmark*

The present study describes the self-assembly of symmetric dicarboxylic acid molecules, $HOOCC_{22}H_{44}COOH$, on aqueous subphases containing divalent Cd, Pb, Ca, Cu or monovalent Ag ions. These positive ions have a dramatic influence on the packing of the diacid molecules: they bind to both ends of the molecules and force the long hydrocarbon chain to lie parallel to the water surface and to crystallise as multilayer domains about 50-60Å thick. In these crystalline multilayers the bound ions are aligned in columns perpendicular to the surface, with a lateral coherence length in the range of 700-1000Å.

Diacid films spread on a 1.0 mM $CdCl_2$ subphase yield a diffraction pattern exhibiting Bragg peaks up to 15$^{th}$ order, (Fig. 1, left) and, on a 1mM $PbNO_3$ subphase, up to 20$^{th}$ order (Fig. 1, right), much stronger than observed on any other Langmuir film. All normalised peak positions $Q_{xy}/a^* = a\,Q_{xy}/2\pi$ are precisely on integer values corresponding to a lattice spacing of $a$=33.11Å for Cd salt and $a$=33.36Å for the Pb salt, very close to the estimated length of an extended molecule. The $Q_Z$-width of the corresponding Bragg rods yield an estimate of the multilayer thickness of ~55Å.

Some information about the packing of the molecules in the plane normal to the molecular axis is obtained from two peaks at $Q_z > 0$ (not shown). For the $Cd^{++}$ system the peaks occur at total scattering vectors $Q_{tot}$ =1.55Å$^{-1}$ and $Q_{tot}$ =1.69Å$^{-1}$ corresponding to lattice spacings of 4.05 and 3.72Å, respectively. These spacings are close to those found in crystal packing of long-chain molecules. The widths of the peaks correspond to coherently diffracting regions of about 50 Å, i.e. similar to the thickness deduced from the widths of all the harmonic Bragg rods. Independent information on the total thickness, of ~59Å, of the multilayer crystallites was obtained from specular reflectivity data measured for the $Cd^{++}$ system.

For the $Pb^{++}$ system the two peaks occur at $Q_{tot}$= 1.41Å$^{-1}$ and 1.48Å$^{-1}$ corresponding to lattice spacings of 4.56Å and 4.24Å, respectively.

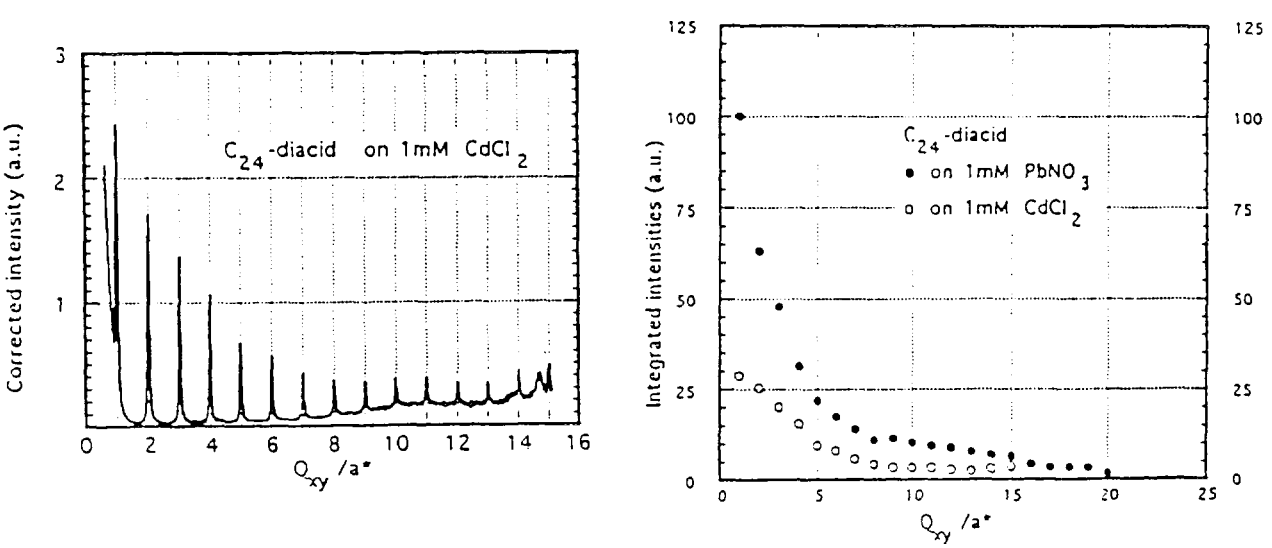


Fig. 1. Left: Scattered intensity vs. $Q_{xy}$ for the $Cd^{++}$ system. Right: Integrated intensities for $Cd^{++}$ and $Pb^{++}$ systems.

## Chiral Separation of Diastereomeric Monolayers at the Air/water Interface

I. Kuzmenko, M. Lahav, L. Leiserowitz, *Department of Materials & Interfaces, Weizmann Institute of Science, Israel*, J. Als-Nielsen, *Niels Bohr Institute, H. C. Ørsted Institute, Denmark* and K. Kjær, *Department of Solid State Physics, Risø National Laboratory, Denmark*

In bulk, racemic mixtures (R,S) can sometimes be separated by co-crystallisation with suitable chiral agents R' (or S'), utilising differences in solubility and enthalpies of formation of the resulting diastereomeric compounds (R,R' and S,R'). In two dimensions, spontaneous chiral separation of long chiral aminoacids in Langmuir films has recently been observed by grazing-incidence X-ray diffraction (GIXD).[1,2] Here we demonstrate that strong diastereomeric interactions may be used to achieve chiral segregation in 2D crystallites at the air/water interface. A 1:1 mixture of (R)-para-pentadecylmandelic acid [$C_{15}H_{31}$-$C_6H_4$-CH(OH)-COOH, (R)] and (R)-para-tetradecylphenylethylamine [$C_{14}H_{29}$-$C_6H_4$-$CH(CH_3)$-$NH_2$, (R')] forms stable highly crystalline Langmuir monolayer films according to GIXD data (Fig.1, top curve). Indexing of the diffraction pattern brings out an oblique cell ($a$=5.59 Å, $b$=9.45 Å, $\gamma$=101.45°). The unit cell contains two independent molecules: acid and amine. The GIXD pattern of the second diastereomeric mixture (R,S') (Fig.1, bottom curve) is different from that of (R,R'). The constants of the oblique unit cell are ($a$=5.55 Å, $b$=9.55 Å, $\gamma$=104.72°). An equimolar mixture of the four components (R,R',S,S') gives rise to a diffraction pattern almost identical to that of the (R,R') mixture (Fig.1 middle curve). Since the oblique unit cell contains only two molecules and the monolayer is highly crystalline, we may conclude that the (R,R',S,S') mixture is separated into (R,R') and (S,S') domains.

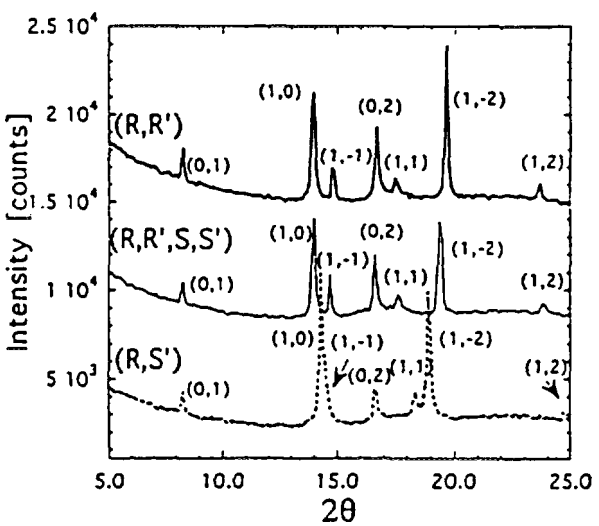


Fig.1

[1] Nassoy, P., Goldmann, M., Bouloussa, O. & Rondelez, F. *Phys. Rev. Letters* 75, 457 (1995)
[2] Weissbuch, I., *et al. J. Am. Chem. Soc.* (submitted) and Annual Report for 1995

## Interdigitated Chiral Architectures at the Air/liquid Interface: Role of Diastereomeric Interactions

I. Kuzmenko, S. Isz, M. Lahav, L. Leiserowitz, *Department of Materials & Interfaces The Weizmann Institute of Science, Israel,* J. Als-Nielsen, *Niels Bohr Institute, H. C. Ørsted Institute, Denmark,* P. Howes and K. Kjær, *Department of Solid State Physics, Risø National Laboratory, Denmark*

The long-chain chiral water-insoluble molecules [(R)-*para*-pentadecylmandelic acid, $C_{15}H_{31}$-$C_6H_4$-CH*(OH)-COOH, $C_{15}$-MA] may interact with their water-soluble chemical counterparts [phenylethylamine, $C_6H_5$-CH*($CH_3$)-$NH_2$, PEA] at the air/solution interface and form mixed amorphous monolayers that, upon compression, transform into crystalline interdigitated trilayers.[1] Grazing incidence X-ray diffraction (GIXD) was used to monitor the process of two-dimensional crystallisation *in-situ* and provide data of near-atomic resolution. The crystallisation is dependent upon the chirality (R,S,R',S') of both components (in these experiments every molecule had one chiral centre) and is likely to be correlated with crystallisation properties of the analogous water-soluble diastereomeric salts (MA, PEA).[1]

We have now extended our surface studies to a more complex system that included the same surfactant $C_{15}$-MA molecules [of (R)-handedness], whereas ephedrine ($C_6H_5$-CH*(OH)CH*($CH_3$)NH-$CH_3$, EPH) bearing two chiral centres [(R',R"), (R',S"), (S',R") or (S',S")] served as a water soluble component. All the four diastereomeric systems [(R,(R',R")), (R,(R',S")), (R,(S',R")) or (R,(S',S"))] display similar pressure-molecular area ($\pi$ *vs.* $A$) isotherms (not shown). They are very expanded and reach a plateau region at $A$~45Å$^2$ to ~15Å$^2$/molecule as for the mixtures of ($C_{15}$-MA, PEA),[1] suggesting intercalation of the solute molecules between long-chain amphiphilic molecules. Only one chiral combination, namely [R,(R',R")] gave rise, upon compression, to a strong GIXD diffraction pattern (Fig.1) that appears to correspond to an interdigitated crystalline film with a rectangular lattice ($a$=11.6Å, $b$=11.91Å; two acid and two amine molecules per unit cell).

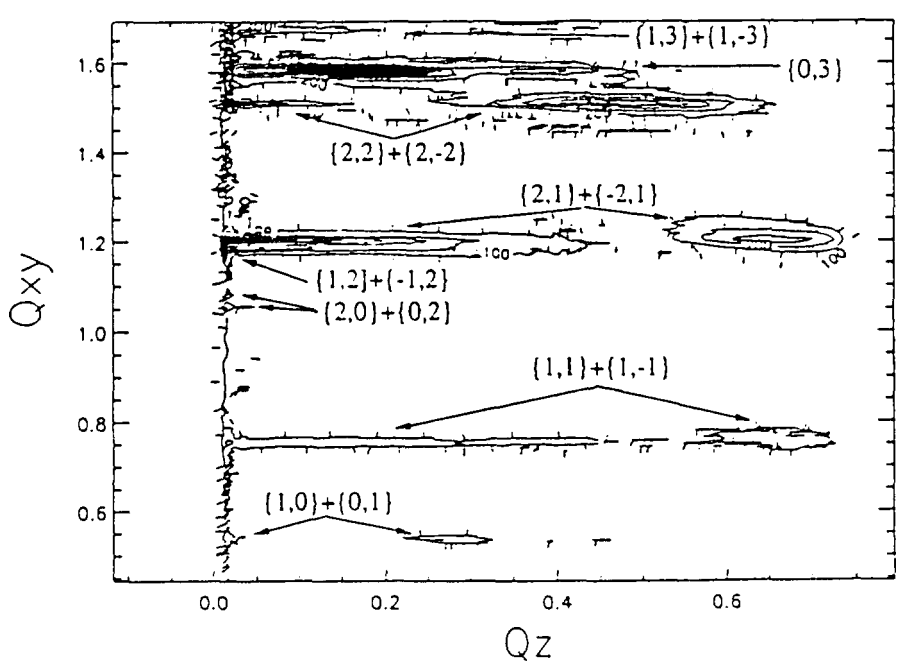


Fig.1

[1] Kuzmenko, I., *et al. Science* (in press) and Annual Report for 1995

## X-Ray Synchrotron Studies of Polymer-Modified Lipid Monolayers on Water.

J. Majewski, G.S. Smith, *MLNSC, Los Alamos National Laboratory, USA*, T. Kuhl, J. Israelachwili, *Department of Chemical and Nuclear Engineering, University of California at Santa Barbara, USA, Denmark*, J. Als-Nielsen, *Niels Bohr Institute, Copenhagen University, Denmark*, K. Kjær, M. Gerstenberg, *Department of Solid State Physics, Risø National Laboratory, Denmark.*

An exciting idea in the area of advanced drug delivery is the use of liposomes composed of macromolecular assemblies of lipids and cholesterol molecules to encapsulate drugs[1]. However, simple liposomes tend to be removed from the bloodstream by the macro phage system (MPS)[1]. Recently, it was discovered that by including a small percentage of PEG-lipids (phosphatidyl choline with poly-ethylene oxide or poly-ethylene glycol (PEG) chemically bound to the head group) in the bilayer membrane, the removal of the liposomes by the MPS is greatly reduced and the *in-vivo* bloodstream half-life is increased from hours to days[2]. To gain insight into the physical properties of lipid-polymer/lipid system we performed a series of x-ray reflection and grazing incidence diffraction (GID) experiments at BW1 beamline at HASYLAB. We studied monolayers composed of mixtures of distearoyl phosphatidyl ethanolamine (DSPE) mixed with 1.3 and 9% of the same lipid but modified by polyethylene glycol chains (PEG, MW=2000) covalently linked to its head group (DSPE-PEG). Monolayers were spread on a water subphase in a thermostated Langmuir trough. The GID data for the pure DSPE and DSPE/DSPE-PEG monolayer yielded three in-plane reflections: {1,0}, {1,1} and {2,0} leading to a hexagonal unit cell of the hydrocarbon chains ($a_H$ =4.7Å, area per lipid molecule for the *crystalline phase* = 38.26Å$^2$ independent of PEG concentration). The coherence lengths of the 2-D lipid crystallites decreased from 360Å for the pure lipid to 280Å and 230Å for 1.3% and 9.0% DSPE-PEG, respectively. The FWHM($q_z$) of each of the Bragg rods increased with PEG-lipid concentration suggesting that the lengths of the coherently diffracting part of the hydrocarbon chains changed from 23Å for the pure lipid to 20Å and 18Å, for 1.3% and 9.0% of the PEG-lipid, respectively. X-ray reflectivity profiles show that both the density and the extension of the polymer segments increase with DSPE-PEG concentration and can be well modelled with a parabolic density profile despite a very weak electron density contrast between the PEG polymer and the water subphase. The roughness of the interface increases with the DSPE-PEG concentration, perhaps indicating that the bulky hydrophilic polymer disrupts the lipid monolayer (Fig.1). The disruption is attributed to two mechanisms: an increase in lipid protrusions due to the increased solubility of the PEG-lipids, and a relaxation of the lateral force between PEG portions by staggering of the lipid headgroups.

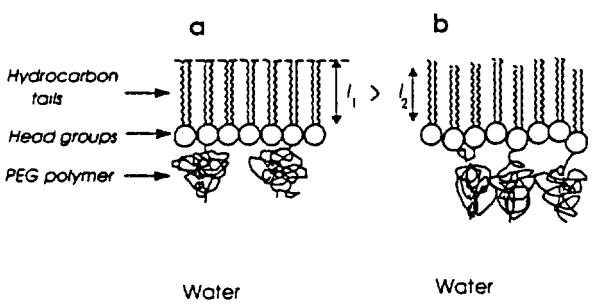


Fig.1. Schematic structure of mixed DSPE with (a) 1.3% and (b) 9.0% DSPE-PEG monolayers showing the decrease in length $l$ of the coherently scattering lipid tails due to the greater out of plane protrusions of the DSPE–PEG molecules.

[1] D. R. Woodle, D. D. Lasic. Biochim. Biophys. Acta, **1113**, 171 (1992). and references therein.
[2] T. M. Allen, *et al*, Biochim. Biophys. Acta, **1061**, 56 (1991).

## Cyclic Peptides Forming Nanotubes at the Air-Water Interface

H. Rapaport, M. Lahav, L. Leiserowitz, *Department of Materials and Interfaces, The Weizmann Institute of Science, Israel,* J. Als-Nielsen, *Niels Bohr Institute, H. C. Ørsted Institute, Denmark,* P. Howes, K. Kjær, *Department of Solid State Physics, Risø National Laboratory, Denmark,* M.R. Ghadiri and H.S. Kim, *Department of Chemistry, Scripps Research Inst., California, USA*

Cyclic peptides made up of even number of alternating *D*- and *L*- amino acids are ring-shaped and form intermolecular hydrogen bonds, creating tubular structures with a hydrophilic core and a hydrophobic rim[1] (shown schematically for *cyclo*[-*L*-Ser-*D*-Leu-(*L*-Trp-*D*-Leu)3-] in Fig.1). These architectures are expected to have applications as size selective channels in artificial membranes. Three types of cyclic-peptide films spread at the air-water interface, that provides a simple model of membrane environment, were studied by Grazing-Incidence X-ray Diffraction (GIXD).

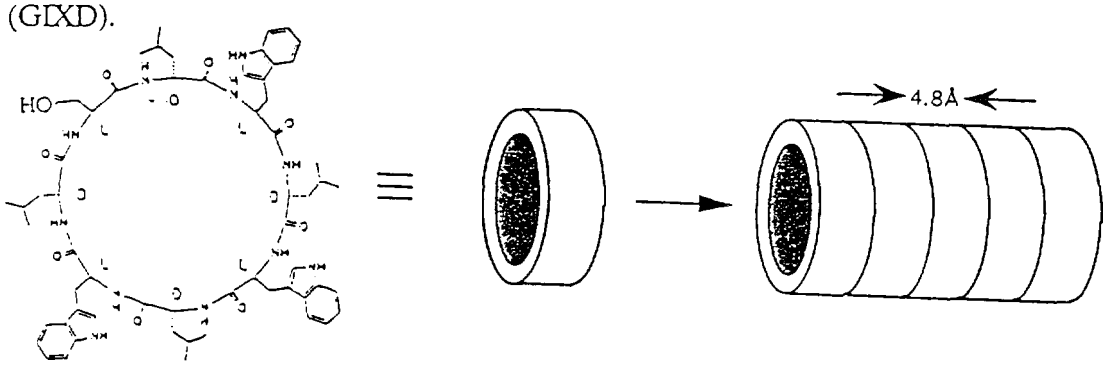


Fig. 1.

For films of *cyclo*[-*L*-Ser-*D*-Leu-(*L*-Trp-*D*-Leu)3-] the GIXD pattern (Fig. 2) exhibits a Bragg rod at $q_{xy}$=1.3Å$^{-1}$, peaking at $q_z$=0, thus corresponding to nanotubes aligned with the ring plane normal to the water surface and stacked with a 4.8Å lateral spacing. The skewed Bragg rod suggests that the tubes have a mosaic distribution on the water surface. The width of the Bragg rod indicates a film ~35Å thick corresponding to two layers of tubes. The extent of crystalline order along the nanotube is ~60 stacked rings according to the width of the Bragg peak. The film of the similar derivative *cyclo*[-(*L*-Trp-*D*-Leu)4-] formed no ordered structures.

*Cyclo*[-(*L*-Phe-*D*-N-MeAla)4-] (designed by addition of methylene groups to be devoid of hydrogen-bond donation from one face of the molecule, formed a 2D crystalline film of horizontal rings stacked in antiparallel dimers (Fig. 3). A tetragonal unit cell *a*=*b*=16.8Å was assigned to the GIXD pattern. The widths of the Bragg rods indicate film 25-35Å thick (≅3 layers). The positions of the Bragg rod maxima are in keeping with a body centred unit cell as found in the 3D crystal structure[2].

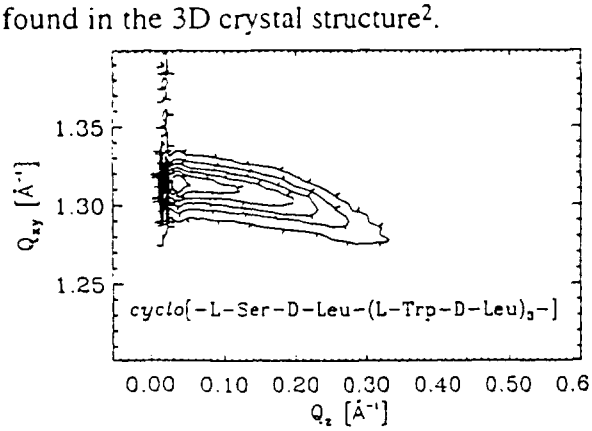


Fig. 2 Bragg rod of *cyclo*[-*L*-Ser-*D*-Leu-(*L*-Trp-*D*-Leu)3-]

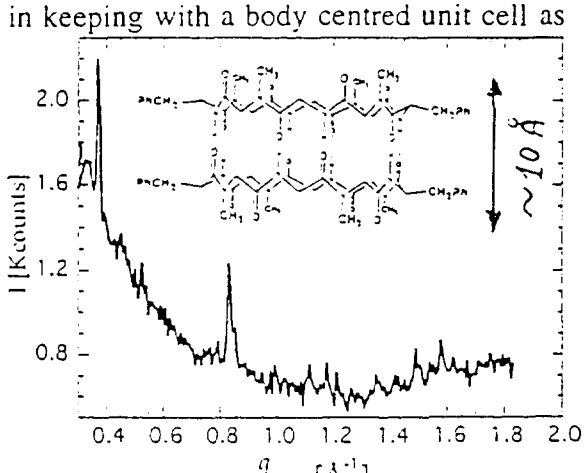


Fig. 3 GIXD pattern of *Cyclo*[-(*L*-Phe-*D*-N-MeAla)4-] inset shows the horizontal ring-dimers.

[1] M. R. Ghadiri *et al.*, Nature, **369**, 301 (1994). [2] M. R. Granaja *et al.*, Angew. Chem. Int. Ed. Engl., **34**, 93 (1995).

## Crystallography of Monomolecular Protein Surface Layers Using X-ray GIXD

P. Howes, K. Kjær, *Risø National Laboratory, Denmark*, B. Wetzer, D. Pum, U. B. Sleytr, *University for Agriculture, Austria*, S. A. W. Verclas, N. A. Dencher, *Hahn-Meitner-Institute, Germany*, M. Weygand and M. Lösche, *University of Leipzig, Germany*

Protein crystallography has revolutionised our understanding of biological processes, enabling a correlation, in molecular detail, of structure and function for a steadily growing number of biomolecules. The bottleneck is the formation of well-ordered three-dimensional (3D) crystals.[1] Many important biological processes are mediated by proteins which in their functional state are either associated with or incorporated into biomembranes.[2] Unfortunately, such proteins are the least amenable to 3D crystallisation, and only a handful of structures of membrane proteins have been solved by crystallography to date.[3] Because of this problem, electron crystallography has been developed,[4] for which 2D protein crystal sheets are prepared at an interface and analysed under UHV conditions in the electron microscope after heavy ion staining or cryo-fixation. A problem here is the inaccessibility of the surface normal ("hidden cone problem").[5] Using a different approach, we have attempted crystallography of monomolecular protein layers floating on the surface of an aqueous buffer, by means of grazing-incidence X-ray diffraction (GIXD). While GIXD has been widely employed for the structural characterisation of lipid surface layers,[6] its application to proteins[7] met with a number of technical problems which we have solved at HASYLAB's beam line BW1. Advantages of the method are its extreme sensitivity (diffraction from samples that contain as few as $10^{12}$ molecules!), the "natural" environment of the proteins during investigation that reduces preparation artefacts (sample on top of buffer interface; no need for stain or cryo-fixation) and an increased probability for the formation of 2D protein crystals, as opposed to 3D crystals, in particular of interface-bound membrane proteins. On the other hand, GIXD from 2D protein crystals currently has a quite limited signal-to-noise ratio, limiting the resolution to about 8Å. Also, the data evaluation has yet to be rigorously established. So far, we have investigated 4 proteins bound in different ways to the buffer/air interface. After completing test measurements with streptavidin we obtained useful GIXD also from:

(•) Purple membrane patches, the protein/lipid crystal films containing bacteriorhodopsin (bR) trimers.[8] The preparation procedure was optimised earlier in fluorescence microscopy experiments using labelled membrane patches. Diffraction was observed up to order (h,k)=(4,3) (hexagonal unit cell), corresponding to a resolution of ~ 8Å. Beam damage was not a problem.

(•) Two different bacterial S(urface)-layer proteins (from *B. sphaericus* CCM2177[9] and from *B. coagulans* E38-66[10]) were crystallised under phospholipid monolayers at buffer surfaces and were found to diffract with higher efficiency than bR. Beam damage was severe but careful dose management meant that samples could survive for 10 hours. Data was collected out to $Q_{xy}$ ~ $2\pi/8$Å (*cf.* Fig. 1).

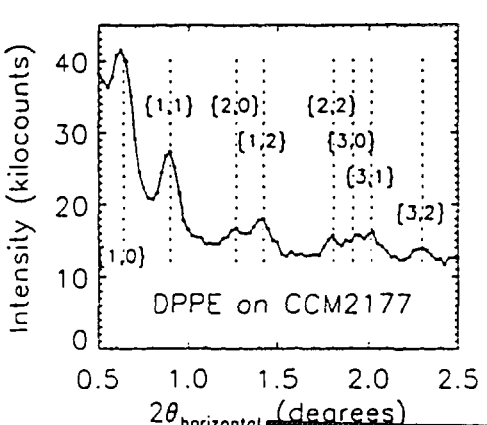



1 Feher & Kam, in: Methods in Enzymol., 114, 77 (1985)
2 Travis, Science, 260, 906 (1993)
3 Deisenhofer *et al.*, Nature, 318, 618 (1985)
4 Uzgiris & Kornberg, Nature, 301, 125 (1983)
5 Darst *et al.*, Biophys. J., 59, 387 (1991)
6 Als-Nielsen *et al.*, Physics Reports, 246, 251 (1994)
7 Haas *et al.*, Biophys. J., 68, 312 (1995)
8 Grigorieff *et al.*, J. Mol. Biol., 259, 393 (1996)
9 Pum & Sleytr, Coll. Surf. A, 102, 99 (1995)
10 Pum *et al.*, J. Bacteriol., 175, 2762 (1993)

The Danish Space Research Institute (DSRI) has produced two high throughput X-ray telescopes to be flown on the international Spectrum Roentgen Gamma satellite. The telescopes are the most efficient telescopes ever to be produced in the energy band from 0.1 to 15 keV. They are based on a highly nested geometry of grazing incidence Au coated mirrors in a 600 mm diameter structure. Calibration of these requires a full aperture illumination of the telescopes at selected energies and with sufficient collimation that the X-ray beam simulates a celestial X-ray source at infinity. To this end DSRI has established at the Daresbury synchrotron an expanded beam X-ray optics facility which operates by an extreme asymmetric reflection in a single 300 mm large Si crystal. The experimental set up including the telescope is shown in fig. 1.

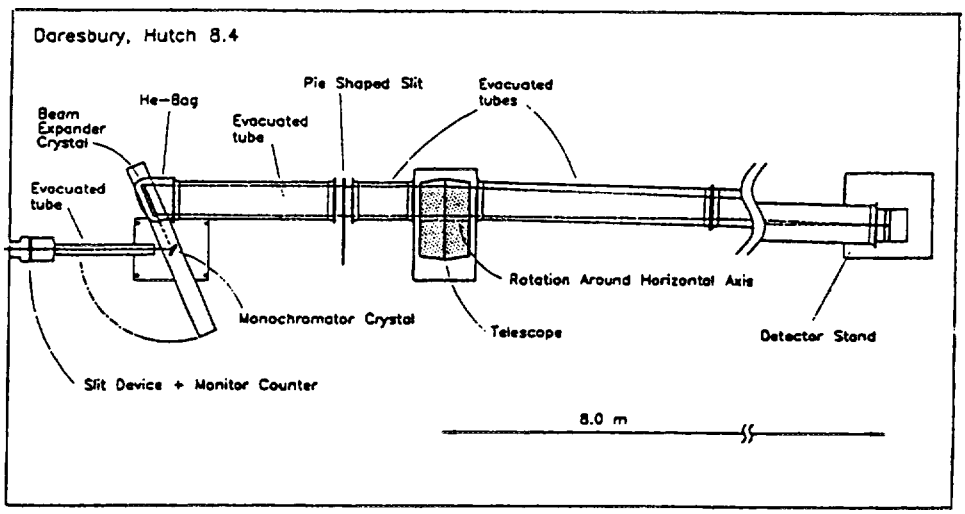


*Figure 1. An overview of the arrangement used in the study of the imaging properties of a flight telescope. A slit device plus monitor detector is located at the entry of Daresbury hutch 8.4. They are followed by the monochromating and beam expanding crystals. The beam expanding crystal is enclosed in a He atmosphere to insure that the far side of the expanded beam is not abosrbed more than the near side that would be the case for the different path lengths in air. The expanded beam passes through a pie shaped slit that insures correct weighting of illumination on the telescope aperture.*

One of the essential performance characteristics of an X-ray telescope is the encircled energy curve for an on-axis source. This curve quantifies the number of photons, normalized with the total number of photons in the image, which falls within a given angular diameter in the focal plane. The result for the first flight telescope produced are given in fig. 2. In additon to this a complete investigation of the telescope was performed including the on- and off-axis imaging, the effective area and mapping of the telescope performance as a function of the azimuthal angle which is responsible for the composite image in the focal plane of an on- and off axis source.

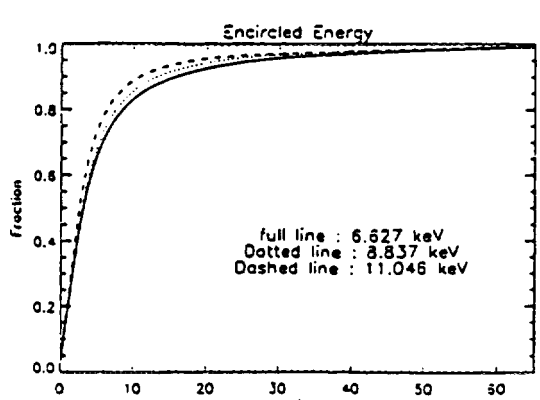


*Figure 2. Encircled energy curve at 6.627 keV (full line), 8.837 keV (dotted line) and 11.046 keV (dashed line).*

**Dynamics of Oxygen Ordering in $YBa_2Cu_3O_{6+x}$ Studied by Neutron and High-Energy Synchrotron X-ray Diffraction.**

T. Frello, N.H. Andersen, J. Madsen, M. Käll, O. Schmidt, *Department of Solid State Physics, Riso National Laboratory, Denmark,* M. von Zimmermann, J.R. Schneider, *HASYLAB, Hamburg, Germany,* Th. Wolf, *Forschungszentrum Karlsruhe, Germany,* H.F. Poulsen, *Materials Department, Riso National Laboratory, Denmark*

The close relation between oxygen ordering and superconductivity in $YBa_2Cu_3O_{6+x}$ with $0 \leq x \leq 1$ has stimulated many structural studies of this material. Of particular interest has been the orthorhombic double cell structure, called ortho-II, which is found for oxygen stoichiometries $0.35 \leq x \leq 0.67$ and leads to a plateau of $T_c \approx 60$ K. It results from oxygen ordering in CuO chains along the *b* axis in the basal plane of the unit cell with the oxygen being preferentially on every second chain. Among the unsettled structural properties are the reasons why the ortho-II structure does not develop long range order, and why the single cell ortho-I structure remains stable down to temperatures that are significantly lower than predicted by most theoretical models. We have studied the dynamics of the ortho-II ordering process in a high purity single crystal by neutron and high-energy synchrotron X-ray diffraction in time intervals from a few seconds to several weeks, and for temperatures from 20 to 200 °C. Our studies reveal a two-step ordering process. When the temperature is changed below 100 °C, an initial change in the ordering properties occurs instantaneously (within seconds) followed by a very slow ordering process, that does not seem to develop long range order even on a time scale of several years. Our data show that the optimal temperature for developing ortho-II ordering is around 80 °C. The observed properties may be interpreted on the basis of recent theoretical model predictions that suggest a strong variation of the oxygen chain length distribution function as function of temperature[1]. As the temperature is lowered a rapid increase of the average chain length is predicted[1]. Locally the chains may combine but thermodynamic equilibrium is only established via a more long range oxygen diffusion process that is frozen out before the chain length distribution saturates.

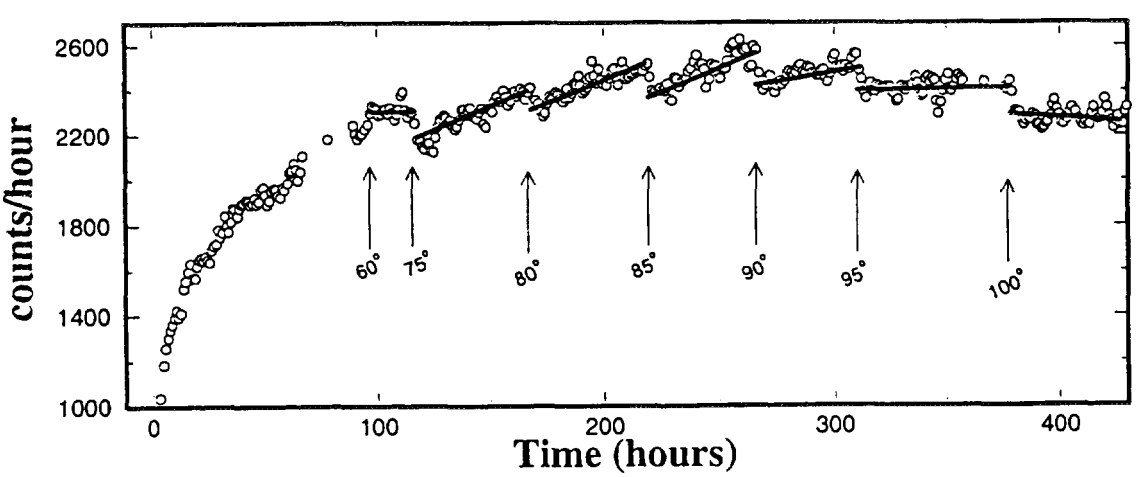


Fig.1. The time-development of the intensity of the (½ 0 0) reflection (the ortho-II phase) measured by neutron diffraction at the TAS1 Risø neutron spectrometer. The sample was quenched from 170 °C to 70 °C at t=0 hours. Additional temperature changes are indicated on the figure by arrows. Circles are experimental data, the lines are guides to the eye.

[1] G. Uimin. Phys. Rev. B. 50. 9531 (1994)

## New Superstructures in $YBa_2Cu_3O_{6+x}$ Observed by High Energy X-Ray Diffraction

T. Frello, J. Madsen, O. Schmidt, N.H. Andersen, *Department of Solid State Physics, Riso National Laboratory, Denmark*, M. von Zimmermann, J. Schneider, *HASYLAB, Hamburg, Germany*, R. Liang, P. Dosanjh and W.N. Hardy, *UBC, Vancouver, Canada.*

The oxygen ordering in the $CuO_x$ basal plane has significant influence on the charge transfer leading to superconductivity in $YBa_2Cu_3O_{6+x}$. The tendency of the system to form Cu-O chains along the *b* axis for $0< x < 1$ leads to weak orthorhombic distortions of the basic tetragonal structure with different sequences of superstructure ordering of *full* (CuO) and *empty* (Cu) chains along the *a* axis. Most notably we have observed the double cell ortho-II[1] and the triple cell ortho-III[2] superstructures with chain ordering sequences: *full-empty* and *full-full-empty*, at ideal oxygen stoichiometries of $x = 0.5$ and $x = 0.67$, respectively. Weak superstructures of more complex ordering sequences have been observed by electron microscopy[3], but so far never by structural techniques that probe the bulk of the material. We have prepared well equilibrated single crystals with stoichiometries, $x = 0.62$ and $x = 0.67$ and studied their oxygen ordering properties with high energy synchrotron X-ray diffraction. In the $x = 0.62$ crystal we find commensurate superstructure peaks with modulation vectors (2/5,0,0), and finite correlation lengths which at room temperature are 10.2 Å along the *a* axis and 73 Å along the *b* axis (see Fig. 1). We interpret the (2/5,0,0) peaks to be the second harmonic of an ortho-V superstructure with periodicity 5*a* and a chain ordering sequence of *full-full-empty-full-empty*, which has ideal oxygen stoichiometry, $x = 0.6$. Simple structure factor calculations show that the intensity of primary peaks at (1/5,0,0) is almost an order of magnitude smaller than that of the (2/5,0,0) peak and may therefore hardly be seen on the background and the tails of the Bragg peaks. The ortho-V peaks are centred around ortho-II peaks at (1/2,0,0) which have correlation lengths at room temperature of 17 Å along the *a* axis and 83 Å along the *b* axis. There is a clear *c* axis modulation of the ortho-II superstructure and a weaker one for ortho-V, but it is not possible to deduce values for the correlation lengths. The ortho-II intensity increases slightly when the ortho-V superstructure starts to decrease at 55 °C, before it disappears at around 110 °C. In the crystal with $x = 0.67$ we observe incommensurate superstructure peaks with ordering vector (0.38,0,0). The correlation lengths at room temperature are 11.5 Å along the *a* axis, 56 Å along the *b* axis, and rather weak correlations along the *c* axis similar to those found for the ortho-III superstructure[2]. Although the superstructure peaks may be fitted nicely with a single Lorentzian we cannot preclude that the apparently incommensurate superstructure peaks are combinations of ortho-III and ortho-V peaks. Neither can we preclude weak traces of ortho-II superstructure peaks. The (0.38,0,0) superstructure has a broad transition between 45 and 140 °C. Our eksperimental observations are in good agreement with recent Monte Carlo simulation model studies.

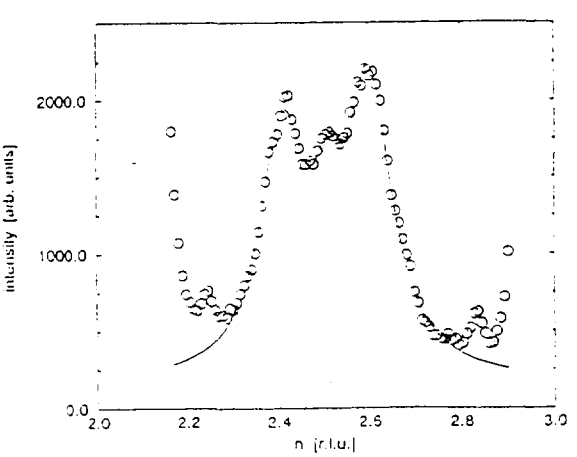


Fig. 1. Observation of combined ortho-V ($h = 2.4$ and 2.6) and ortho-II ($h = 2.5$) superstructure peaks at room temperature in $YBa_2Cu_3O_{6.62}$. Full line is a fit with three Lorentzians. The peaks at $h \approx 2.24$ and 2.83 have not been identified. The scattering densities at $h \rightarrow 2$ and 3 are the tails of the Bragg peaks.

[1] P. Schleger, *et al.*, Phys. Rev. Lett., **74**, 1446 (1995).
[2] P. Schleger, *et al.* Physica C **241**, 103 (1995).
[3] R. Beyers *et. al.* Nature **340**, 619 (1989).

## Verification of Stripe Charge Correlations in $La_{1.775}Sr_{0.225}NiO_4$ by Hard X-Ray Diffraction.

M. von Zimmermann, J.R. Schneider, *HASYLAB, Hamburg, Germany,* T. Frello, J. Madsen, N.H. Andersen, *Department of Solid State Physics, Risø National Laboratory, Denmark,* A. Vigliante, J.M. Tranquada, D. Gibbs, *Department of Physics, Brookhaven National Laboratory, USA,* and D.J. Buttrey, *University of Delaware, USA.*

Recent neutron scattering studies have shown very intriguing stripe correlations of spins and holes in nickelates and cuprates[1], but no X-ray diffraction experiment has confirmed the neutron results. We have carried out an X-ray diffraction study of $La_{2-x}Sr_xNiO_4$ ($x$ = 0.225) at the hard X-ray wiggler beamline BW5 at HASYLAB and verified the presence of stripe charge correlations in this material. We use 100 keV photons, which imply an absorption length of 0.08 cm and allow us to perform the experiment in Laue geometry and study the bulk of the same crystal as in the previous neutron experiment[2]. Ta-$SiO_2$ crystals with a mosaicity of 50 arc seconds used as monochromator and analyzer gave a resolution of 0.009 $Å^{-1}$ (longitudinal) and 0.001 $Å^{-1}$ (transverse). The sample was initially cooled to 10 K where eight independent incommensurate superstructure reflections at $Q = G \pm g_{2\varepsilon}$ were observed. $G$ is a reciprocal lattice vector and $g_{2\varepsilon}$ = $(2\varepsilon,0,1)$ is the charge density modulation vector for which it is expected that $\varepsilon \approx x$. In Fig. 1 are shown $h$ scans (along $a^*$) through $(4\text{-}2\varepsilon,0,3)$ at 10 K in the stripe ordered phase and at 170 K, where the ordering has disappeared. After the initial cooling to 10 K the $(4\text{-}2\varepsilon,0,3)$ peak intensity was measured as function of increasing temperature, and subsequently for decreasing temperature. The results are shown in Fig. 2. Below 40 K the peak intensity decreases steadily, and hysteresis is observed when the sample is cooled after the initial heating study. The temperature dependence of the incommensurate splitting parameter, $\varepsilon$, and the correlation lengths were measured, and the results are comparable with those obtained by neutron diffraction[2]. The largest correlation lengths of 46 Å in the $a$ direction, 74 Å along $b$ and 14 Å along $c$ were found at 50 K close to where the peak intensity is maximum

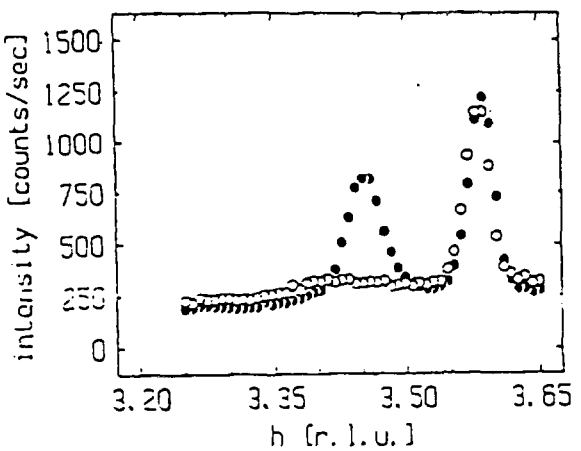


Fig. 1. $h$ scan through the charge-order peak at $(4\text{-}2\varepsilon,0,3)$ at 10 K (filled circles) and 170 K (open circles). The temperature independent peak at $h$=3.58 is an Al powder line from the cryostate.

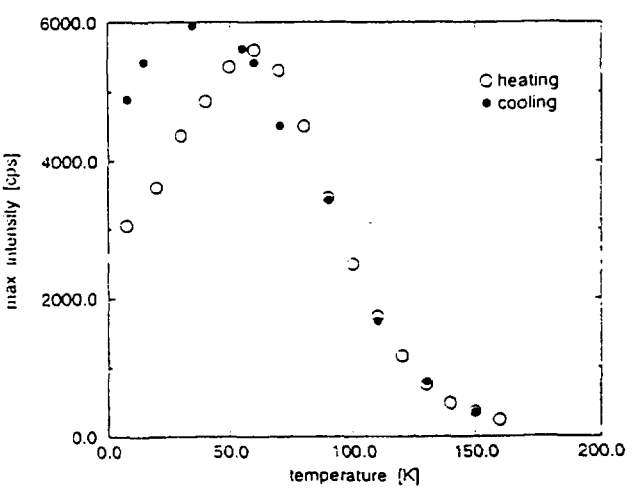


Fig. 2. Temperature dependence of the $(4\text{-}2\varepsilon,0,3)$ charge order peak measured during initial heating (open circles) and subsequent cooling (closed circles).

[1]J.M. Tranquada *et al.*, Nature 375, 561 (1995) ; J.M. Tranquada *et al.*, Phys. Rev. B 54, 7489 (1996)
[2]J.M. Tranquada *et al.*, Phys Rev. B 54, 12318-12323 (1996).

# $L_{II,III}$-XANES study of rare earth valency in $Pb_2Sr_2Ce_{1-x}Ca_xCu_3O_8$ for x= 0.0 to 0.4.

Jens-Erik Jørgensen and Kristian Rønning Pedersen
Department of Chemistry,University of Aarhus , DK-8000 Aarhus C, Denmark

Compounds with formula $Pb_2Sr_2Ln_{1-x}Ca_xCu_3O_8$, where Ln represents a trivalent rare earth ion, are high temperature superconductors. The $Pb_2Sr_2Ln_{1-x}Ca_xCu_3O_8$ compounds have been prepared for all the rare earths but superconductivity has not been found in the $Pb_2Sr_2Ce_{1-x}Ca_xCu_3O_8$ compounds. The rare earth valency in $Pb_2Sr_2Ln_{1-x}Ca_xCu_3O_8$ compounds with Ln= Ce, Pr and Tb has recently been studied by a number of groups using XANES spectroscopy.[1-3] These studies showed that Pr and Tb are trivalent in the $Pb_2Sr_2Ln_{1-x}Ca_xCu_3O_8$ compounds for x= 0.0 and 0.5, while Ce was found to be tetravalent in the corresponding compounds. The superconducting properties of these compounds are affected by the rare earth valency and $Pb_2Sr_2Pr_{0.5}Ca_{0.5}Cu_3O_8$, as well as $Pb_2Sr_2Tb_{0.5}Ca_{0.5}Cu_3O_8$, are high temperature superconductors while $Pb_2Sr_2Ce_{1-x}Ca_xCu_3O_8$ is semi-conducting for any value of x. The fact that Ce is tetravalent in undoped $Pb_2Sr_2CeCu_3O_8$ is rather surprising, and we have therefore measured Ce $L_{II,III}$ XANES spectra of $Pb_2Sr_2Ce_{1-x}Ca_xCu_3O_8$ for x= 0.0 to 0.4 as well as spectra of $Pb_2Sr_2Y_{1-x}Ce_xCu_3O_8$ for x= 0.1 and 0.2. As seen from Fig. 1 our study shows that the shape of the Ce $L_{III}$ XANES spectra of the studied compounds are very similar and numerial analysis of the spectra within the frame work of the simplified version of the Anderson single-impurity model also shows that 4f electron occupancy and hybridization with the ligand electrons is independent of the Ca-doping level. The tetra-valency of Ce in $Pb_2Sr_2CeCu_3O_8$ raises the question about the true oxygen content of this compound and preliminary EXAFS measurements at the Ce $L_{III}$ edge were performed to study the local Ce environment. No excess oxygen was observed but EXAFS measurement at the Ce $L_{III}$ edge is difficult due to the limited k-range available. Additional EXAFS measurements will therefore be performed at the Ce K edge. The present measurements were performed at the EXAFS II spectrometer at HASYLAB, Hamburg.

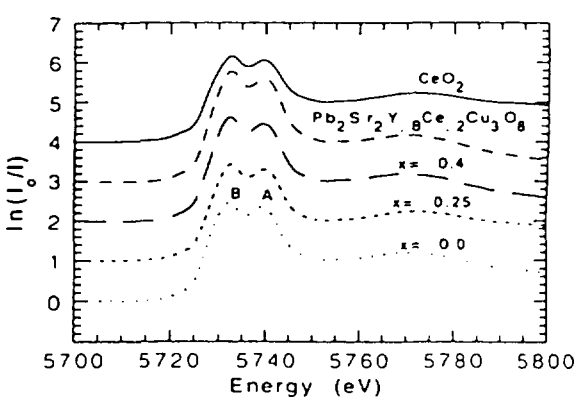


Fig. 1 Selected Ce $L_{III}$ XANES spectra of $Pb_2Sr_2Ce_{1-x}Ca_xCu_3O_8$ for x=0.0, 0.25 and 0.4 as well $Pb_2Sr_2Ce_{0.8}Ce_{0.2}Cu_3O_8$ and $CeO_2$. All spectra exhibit double peaked white lines indicating tetra-valent Ce.

References: [1] S. Skanthakumar and L. Soderholm, Phys. Rev. B53, 920 (1996).
[2] K. R. Pedersen and J.-E. Jørgensen, Physica C264, 185 (1996).
[3] U. Staub et. al., Phys. Rev. B52,9736 (1995).

# PETRA-1: Phase I commisioning

J. Als-Nielsen, K. D. Joensen, H. Schulte-Schrepping

The "lower" energy beamline at Petra is intended to be capable of delivering a monochromatic semi-focused beam with energies ranging from 16 keV to 54 keV into an experimental hutch. This is achieved by using three consecutive x-ray optical elements: 1) a diamond(C*) Laue-crystal 2) a Ge-crystal and 3) and a W/Si multilayer, all stationed in the optics hutch. The curvature of the Ge-crystal (sagittal) and the multilayer (tangential) can be varied to obtain focussing independently in the two directions. The large range of energies is obtained by using different combinations of crystal planes: C*(111)-Ge(220) for the 16 to 23 keV range and C*(004)-Ge(620) for the 19-53 keV range. The setup has already been described in detail.[1]

The main goals of the primary commisioning phase was to ensure that all components functioned as intended, and that for the energy range of 16 to 23 keV a monochromatic focused beam could be brought into the experiment hutch. These goals have been reached, with a redesign of the Laue-crystal holder. The original design relied on accurate pre-alignment of the crystal with no means of in-situ correction. Commisioning showed, however, that this was insufficent. Consequently a mini-goniometer, based on a ball-bearing principle and motored by inch-worm motors, was constructed.[2] Although some improvements may still be made, this design enabled the accomplishment of the commisioning goals. The following results have been obtained during the Phase 1 commisioning.

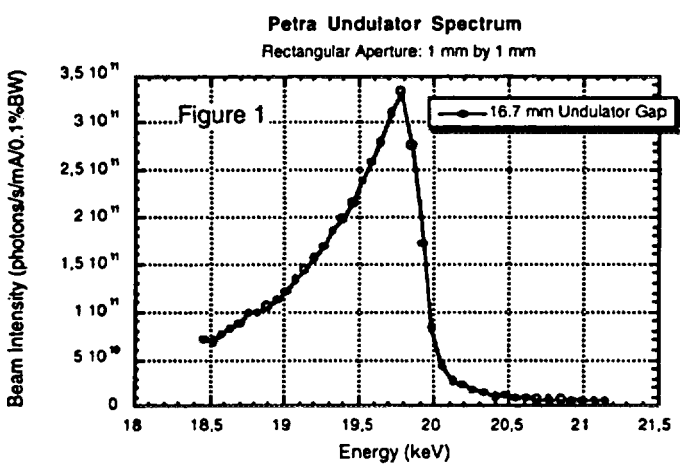


Undulator spectra from 15 to 35 keV were obtained by crystal spectroscopy with the C*(220) reflection. Spectra were taken with undulator gaps ranging from 15 mm to 23 mm, providing first harmonics in the range from 16 keV to 32 keV. A sample spectrum is seen in Figure 1, which was obtained at Petra settings of 12 GeV, 3.1 mA, using the Compton scattered radiation from 0.42 mm thick Kapton foils. Theoretical calculations show an expected peak beam intensity of $3.75 \times 10^{11}$, which is within 5% of our result. The vertical beam size at the diamond crystal position, 106 m from the source, was also determined and found to be 2.0±0.2 mm FWHM. The horizontal width was found to be larger than 8 mm. Both of these numbers are in good agreement with previous results.[3]

The three optics can be positioned such that a monochromatic beam arrives at a predetermined position in the experimental hutch. Although this has not been extensively tested yet, the beam characteristics for one particular energy have. With the Petra-ring running at 12 GeV/4 mA, an undulator gap of 16.7 mm, a crystal configuration of C*(111)-Ge(220), an19.7 keV unfocused x-ray beam was obtained in the experimental hutch with an absolute intensity of 8.1 x $10^9$ photons per second. This corresponds fairly well with the expected value of 10.3 x $10^9$ calculated by using the theoretical beam intensity and applying the diamond crystal Darwin width, the reflectivity of the optical components and absorption in the 13.4 meters of air.

For this 19.7 keV configuration, horizontal focusing with the W/Si multilayer was demonstrated to reduce the 1 mm (FWHM) incoming beam to a size of 0.59 mm, correspondingly increasing the peak intensity by 53%. The horizontal beamsize should be source-size limited and should result in a focal size of 0.2 mm. We do not presently understand this disagreement. Vertical focusing by the sagitally bent Ge-crystal was also demonstrated with a 1 mm beam being reduced to 0.34 mm, with peak intensity increasing by a factor of 3.

Activities in the immediate future will concentrate on verifying performance for the whole energy range, and improving the focusing capabilities of the beamline.

References:

1) "Petra Undulator Beamline", 1995 Hasylab Annual Report I, Section 2.8, p. 154- 159.
2) Built by JJ X-ray, Center for Advanced Technology, RISØ, Denmark.
3) "Petra Undulator Beamline", 1995 Hasylab Annual Report I, Section 2.5, p. 148- 150.

**Focusing optics for high energy bulk diffraction with high spatial resolution: First results**

U. Lienert, V. Honkimäki, O. Hignette, M. Lingham, E. Ziegler, ESRF
S. Garbe, H. F. Poulsen, A. Horsewell, Risø
N. B. Thomsen, Risø / Danfoss A/S

**Aim:** The aim of the experiment was to determine the bulk strain gradient in layered structures. This is only feasible in transmission geometry and requires high energies and (one-dimensional) focusing. Conventional techniques based on x-ray tubes are only sensitive to a surface region.

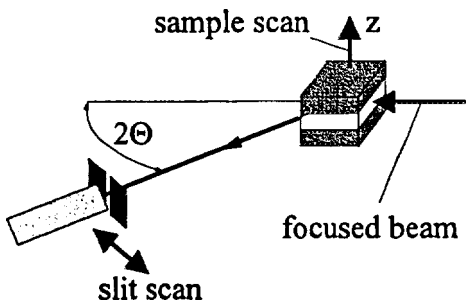


**Experimental:** Samples were Cu/Ni multilayers grown on Cu substrates by 'dual bath technique' (layer thickness 1 and 50 μm, total thickness 200 μm) and single 10 μm thick CrN layers grown on Fe substrates. Due to the novel optics approach sufficient intensity and a spatial resolution of 4 μm were obtained on a bending magnet source. Broadening of the diffraction peaks due to the horizontal focusing was avoided by dispersion compensation. The peak width was limited by the sample thickness, detector slit and incoming beam widths and by the intrinsic energy band of the monochromator ($\Delta E/E = 2 \cdot 10^{-4}$). Best resolution would be obtained by a large sample-detector distance which was, however, prevented by the hutch dimension. Still, the minimum peak width of a Fe calibration powder was obtained for the (2 1 1) reflection as expected by the dispersion contribution.

**Results:** The contour plot of the (3 1 1) diffraction peaks clearly shows that the peaks of the Ni layers are wider than for the Cu layers indicating sensitivity to micro structure (grain size). It is also clear that the spatial z-resolution is sufficient to obtain strain profiles within single layers. The quantitative evaluation of the strain gradient by peak fitting is under way but is also discernible by the slight tilt and waviness of the Cu ridge. The intensity variations are most likely due to texture. The detailed evaluation is in progress.

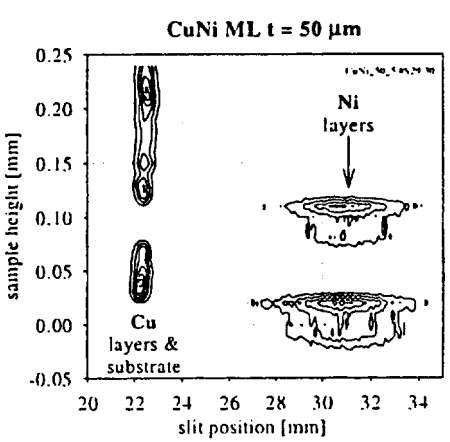

## Focusing optics for high energy bulk diffraction with high spatial resolution: Optics

U. Lienert, V. Honkimäki, O. Hignette, M. Lingham, E. Ziegler, ESRF
S. Garbe, H. F. Poulsen, A. Horsewell, Risø
N. B. Thomsen, Risø / Danfoss A/S

**Aim:** At present, no routinely usable focusing, energy tuneable, fixed exit monochromator exists for high x-ray energies. A prototype version of such a monochromator, based on bent Laue and Bragg crystals, was installed at the ESRF beamline BM5 but no diffraction experiments were performed yet. This experiment was aiming at:
(i) testing the performance of the monochromator in an actual diffraction experiment
(ii) combining the monochromator with a vertically focusing multilayer
(iii) demonstrate that a broadening of diffraction peaks by the divergence due to focusing can be avoided.

Laue-Bragg Monochromator: The intrinsic energy band path of the LBM is $\Delta E/E = 2 \cdot 10^{-4}$. 35 mm of the horizontal radiation fan was accepted. The focus size is limited to 1 mm by the penetration of the x-rays into the crystals. The focus was slit down to 100 - 300 μm to obtain sufficiently narrow diffraction peaks. By detuning the crystal bending such that the source went off-Rowland circle, an horizontal energy gradient was selected to match the dispersion of the Cu and Ni (311) reflections.

MultiLayer: The $W/B_4C$-ML (d-spacing of 25 Å, laterally graded) was grown by the ESRF ML group. The distance from the ML to the focus was 0.75 m and 220 mm of the ML were illuminated, equivalent to 800 μm beam height. Elliptical bending was achieved by a two moment bender which was calibrated by optical metrology. The x-ray energy was chosen to be just below the W K-edge.

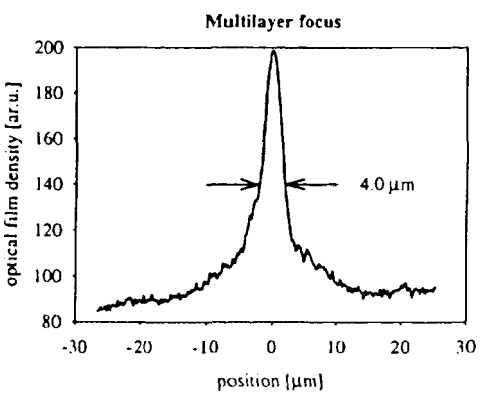


**Results:** The vertical size of the line focus was measured to be 4±1 μm by high resolution film exposure, absorption knife-edge and slit scans. The focus width is limited by the remaining slope error of the ML substrate. A peak reflectivity of 80 % was measured at the centre of the ML decreasing down to 30% at the edges. The all over gain factor (as compared to a 4 μm wide slit) is around 50. The proposed monochromator provides an intensity gain factor larger than 1000 as compared to existing non-focusing optics. The selection of an horizontal energy gradient by the LBM for dispersion compensation posed no problems.

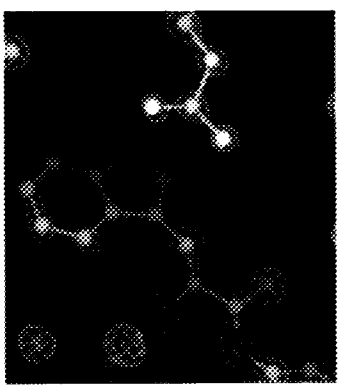

# Protein Structures

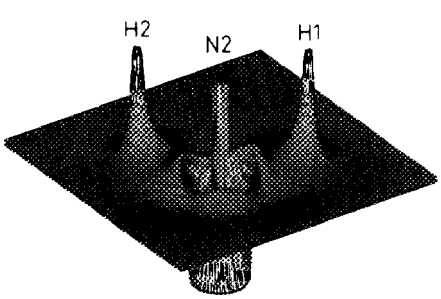


# Electron densities

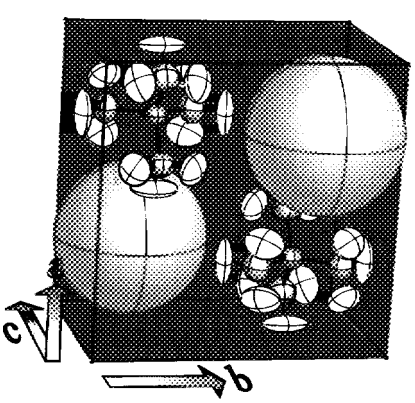


# Crystallography

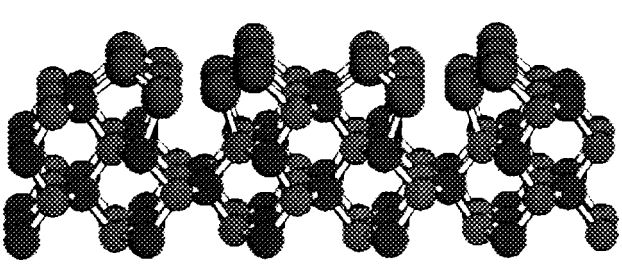

# Surface Science

klæbel's offset tryk a-s